Influenza A Virus Pathogenesis in a Non-Human Primate Model of Pregnancy

Orlando Cervantes

A dissertation

submitted in partial fulfillment of the

requirements for the degree of

Doctor of Philosophy

University of Washington

2025

Reading Committee:

Kristina Adams Waldorf, Chair

William Altemeier

Tristan Jordan

Program Authorized to Offer Degree:

Global Health

©Copyright 2025

Orlando Cervantes

University of Washington

Abstract

Influenza A Virus Pathogenesis in a Non-Human Primate Model of Pregnancy

Orlando Cervantes

Chair of the Supervisory Committee:

Kristina Adams Waldorf

Department of Obstetrics & Gynecology

Influenza A viruses (IAVs) have caused pandemics throughout the last 100+ years and remain a danger to global health due to their evolutionary mechanisms and persistence in worldwide avian populations. Pregnant women infected with pandemic IAVs have greater risk of respiratory disease severity and pregnancy complications. We hypothesized that aberrations in the pregnant primate's innate immune response to pandemic IAV predisposes them to severe IAV lung disease and atypical placental function. We infected pregnant and non-pregnant non-human primates (NHPs) with 2009 H1N1 and euthanized them at 5 days post-infection. Pulmonary physiology tests showed that severe IAV respiratory disease emerged at a similar frequency in both pregnant and non-pregnant macaque females. We observed that upregulation of antiviral gene expression in the lungs was similar in both infected pregnant and non-pregnant females relative to uninfected females. However, frequencies of IAV-infected alveolar macrophages are significantly higher in pregnant macaques relative to non-pregnant females. A multivariate linear regression model suggests that pulmonary TLR9 expression combined with baseline oxygenation values predict endpoint disease severity, regardless of pregnancy status. We did not find evidence of viral infection in most placentas or any fetuses. We encountered no

significant differences in frequency of injury between placentas from infected and uninfected NHPs. In spite of this, we found evidence of elevated antiviral gene expression and pro-inflammatory cytokine circulation in placentas from infected versus uninfected NHPs. We calculated that maternal lung viral load correlated significantly and positively with antiviral gene expression, suggesting that the extent of maternal infection is triggering placental innate immunity. We believe that our translational NHP model reveals interesting insights into the maternal innate immune response to IAV infection and crosstalk with placental immune activation. Future studies should use longer experimental timelines to quantify enhanced mortality and pregnancy complication risks from maternal IAV infection.

Table of Contents

Acknowledgements

I thank the many people involved in the nonhuman primate experiments at the Washington National Primate Research Center including Brenna Menz and Solomon Wangari. I thank the members of the Institutional Animal Care Use Committee that reviewed and approved the experimental plan. Nearly all members of our laboratory assisted in collecting or processing tissues in collecting or processing tissues. Many lab members also assisted with molecular biology experiments that supported this work including Hazel Huang, Briana Del Rosario, Hong Zhao, Amanda Li, Andrew Vo, Sidney Sun, and Roslyn Van Abel. The flow cytometry assays were performed in collaboration with the Fuller laboratory and within this lab, I would like to thank Thomas Lewis, Megan Fredricks, Mara Vaughan, and Dr. Deborah Fuller. Drs. Jeff Munson and John Cornelius assisted with data management and/or analysis. Dr. Raj Kapur at Seattle Children's Hospital and Dr. Audrey Baldessari at the Washington National Primate Research Center interpreted placental and lung pathology, respectively. My thesis committee was extremely helpful in guiding this project and my intellectual development and included Drs. Bill Altemeier, Tristan Jordan, Whitney Harrington, Deborah Fuller, and Michael Gale, Jr. I would also thank Dr. Kristina Adams Waldorf, my thesis mentor, for her guidance over the past five years. Finally, I am eternally grateful for the endless support from my friends, family, and God.

Chapter I: Introduction

Influenza Viruses and Pandemic Potential

Influenza A viruses (IAVs) have caused major pandemics over the last 110 years. IAVs are one of four types of influenza viruses in the *Orthomyxoviridae* family.[4,5] These pandemic IAV subtypes include the 1918 “Spanish” H1N1, 1957 “Asian” H2N2, 1968 “Hong Kong” H3N2, and 2009 swine H1N1.[6,7] Pandemic IAV remains a global health threat due to antigenic shift or drift. Currently, there is concern that a highly pathogenic avian influenza (HPAI), such as H5N1, might spill over into human populations as large outbreaks from poultry or other animal reservoirs. In the last year, H5N1 has even been detected in dairy cattle herds in the United States (USA), a sign of the growing danger of HPAIs.[8]

HPAIs have been endemic in Africa and Asia for decades, owing to the widespread presence of suitable reservoir populations in poultry farms, but have steadily spread across the globe. From these farms, HPAIs can spread to migratory waterfowl and continue to persist in the region through continuous evolution even with the culling and vaccination practices used to control epizootic outbreaks experienced on these farms.[9] While last year was not the first time that HPAI has reached the Western Hemisphere, it is the first time that the infections spilled over in high frequencies in mammal populations (dairy cows, cats, dogs, and humans) in the USA.[10] Notably, almost 300 herds in 14 states have been affected by the outbreak with cows experiencing lethargy, loss of appetite, reduced milk production, and infected milk.[11] This infected milk was likely consumed by domestic cats in the area, resulting in feline deaths with viral infection of the central nervous system.[12] While 70 human cases have been identified, all except one have resulted in mild disease after adequate treatment and therapeutic intervention.[13] The only severe case of H5N1 resulting in death in the USA occurred in an older male Louisianan with underlying health conditions.[14] At the time of writing, HPAIs have not been able to spread person-to-person.

Still, health authorities continue to maintain rigorous surveillance, even in the face of an anti-science political climate.

There are several other types of influenza viruses, but they lack the ability to undergo rapid genetic changes like IAVs and jump from humans to other species. Influenza B viruses (IBV) can cause seasonal epidemics but lack the ability to undergo rapid genetic changes like IAVs and jump from humans to other species; these two factors make IBVs less likely to start pandemics. Influenza C viruses (ICV) only cause mild illness in humans and do not cause epidemics. Influenza D viruses (IDV) do not infect humans and have only been documented to cause mild animal infections. This dissertation focuses on IAV due to its propensity to cause pandemics and severe lung disease in humans.

IAV Genomic Organization and Evolution

Orthomyxoviruses have bilayered, enveloped virions containing a negative sense, single-stranded RNA genome. While all influenza viruses have segmented genomes, IAV possesses 8 segments (PB1, PB2, PA, HA, NA, NS1, NP, M, and NS) that encode 11 proteins after RNA splicing.[15,16] The viral RNA-dependent RNA polymerase is made up of proteins from the PB1/PB2/PA segments. The PB1 segment also encodes for the pro-apoptotic PB1-F2 protein while PB2 and PA only encode their respective polymerase subunits. NA encodes neuraminidase and HA contains only the gene for hemagglutinin; both NA and HA are key for subtype classification. The M segment contains the genes necessary to build the M1 matrix protein and the M2 ion channel. M1 is also needed to hold the viral ribonucleoproteins (vRNPs) in place along the inner membrane. The NS1 segment encodes the interferon antagonist and NEP/NS2, which supports vRNP export from the host nucleus.

Of the gene products contained in this genome, the surface glycoproteins HA and NA guide further characterization of IAVs into HxNy subtypes.[4,5] HA contains the machinery needed to interact with

host surface sialic acids and initiate entry via membrane fusion. NA facilitates the release of assembled virions by cleaving the very same host surface glycans as the virion buds off the host cell membrane. At the time of this work, the CDC has recorded 18 different HA and 11 different NA.[17] Given the propensity of IAV reassortment in animal reservoirs due to their segmented genomes, the possible combinations of HxNy equate to nearly 200 unique subtypes. Most of these subtypes are found in the main animal reservoir, wild birds, which only experience asymptomatic infection.[18]

Reassortment involves the mixing of viral genes between multiple IAV strains after infection of the same host cell and is a mechanism that allows IAV to thrive in a range of animal hosts such as swine, avians, mustelids, and humans.[18] These antigenic shift events, the integration of animal IAV genes into strains already capable of infecting human cells, is what can lead to new pandemic IAVs. Antigenic drift, on the other hand, is the gradual accumulation of mutations in the HA and NA genes, allowing for IAV's evasion of antibody-dependent immune responses.[5,18] This mechanism provides an evolutionary advantage to the error prone viral RNA-dependent RNA polymerase encoded by the PB1/PB2/PA genes and has given rise to the seasonal, antigenically distinct IAV strains originating from pandemic H1N1 and H3N2 subtypes.

IAVs are classically recognized as respiratory viruses but have the capacity to infect a wide range of organs. IAVs main host receptors are the a-2,3 and a-2,6 sialic acid, part of the N-glycan family, which are most abundant in epithelial cells of the respiratory tract, but are also expressed in the placenta, brain, heart, and intestinal mucosa.[19] A recent publication has also highlighted that alternative entry receptors for IAV infection include phosphoglycans, O-glycans, and glycosphingolipid-glycans that expand the viral entry routes.[20] Viral tissue tropism is also expanded by mutations in the HA gene and host proteases capable of cleaving the HA.[21] Therefore, it is worth considering multi-organ dissemination during the time course of a severe IAV infection.

IAV Infection in Pregnant Women (adapted from Cervantes et.al., *Immunol Rev*., 2022)[22]

Pregnant women stand at greater risk of severe pandemic IAV disease and pregnancy complications. The first reports of pregnancy as a high-risk condition for severe IAV disease occurred during the 1918-1919 IAV pandemic ('Spanish flu'). An analysis of death certificates in London found that the mortality rate for all women (15-49 years) was 4.9/1,000, but in pregnancy was 5.3-5.7/1,000.[23] As many pregnant women who died did not have their pregnancy noted on their death certificate, this is likely an underestimate. Similarly, in the U.S., reports of pregnancy mortality obtained from a questionnaire of obstetricians surveying 1,350 pregnancies found that 678 of these patients developed pneumonia (50%), 365 died (27%) and there were high rates of stillbirths.[24] Reports of higher mortality, hospitalization, preterm birth and stillbirth also occurred during the 1957 pandemic ('Asian flu') and the more recent 2009 H1N1 pandemic ('swine flu').[25-36] The postpartum period after delivery represents a particularly high-risk time for mortality due to IAV.[37] This is a time of rapid physiological changes, fluid shifts and a precipitous drop in sex hormones. In a systematic review of more than 610,000 participants identified the women less than four weeks postpartum as one of the few risk factors associated with a significantly increased risk of death from pandemic influenza [odds ratio: 4.43, 95% Confidence Interval (C.I.): 1.24-15.81].[37] The impact of changes in immune defenses, sex hormones and other physiological changes on the immunity and health of pregnant and postpartum women is unknown.

H5N1 infections in pregnant women have high risks of maternal and fetal death. A recently published systematic review of documented cases found that pregnant women infected with HPAIs were usually young (20-35 years) and represented at each trimester[38]. The maternal and fetal death rates were high (90% and 87%, respectively). Surviving fetuses had a greater risk of being born prematurely (80%). However, stronger disease surveillance infrastructure in countries where HPAIs are endemic is necessary to better capture the etiology of severe disease risk in pregnant women, especially if H5N1 becomes endemic in the United States.

The high fetal death rate may be a result of H5N1's ability to more consistently infect and thrive in the placenta. Placental syncytiotrophoblast cells, responsible for nutrient and gas exchange between mother and fetus, are permissive for HPAI infection.[39] Infection can also disrupt normal secretion of essential pregnancy-related hormones. Viral infection of the placenta and fetus was demonstrated in a pregnant mouse model and a human case of H5N1, providing evidence that HPAIs can be vertically transmitted from mother to fetus.[40,41] The placenta may initially become infected from the dissemination of infected neutrophils from the lungs to other organs.[42] It is interesting that vertical transmission is not well-documented in H1N1 literature so this phenomenon may reflect a unique and dangerous facet of HPAI pathogenesis.

Central Hypothesis and Rationale

To address these unknowns, this dissertation project will use a nonhuman primate model, which is a highly translatable model of human pregnancy and IAV disease. The central hypothesis of this dissertation is that aberrations in the pregnant primate's innate immune response to IAV H1N1 predisposes to severe IAV lung disease and aberrant placental function in pregnant nonhuman primates (NHPs). In the remaining introduction, we will describe pregnancy-associated changes in lung physiology and immunologic subsets, which may play a key role in development of enhanced lung disease due to IAV in pregnancy. T cell populations are known to be heavily impacted in function and frequency by pregnancy-related hormones; they also occupy important niches during IAV infection. Pigtail macaques (*Macaca nemestrina*) have a gestational period of approximately 6 months (~172 days) with a similar timeline of fetal development as in humans; they have also been found to be an excellent model of IAV disease.[43]

Lung Physiology and Changes Induced by Pregnancy

IAV infection usually presents mild to severe depending on various factors such as comorbidities, age, previous vaccinations, and pregnancy status. Severe cases can develop as soon as 2 days

post-infection and usually involve viral pneumonia and acute respiratory distress syndrome (ARDS).[44,45] ARDS diagnosis in humans requires specific criteria: proof of bilateral infiltrates on chest radiograph, acute onset within 1 week of new/worsening symptoms, and PaO_2/FiO_2 <300 with a positive end expiratory pressure equal to 5.[46] Bilateral opacities must not be the results of abnormal fluid accumulation (effusion), lung/lobar collapse (atelectasis), or abnormal tissue growth (nodules). Pulmonary edema origin must be objectively assessed via ultrasound to rule out hydrostatic edema and not fully explained by cardiac failure or fluid overload. A more recent recommendation by critical care experts to facilitate diagnosis in resource-limited settings globally recommends high flow nasal oxygen <30 L/min, SpO_2/FiO_2 <315, and ultrasound imaging of bilateral opacities to be considered as well.[47] The oxygenation measure PaO_2/FiO_2, the ratio between partial pressure of arterial oxygen and fraction of inspired oxygen, has emerged as a dependable predictor of clinical outcomes and ARDS in clinical literature.[48,49] Oxygenation measures have been used to find association with immunological variables in a mouse model of IAV infection, but not in the context of pregnancy or a highly translational model like nonhuman primates.[50]

Pregnancy brings temporary but important changes to the respiratory system thanks to hormones and the needs of a growing fetus. As progesterone increases during pregnancy, it alters the tone of the smooth muscles in the airways resulting in dilation of the airways and an increase of oxygen consumption.[51] As the fetus grows and the uterus expands, the diaphragm is displaced upwards, and the negative pleural pressure increases.[52] This, in turn, leads to a reduction of the expiratory reserve volume and functional residual capacity (FRC) as the small airways close[53]. FRC can also be decreased during respiratory infection, making a delicate situation worse for pregnant women.[54] Airway resistance, the change of pressure needed to move air from the mouth through to the alveoli, tends to decrease in later pregnancy as pregnancy-specific hormones relax tracheobronchial smooth muscles.[53,55] However, the total lung capacity stays constant since the

rib cage expands to compensate for the shorter chest height.[56] Static and dynamic compliance, the ability for the lungs to expand and stretch, also stays consistent during pregnancy.[52] Pregnant women tend to experience hyperventilation, which can be exacerbated further in the context of respiratory infection.[55,57] The pregnancy-induced physiological changes to the respiratory system put pregnant women in a delicate balance that IAV infection can disrupt to a greater degree than when women are non-pregnant.

Innate Immune Signaling in Pregnancy and IAV

An essential early response to IAV infection by the host is to activate the inflammasome and antiviral immune signaling via Type I IFNs. Inflammasome activation relies on two signals.[58] Once IAV gets taken into the endosomes due to membrane fusion, Toll-like receptors (TLRs) 3 and 7 will recognize the viral RNA and trigger a signaling cascade to activate the nuclear factor κ-light-chain enhancer of activated B cells (NF-κB) transcription factor.[59,60] NF-κB would then enter trigger expression of the inflammasome components and inactive pro-IL-1β/pro-IL-18; this process is referred to as the first signal. The second signal occurs when NLR family pyrin domain containing 3 (NLRP3), one of the components, recognizes damage associated molecular patterns which include IAV M2 channel and PB1-F2 proteins.[61,62] NLRP3 then forms the inflammasome complex by associating with adapter protein apoptosis associated speck-like protein containing a CARD (ASC) and caspase-1.[63] Activated inflammasome complex would then cleave the pro-IL-1β/pro-IL-18 into active forms for secretion along with processing of gasdermin D for pyroptosis. However, in severe IAV cases, hypercytokinemia results when IL-1β and IL-18 levels are greatly elevated system-wide.[64,65] Inhibition of the NLRP3 inflammasome has been suggested to improve patient outcomes from IAV infection.[66,67]

Inflammasomes during pregnancy are necessary to facilitate inflammation during parturition (childbirth) but have also been linked to adverse pregnancy outcomes. The initiation of

physiological labor at term requires a form of sterile inflammation and is coordinated among immunological elements in the placenta, myometrium, and cervix.[68] Inflammasome components such as ASC and caspase-1, along with elevated levels of active IL-1β have been detected in the amniotic fluid and the placental chorioamniotic membranes of pregnancies at term.[69-72] However, studies have suggested that the introduction of pathogen-associated stimuli can induce the activation of NLRP3 inflammasomes in the placenta and, therefore, contribute to poor pregnancy outcomes (preterm parturition and hypertensive complications).[73-76] Therefore, it is possible that viral infection of the placenta could result in adverse pregnancy outcomes, such as preterm birth, from inflammasome hyperactivation.

Interferons (IFNs) are a key element of the antiviral, innate immune response to IAV. Type I IFN, defined classically as IFNα and IFNβ, are produced by almost all nucleated cells. Due to the diversity in the distribution of Type I IFN producing cells, these IFNs are the most important in restricting IAV replication and enhancing spread to neighboring cells and organs.[77] In the respiratory system, epithelial and antigen-presenting cells are the first to encounter the IAV. In these cells, the viral RNA is recognized as foreign material by the pattern recognition receptors TLR 3/7-9 and RIG-I. This triggers a signaling pathway to produce Type I IFNs, which are then secreted by the cells for paracrine or autocrine signaling. Once docked with the Type I IFN receptor (IFNAR), this triggers the JAK-STAT signaling pathway, leading to the expression of interferon stimulated genes (ISGs).[78] These ISGs help prevent viral replication and dissemination directly and indirectly, by enhancing cytokine production and cellular immunity.[79] The Mx (myxovirus) GTPases can form oligomeric rings around vRNPs to inhibit nuclear import/export. IFITM (IFN-inducible transmembrane) family members can interfere with membrane fusion between the viral envelope and host endosome, restricting viral replication within the cell[80] The Type I signaling pathway represents the first line of the immune defense to IAV but also occupies special functions to promote a healthy pregnancy in humans.

Type I IFNs also occupy important roles in ensuring a safe and normal pregnancy. Lack of type I IFN signaling can result in high viremia and greater risk of mortality even in the later stages of murine pregnancy.[81] In mice, Type I IFNs and their accompanying ISGs support placental implantation and so are expressed on the preimplantation blastocyst's outer layer and post-implantation decidua.[82] However, overexpression, especially in the context of pregnancies complicated by maternal infection or autoimmunity, can lead to developmental deficiencies or even death in the fetus.[83-85] Type I IFN signaling is instrumental to placental implantation and antiviral defense, but dysregulation is attributed to poor pregnancy outcomes.

The Th17/Treg Balance in Pregnancy and IAV (adapted from Cervantes et.al., *Immunol Rev*., 2022)[22]

Th17s and its effector cytokines have been described as an element in the anti-IAV response and were examined in this dissertation. Th17 cells are a key mediator of the inflammatory response to pathogens by recruiting neutrophils to sites of infection. Th17 cells are a CD4+ T helper lineage characterized by retinoic acid receptor-related orphan receptor transcription factors (RORγt and RORα) and the production of pro-inflammatory cytokines (IL-17, IL-21, IL-22).[86,87] Naive CD4+ T cells differentiate into Th17 cells after stimulation with IL-6 and TGF-β. In a murine model of H3N2 infection during pregnancy, IL-17 was elevated in circulation. RORγt levels were upregulated in the intestines in parallel with maternal pulmonary inflammation and dam weight loss.[88] In line with this, higher levels of IL-17 and Th17-linked cytokines (IL-6, IL-8) were found in human patients infected with the 2009 H1N1 strain.[89] Another study suggested that elevation in the Th17 cytokine profile (IL-17, IL-6, IL-8, IL-9) is a hallmark of early, severe influenza disease.[90] Reduced production of Treg-produced IL-10 can improve Th17 effector functions, but strong maternal immune activation have been linked to fetal abnormalities.[91,92] Due to the function of Th17 as a

mediator of inflammatory responses, it is important to study this cell population in the context of IAV infection.

Regulatory T cells (Tregs) occupy an important role in mediating the immune response to IAV and promoting recovery of the affected tissues; this population is also increased in pregnancy. Tregs are a subset of $CD4^+$ T cells characterized by their expression of the transcription factor forkhead box P3 (FoxP3) and their ability to regulate inflammatory responses, establish self-tolerance, and suppress effector T cells and other immune cells.[93,94] FoxP3 is essential for Tregs immunosuppressive function and is the master regulator of Treg development, function, and differentiation.[95,96] They express anti-inflammatory cytokines, such as TGF-β and IL-10 and rely on these same cytokines to differentiate new Tregs.[97,98] Treg differentiation from CD4+ T cells also relies on TGF-β, in addition to IL-2, and this key similarity to Th17 underlies the Th17/Treg ratio.[99,100] Shifts in this balance allows the immune system to respond appropriately to different circumstances such as infection or pregnancy. Interestingly, another study showed that estriol treatment of female mice following IAV infection resulted in a skewing of T helper responses an increase of Treg frequencies in lung tissue; these changes to the immune profile were associated with decreased disease severity, though viral replication and clearance was unaffected.[101] In addition to their immunosuppressive capabilities, Tregs also contribute to tissue healing and integrity through the expression of epidermal growth factor receptor ligands, such as amphiregulin and keratinocyte growth factor, during viral infection.[102-105]

During pregnancy, there are changes in the maternal immune system that facilitate a tolerogenic environment to the fetus. The Th17/Treg ratio shifts during pregnancy, which may help to support tolerance to the developing fetus. Treg frequencies rise in pregnancy and Th17 frequencies decrease, which may increase the likelihood of severe IAV disease. This shift occurs largely through the influence of pregnancy-specific hormones such as estrogens and progesterone. Estradiol, a type of estrogen, at pregnancy levels suppresses the differentiation of Th17 cells from

CD4+ via a PD-1 signaling pathway.[106] Estradiol also enhances the expansion of Tregs, their ability to effectively suppress the activation and proliferation of effector T cells, increases *FoxP3* expression, and decreases production of IL-17 by Th17 cells in mice.[107,108] Pregnancy and pregnancy-like levels of estrogen can downregulate Th17 transcription factors and cytokines and upregulate Treg transcription factors.[109] Estriol, another type of estrogen produced at high levels only during pregnancy, dampens Th17 responses by decreasing the Th17/Treg ratio and increasing IL-10 secretion while inhibiting IL-17 secretion and neutrophil function.[110,111] Progesterone can bias the naive CD4+ T cells towards differentiation into Tregs and suppress differentiation into Th17s.[112-115] These findings demonstrate the importance of evaluating changes in Th17 and Treg populations over the course of IAV infection and disease.

Nonhuman Primate (NHP) Models of Pregnancy and IAV

Animal models that share human pulmonary physiology, such as nonhuman primates, are the most ideal for studying how pulmonary physiology and function are impacted during respiratory viral infection (Tables 1.1 and 1.2).

Of the models highlighted in Table 1.1, mice have the cost-advantage and are available in a wide range of inbred, transgenic strains. Their key disadvantages are they do not recapitulate human IAV disease and require mouse-adapted IAV strains (such as the 1934 H1N1 PR8 virus) to achieve ideal results, making it difficult to easily extrapolate results to humans. Ferrets do have comparable viral pneumonia and anatomical similarities in their respiratory systems to humans, but they are not ideal models due to the dearth of species-compatible biological reagents.

Table 1.1. Advantages & Disadvantages of IAV Animal Models

	Mice	Nonhuman Primates	Ferrets
Advantages	• Low cost barrier • Well-characterized genetics; easily manipulated genome • Many species-specific reagents	• Comparable viral pneumonia pathology to humans • Histology of respiratory tract most similar to humans • Close genetic/anatomic similarity to humans • Most similar immune response and systemic disease • Many compatible reagents due to cross-reactivity with human-specific reagents • Excellent translational value	• Comparable viral pneumonia pathology to humans • Anatomy/histology of respiratory tract similar to humans • Suitable for airborne transmission studies
Disadvantages	• Anatomy/histology of respiratory tract and distribution of sialic acids dissimilar to humans • Disease manifestation differs from humans • IAVs, aside from some highly pathogenic strains, require adaptation to species for ideal pathology • Cannot transmit IAV • Data not easily extrapolated to humans	• Genetically outbred, host response variability expected • Expensive to acquire and maintain • Ethical concerns	• Genetically outbred, host response variability expected • Systemic disease differs from humans • Few molecular biological reagents available

Modified from references[2,3]

The need for translational models of IAV pathogenesis has led researchers to seek answers in nonhuman primate models. The dominant species used in NHP IAV studies are macaques (genus *Macaca*), specifically rhesus (*M. mulatta*), cynomolgus (*M. fascicularis*), and pigtail macaques (*M. nemestrina*). It is well-documented that macaques are naturally susceptible to human IAV infection due to their similar distribution of sialic acid receptors in the airways.[116-118] However, there could be species-specific differences in the extent of viral replication and symptoms.[119] Macaques have proven useful as important tools to prove the translational potential of novel therapeutic interventions against IAV disease.[120-122] Macaque models have also been utilized to study pathogenesis from different IAVs, including 1918 H1N1 and HPAI H5N1, and helped develop insight into innate immune responses.[123-127] Furthermore, they have also been used in studying differences in IAV antiviral responses between age groups.[128]

Alternative NHP model species have also been successful models of human IAV infection. Marmosets (*Callithrix jacchus*), a New World NHP species, have emerged over the last decade as a model that can replicate clinical presentation of IAV disease after infection with HPAI H5N1 and pandemic H1N1 2009.[129,130] Infant African green monkeys infected with H1N1 PR8, an isolate also closely related to 1918 H1N1 IAV, had defective antibody production in the respiratory tract,

Table 1.2. Different models for pregnancy studies

	Human	Mice	Nonhuman primates	In vitro (cell lines, primary cells/explants)
Mean Gestational Period	40 weeks	2-3 week gestation	24-26 weeks (macaques) 20-21 weeks (marmosets)	Can obtain from any gestational age
Mean Litter Size	1	10-12	1 (macaques), 2 (marmosets)	n/a
Uterus	Simplex	Bipartite	Simplex	n/a
Placenta	Hemomonochorial, villous, discoid	Hemotrichorial, labyrinthine, discoid	Hemomonochorial, villous, bidiscoid	Can obtain samples from across placental structure
Advantages/ Disadvantages	Directly translational, but limited to observational analysis.	Low cost, low variation if using inbred strains, transgenic strains available. Different immunological environments to primates, best results from mouse-adapted viruses.	Directly translational, but expensive and limited in availability. Can use human pathogens without issue. High and variable pregnancy losses.	Accessible, low ethical concerns when using cancer cell lines. Techniques available to manipulate basic genetic and translational behavior. Limited by artificial environments and isolation from organ system.

Modified from reference[1]

and therefore higher viral load, than adults.[131] NHPs, across various species, have emerged over the years as an ideal animal model for studying human IAV due to their human-like immune responses and pathology.

Comparing NHPs to the other relevant models of mice and in vitro cell lines/explants highlights the ideal nature of using NHPs to model infections during pregnancy (Table 1.2.). Mice dams (a general term for female parents) have two uterine horns while primates only have one. Mice and humans both have hemochorial placentas, allowing for the limited mixing of maternal and fetal blood, but only primates have a single trophoblast layer separating maternal and fetal blood and mice have three layers.[132-134] In addition, primate placentas have chorionic villi that form the main

structures for the interfacing of fetal blood vessels with maternal blood vessels while mice placentas have a more disordered web (labyrinth) of blood vessels for nutrient exchange.[135,136] While NHPs, such as macaques, have highly similar placentas to humans, NHPs can have bidiscoid placentas (two placental disks linked by a fetal blood vessel), but these are the same morphologically.[137] However, mice remain an attractive model due to their accessibility, short gestational periods, and litter sizes. While using humans is impossible beyond limited cross-sectional studies, researchers could use *in vitro* samples from cancer cell lines or primary tissue direct from the clinic. However, these cell lines cannot recapitulate normal trophoblast gene expression and explant samples are fragile in culture.[138] In addition, elements of the placental microenvironment, such as hormone and growth factors, are lost *in vitro*. However, developments in organoid cultures can allow researchers to study infections in a recreation of the first trimester placenta.[139] Ultimately, NHPs are an excellent model in which to study the complex factors contributing to enhanced lung disease in human pregnancy and the impact of IAV on the placenta.

There have been few studies of IAV disease in pregnant NHPs. A study with African green monkeys infected with H1N1 PR8 found that third trimester females' plasma had diminished IAV neutralization due to lower levels of complement when compared to non-pregnant monkeys.[140] Pregnant rhesus macaques infected with H3N2 A/Sydney/5/1997 in the third trimester and their offspring were studied for postnatal abnormalities. Notably, the offspring had significantly reduced grey and white matter when compared to controls, associating potential cognitive abnormalities with maternal IAV infection during pregnancy.[141] Only one study was found that tested therapeutic interventions in pregnant NHPs, focused on oseltamivir (an anti-IAV drug) pharmacokinetics in pregnant rhesus macaques across the gestational period.[142] This dissertation project addresses the major knowledge gap of IAV pathogenesis in pregnant NHPs and so elucidates aspects of the innate immune response not addressed in prior studies.

Chapter Overview

This dissertation project is based on the many unknowns in the pathogenesis of enhanced IAV disease in pregnancy. Previous literature informed the design of this study to address key questions linking IAV disease and pregnancy outcomes: 1) what is the relationship between pregnancy status and IAV disease severity in the pigtail macaque NHP model; 2) how does the pulmonary innate immune response to IAV differ between pregnant and non-pregnant females; and 3) how does maternal IAV infection affect placental health and innate immune activation. The dissertation is organized into chapters to address the two main organs of interest for these research questions: the lung and the placenta. Chapter 2 reviews the methodology used for data generation and analysis. Chapter 3 addresses questions 1 and 2 by focusing on the maternal lungs, while placental health and innate immune response are addressed in Chapter 4. Finally, I summarize the outcomes of this dissertation project and discuss potential opportunities for improvement alongside new research questions that are emerging from this work.

Chapter II: MATERIALS & METHODS

Research Animals and Ethics Statement

All animal experiments used in this study were approved by the University of Washington Institutional Animal Care and Use Committee (protocol# 4165-03), and in compliance with the U.S. Department of Health and Human Services Guide for the Care and Use of Laboratory Animals and Animal Welfare Act. All animal experiments were performed at the Washington National Primate Research Center (WaNPRC). Experiments described in this thesis used four groups of female pigtail macaques *(Macaca nemestrina*): IAV H1N1 infected-pregnant (n=11), IAV H1N1 infected-non-pregnant (n=18), uninfected-pregnant (n=18), and uninfected-non-pregnant (n=2) animals (Tables 2.1 and 2.2).

At the pre-defined study endpoint, the gestational age of all pregnant NHPs were between 121 and 159.5 days, which corresponds to the third trimester for this species.[143] Animals were housed in comfortable, clean, adequate-sized cages. The ambient temperature in animal quarters was maintained at 72–82°F. Animals were fed a commercial monkey chow, supplemented daily with fruits and vegetables. Throughout the study, animals were checked twice daily by the WaNPRC staff to evaluate their physical and clinical condition. Environmental enrichment activities included grooming contact, perches, toys, foraging experiences and access to additional environment enrichment devices such as paint rollers, grooming devices, foraging devices, activity panels and mirrors. All procedures performed under conscious sedation used either ketamine (10 mg/kg) or telazol 2.5-10mg/kg. Euthanasia prior to necropsy was performed by administration of a barbiturate overdose while the animal was under deep anesthesia in accordance with guidelines established by the 2007 American Veterinary Medical Association Guidelines on Euthanasia. These methods are also consistent with the guidelines described in the Weatherall Report on The Use of Nonhuman Primates in Research.

Table 2.1 Summary of Infected NHP Subjects

ID	AltID	Pregnancy Status	Gestational Age (days)	Fetal Sex	Weight (kg)	Age (years)
A11251	FLU1	Pregnant	130	M	8.5	12.19
L07279	FLU2	Pregnant	131	F	13.9	12.68
Z15060a	FLU3	Pregnant	132	F	7.14	6.56
R06147b	FLU4	Pregnant	143	F	11.68	15.5
Z11366a	FLU5	Pregnant	139	F	9.87	10.61
Z15193	FLU6	Pregnant	140	M	9.45	7.02
L08225a	FLU7	Pregnant	134	M	8.35	13.83
Z14061	FLU8	Pregnant	132	M	8	8.52
Z16319a	FLU9	Pregnant	121	M	8.25	6.99
Z17315	FLU10	Pregnant	131	F	8.95	4.43
Z12072	FLU11	Pregnant	139	M	11.15	11.75
A10026np	FLU12	Non-pregnant	n/a	n/a	8.6	13.46
A10180np	FLU13	Non-pregnant	n/a	n/a	6.75	12.39
T07039np	FLU14	Non-pregnant	n/a	n/a	6.25	13.53
Z14150np	FLU15	Non-pregnant	n/a	n/a	6.3	7.64
Z14367np	FLU16	Non-pregnant	n/a	n/a	7.25	7.06
L07236np	FLU17	Non-pregnant	n/a	n/a	7.05	14.88
Z01237np	FLU18	Non-pregnant	n/a	n/a	10.15	21.05
K01238np	FLU19	Non-pregnant	n/a	n/a	8.9	21.07
Z14186np	FLU20	Non-pregnant	n/a	n/a	11.4	9.21
Z18111np	FLU21	Non-pregnant	n/a	n/a	6.6	5.28
K06218np	FLU22	Non-pregnant	n/a	n/a	9.8	17.02

L05363np	FLU23	Non-pregnant	n/a	n/a	9.85	17.18
J06247np	FLU24	Non-pregnant	n/a	n/a	11.1	17.01
Z16281np	FLU25	Non-pregnant	n/a	n/a	5.7	6.97
Z13135np	FLU26	Non-pregnant	n/a	n/a	9.25	10.72
Z13227np	FLU27	Non-pregnant	n/a	n/a	10.3	10.52
A11186np	FLU28	Non-pregnant	n/a	n/a	10.05	15.08
Z09133np	FLU29	Non-pregnant	n/a	n/a	8.75	14.67

Table 2.2 Summary of Control Subjects

ID	AltID	Pregnancy Status	Gestational Age	Fetal Sex	Weight (kg)	Age (years)
Z15280np	CTRL1	Non-pregnant	n/a	n/a	5	5.5
A12264np	CTRL2	Non-pregnant	n/a	n/a	6.95	11.56
A07083	CTRL3	Pregnant	159	F	9.61	13.96
A10007	CTRL4	Pregnant	155	M	12.92	13.48
A10183a	CTRL5	Pregnant	156	M	9.45	7.85
F09165a	CTRL6	Pregnant	157	F	6.98	7.37
L10152	CTRL7	Pregnant	144	M	8.58	12.88
M10190	CTRL8	Pregnant	154	F	14.12	12.36
Z12353	CTRL9	Pregnant	147	UK	9.1	10.75
M05062	CTRL10	Pregnant	155	F	8.77	11.99
Z15006	CTRL11	Pregnant	158	F	11.35	5.23
L07201	CTRL12	Pregnant	139	M	8.2	11.7
R06147a	CTRL13	Pregnant	138	F	9.1	14.17
Z15060	CTRL14	Pregnant	128	M	7.14	6.56
J08186	CTRL15	Pregnant	136	F	8.44	14.92
M05267	CTRL16	Pregnant	145	M	6.2	5.56
Z15198	CTRL17	Pregnant	134	F	8.3	7.42
R10195	CTRL18	Pregnant	132	F	10.8	12.67
M99183	CTRL19	Pregnant	143	M	8.2	10.53
A07083	CTRL20	Pregnant	156	F	9.61	13.96

H1N1 Virus Cultivation and Harvesting

Madin-Darby canine kidney (MDCK) cells (ATCC) were cultured in Dulbecco's modified Eagle's medium (DMEM) supplemented with 10% fetal bovine serum (FBS), 25 mM HEPES, 100 U/mL penicillin, and 100 µg/mL streptomycin. Cells were incubated at 37°C and 5% CO_2 and confirmed to be free of mycoplasma with the MycoAlert™ mycoplasma detection kit (Lonza, LT07-318) prior to use for virus cultivation. A/California/07/2009 H1N1 influenza virus (CA09) isolate was obtained from Deborah Fuller's research group[144]. Sub-confluent monolayers of MDCK cells in T150 flasks were washed with PBS and infected at MOI 0.5 (5 mL serum-free MEM) at 37°C and 5% CO_2. After 1 hour, the media was removed, cells were washed with 1X PBS and media replaced. The media was harvested at 36 hours and centrifuged at room temperature to clear cell debris (1800 rpm for 5 minutes and then at 3000 rpm for 10 minutes). Virus stock was frozen at −80°C in 1 mL aliquots. The viral titer of each stock was quantified using a TCID50 assay with hemagglutination readout (described below) and converted to plaque forming units/mL. To transform TCID50/mL into PFU/ml, we multiplied TCID50/ml by 0.7. All cell culture and virus amplification procedures were performed according to Biosafety Level 2 protocols.

Figure 2.1 Visual Overview of Experimental Timeline

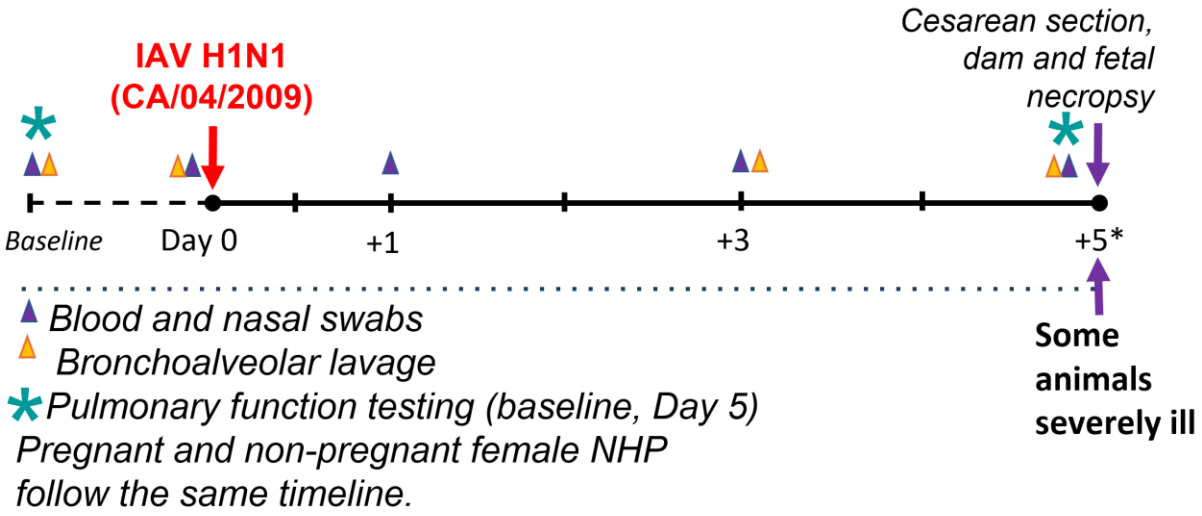

Infection with IAV H1N1pdm09

In line with previous NHP literature, we chose a 5-day time period for infection that would allow us to analyze the subjects at peak infection, innate immune and Th17 response.[119,145] Figure 2.1 outlines this infection timeline and points to the the timepoints in which we collected bronchoalveolar lavage (BAL) and blood. Nine pregnant female pigtail macaques (*Macaca nemestrina*), were sedated using ketamine (10 mg/kg) and inoculated using a combination of intranasal, intratracheal, intraocular, and intraoral routes with $10^{7.4}$ PFU of IAV (A/California/07/2009 (H1N1)). This dose was expected to yield a 100% infection rate according to the supplier.[146] Macaques were observed daily for clinical symptoms of influenza disease. Placentas were extracted during Cesarean section (C-section) 5 days post-infection (dpi), after which animals were euthanized for further sample collection and pathological examination, unless veterinary staff determined that a subject had to be humanely euthanized earlier due to IAV disease severity (Figure 2.1). Uninfected control pregnant adult pigtail macaques were given a mock infection with either cell media or saline and placentas were collected after C-section at endpoints. Samples from non-pregnant female adults were collected under the Tissue Distribution Program at the Washington National Primate Research Center.

Bronchoalveolar Lavage with Tracheal Wash Collection

The animal was fasted overnight, then anesthetized to a surgical plane. The animal was intubated and pre-oxygenated prior to the procedure. Pulse oximetry monitoring was used to monitor oxygen saturation throughout the procedure. Oxygen was provided until pulse oximeter shows oxygen saturation >90%. Care was taken to maintain sterility within the trachea and bronchi. The bronchoscope or a sterile feeding tube/catheter (8-12 Fr.) was passed into the trachea with ideal placement of the tip a few centimeters above the tracheal bifurcation. Trachea flushed with up to 6 ml sterile saline or PBS and fluids were then immediately withdrawn. This step may be repeated up to 2 additional times depending upon the quality of sample retrieved. Sterile feeding

tube/catheter passed more distally to the tracheal bifurcation. Sterile saline or PBS (3 mL/kg, not to exceed 15 mL) was infused into one lung lobe and retrieved by suction. This procedure may be repeated with a second aliquot of similar or lesser volume.

Pulmonary Physiology Testing (procedure adapted from Cervantes et.al., 2024)[147]

To best reflect the degree of impaired lung function in our NHP model, we developed a clinically relevant pulmonary physiology assessment with the support of physicians at the University of Washington. The inspiratory pause was a key feature of this protocol, which allows for calculation of lung compliance when the lungs and ventilator becomes a closed system with static volume; thus, there was no airflow, nor contribution of airway resistance to the measure pressures. The measured end-inspiratory pressure in the absence of airflow was called the plateau pressure (Pplat) and was equivalent to the alveolar pressure. Knowledge of the plateau pressure allows calculation of static lung compliance, which was a key metric of pulmonary mechanics that was not possible to calculate using plethysmography (Fig. 2.2D).

Interpretation of the Pulmonary Physiology Testing Results

Gas exchange includes both oxygenation and ventilation, which are measured using the PaO2 and PaCO2, respectively. An animal's PaO2 can be increased via mechanical ventilation by increasing FiO2, mean airway pressure, or to a lesser extent minute ventilation. As all three are independent variables and positive end expiratory pressure (PEEP) was held constant during our experiments, oxygenation was assessed by the P/F ratio, with lower P/F ratio well known to correlate with severity of lung injury and prognosis in humans.[148] We also assessed the alveolar-arterial oxygen difference (A-aDO2). The A-aDO2 provides a more comprehensive understanding

Figure 2.2 Visual Overview of Pulmonary Physiology Testing Protocol

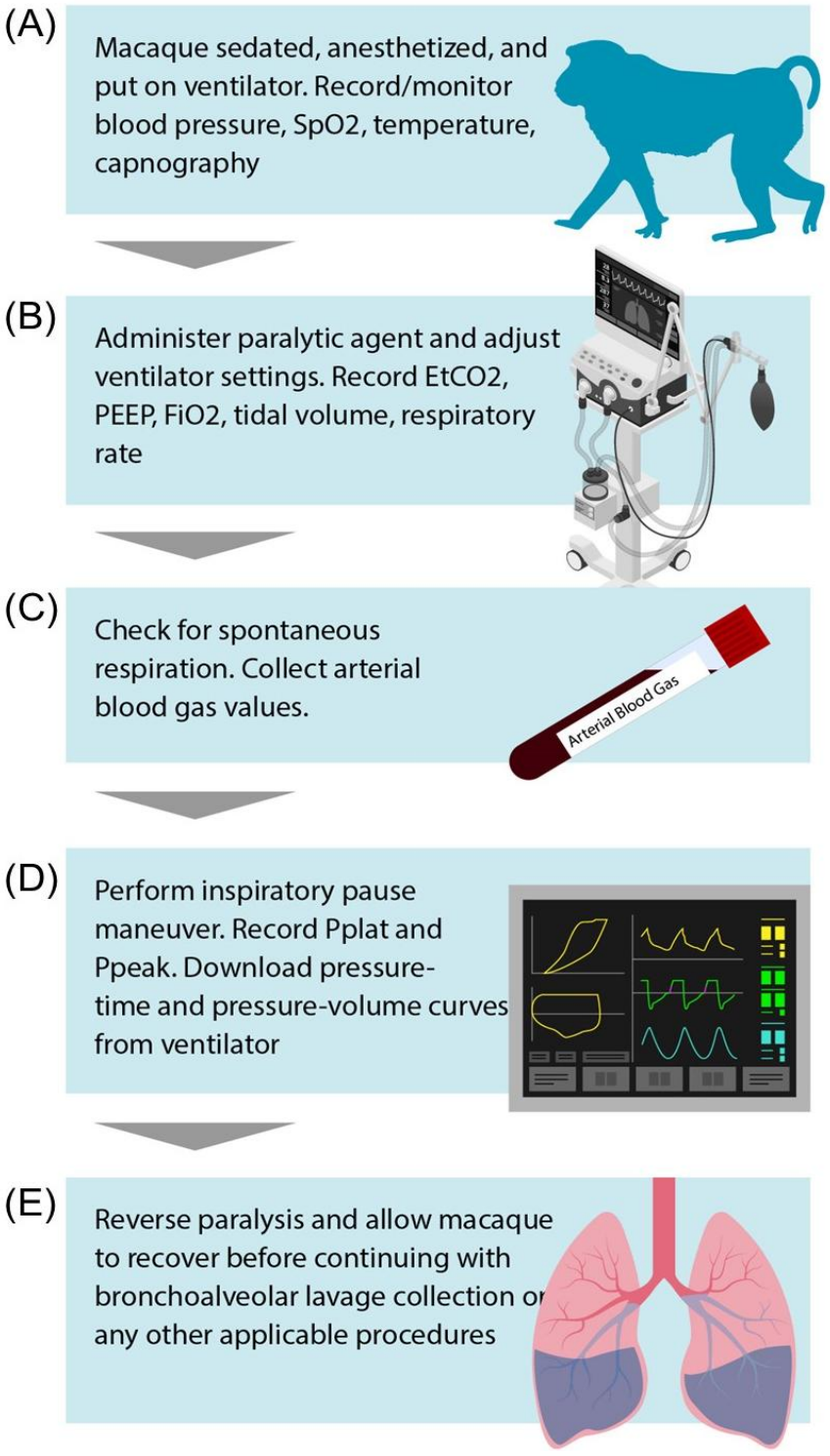

of oxygen transfer from the alveolar space to the arterial blood. An animal's PaCO2 was inversely proportional to alveolar ventilation (alveolar ventilation = respiratory rate x (tidal volume – dead

space volume). Lung pathology can increase PaCO2 via increased dead space, which represents the volume of each tidal breath that does participate in gas exchange. Increased percentage of dead space ventilation was associated with worsening lung injury and reduced survival in humans on mechanical ventilation.[149-151] As the end-tidal CO2 (EtCO2, and thus PaCO2) was held constant during our experiments, a requirement for a higher minute ventilation was therefore indicative of increased dead space.

Assessment of pulmonary mechanics on mechanical ventilation requires measurement of peak and plateau ("static") inspiratory pressures (Figure 2.2). The plateau pressure (Pplat), measured with an inspiratory "pause" (in the absence of airflow) was the summation of PEEP and the pressure required to hold the thorax at the set tidal volume and was thus used to measure thoracic compliance (thoracic compliance = Tidal volume/(Pplat-PEEP)) (Fig. 2.2A)**.** Thoracic compliance was the summation of lung compliance and chest wall compliance. Thus, at a given tidal volume, many conditions outside of the lung (e.g., increased abdominal distention or pressure) will increase Pplat. However, in most instances, increased Pplat results from reduced lung compliance (Fig. 2.2B). The enlarging uterus reduces chest wall compliance and slightly higher Pplat may be necessary to maintain appropriate tidal volume.[152] The peak inspiratory pressure (measured during airflow) reflects starting PEEP, thoracic compliance and the pressure needed to overcome airway resistance and achieve the set flow rate, the latter of which was held constant during our experiments with an inspiratory time consistently 0.6 seconds. Changes in airway resistance were represented as changes in the PIP relative to Pplat. High PIP, Pplat, and high driving pressure (Pplat – PEEP) have been associated with increased degree of lung injury and worse outcomes in humans.[153-155] The pressure-volume waveform on the ventilator was flattened with lung injury reflecting the need for an increase in airway pressure to obtain the same (or reduced) lung volume during inspiration (Fig. 2.2C).

Preparation of NHPs for Procedure

First, we sedated the animal using ketamine hydrochloride (15 mg/kg) and transported the animal to the surgery suite. Next, we collected any biological samples specified by the research protocol (e.g., blood, nasal swabs) except for the bronchoalveolar lavage (BAL). We then prepared the animal for surgery by inserting an intravenous catheter. To induce anesthesia, we administered an intravenous (IV) bolus of propofol 3-6 mg/kg; after approximately 60-90 seconds, we intubated and attached the endotracheal tube to the ventilator all while the animal was on its side. Anesthesia was maintained solely with isoflurane gas. Then, we applied a blood pressure cuff, temperature probe and SpO2 leads. The distal legs were both shaved to enable acquisition of an ABG from the dorsal pedal artery. Animals were maintained in a surgical plane with isoflurane for at least 6 minutes, while we recorded vital signs and oxygen saturation (SpO_2) to ensure that the animal was at an appropriate anesthetic depth prior to administering the paralytic. A lactated ringer's solution was administered (10 mL/kg/hr IV) and the animal was warmed (Fig. 2A).

Inducing Paralysis and Collecting an Arterial Blood Gas

First, we administered rocuronium 0.3 mg/kg IV to achieve paralysis, in preparation for performing an inspiratory pause maneuver (also called an inspiratory hold maneuver). Capnography was monitored to assess for cessation of spontaneous respiration (and as a marker of ventilation during the case), and then the ventilator was turned on. If spontaneous respiration persisted longer than 5 minutes, a second dose of rocuronium (0.15 mg/kg IV) was administered and we waited an additional 5 minutes before proceeding to the next step.

Next, we adjusted the ventilator settings as follows: 1) tidal volume to 8 ml/kg using a square wave inspiratory pattern; 2) respiratory rate to achieve an end tidal CO_2 of 35-45 mmHg; 3) PEEP to 5 cm H_2O; and 4) FiO_2 to maintain an SpO_2 above 95%. A 10-minute waiting period began after the animal was stabilized with these ventilation parameters.

Immediately before the arterial blood draw, we checked for spontaneous respiration using the ventilator's screen display to confirm absence of breaths initiated (triggered) by the animal, which are marked with a small pink line. In the event spontaneous respiratory effort was observed, another dose of rocuronium was administered at 0.15 mg/kg IV, followed by repeat of the 10-minute waiting period. We then checked whether there was any spontaneous respiratory effort and if none, we proceeded with collection of arterial blood (0.1-0.2 mL) from the dorsal pedal artery to obtain an ABG (Fig. 2.2C).

Inspiratory Pause Maneuver

After the arterial blood draw and immediately before the inspiratory pause, we once again checked for spontaneous respiration. If no spontaneous respiration was observed, we proceeded with the inspiratory pause maneuver. To perform an inspiratory pause, the exhalation port must be occluded at end-inspiration for either a percentage of the breathing cycle (10-20%) or for a specific time (0.5-2.0 seconds). Although we performed this maneuver manually, it can also be programmed through the ventilator software.

Reversing Paralysis

After completing the lung mechanics measurements, we reversed the paralysis by administering neostigmine (0.07 mg/kg IV) and atropine (0.04 mg/kg), monitored the animal for spontaneous respiration and documented how many minutes from the reversal (Neostigmine) it took for the animal to start breathing spontaneously without the ventilator. Typically, this took 3-5 minutes. If a BAL was performed as part of the research protocol, we performed this procedure at the conclusion of the pulmonary physiology testing (Fig. 2E).

RNA Isolation

For qPCR and bulk transcriptomics, we needed high quality RNA from various samples. The following protocol and kits yielded high concentrations of pure RNA. Tissue samples were kept in

Trizol reagent (Thermofisher, #15596018) in Precellys homogenizing tubes (Cayman Chemical, #1011152) prior to homogenization with Precellys Evolution machine (Bertin Technologies, #K002198-PEVO0-A.0). RNA was extracted from homogenate using RNeasy Mini Kit (Qiagen, #74106). For cell-free fluid samples such as BAL supernatant samples, RNA was extracted with QIAamp Viral RNA Mini Kit (Qiagen, #52904). All RNA was quantified via NanoDrop™ 2000 spectrophotometer (Thermo Scientific, #ND-2000) and Qubit 4 fluorometer (Invitrogen, #Q33238). The RNA integrity number (RIN) was measured by 4200 Tapestation System (Agilent, #G2991BA).

Viral RNA Load Assay

To quantify viral RNA levels from different sample origins, we used a RT-qPCR protocol and a WHO-approved primer/probe set. cDNA was generated from RNA isolates using iScript™ Select cDNA synthesis kit (Bio-Rad, #1708897) and manufacturer's gene priming method. qPCR was done with H1N1 HA-specific primers and probes (Table 2.3) using Taqman Fast Advanced master mix (Fisher Scientific, #444964) and Quantstudio 3 machine (Thermofisher Scientific, #A28132) following manufacturer instructions. Samples were run in triplicate. Positive results were defined as any sample with an average Ct value less than 38 cycles.

Table 2.3. qPCR Primers and Probe for H1N1 Detection

Name	Sequence
HKUqSW Probe	5`-[FAM] TGGGTAAATGTAACATTGCTGGCTGG [TAMRA]-3`
HKUqSW Forward Primer	GGGTAGCCCCATTGCAT
HKUqSW Reverse Primer	AGAGTGATTCACACTCTGGATTTC

Cytokine Quantification

To better characterize post-transcriptional circulation of immune mediators across various biological samples, we sought to use multiplex and simplex immunoassays tested for use in NHPs to directly quantify cytokine levels. Tissue samples were lysed using Invitrogen™ ProcartaPlex™ Cell Lysis Buffer (Fisher Scientific, #EPX-99999-000) mixed with a protease inhibitor cocktail

(Fisher Scientific, #PI78430) and everything was mixed in Precellys homogenizing tubes (Cayman Chemical, #1011152) prior to homogenization with Precellys Evolution machine (Bertin Technologies, #K002198-PEVO0-A.0). Lysate protein quantification was performed using a Pierce™ BCA assay (Thermo Scientific, #PI23225). Multiplex cytokine assays used the ProcartaPlex NHP Th 14-plex panel (Thermo Scientific, #EPX140-40040-901) and protocol was followed in accordance with manufacturer's guidelines for serum/plasma samples. We also quantified IFNα and IFNβ using the Cynomolgus IFN-Beta and Cynomolgus/Rhesus IFN-Alpha ELISA kits (PBL Assay Science #46415-1 and #46100-1, respectively). All protocols followed the manufacturer's guidelines.

Table 2.4. Immune Cell Definitions

Cell Type	Definition (all live CD45+ singlets)	Panel Used
Th17	CD3+/CD4+CD8-/IL17+IL-22+	ICS
Treg	CD3+/CD4+CD8-/CD25+FoxP3+	ICS
Classical monocytes	CD20-CD3-/HLA-DR+/CD14+CD16−	IMP
Myeloid dendritic cells	CD20-CD3-/HLA-DR+/CD14-/CD123−CD11c+	IMP
Plasmacytoid dendritic cells	CD20-CD3-/HLA-DR+/CD14-/CD123+CD11c−	IMP

Overview of antibody targets used to define immune cell subsets of interest and panels that were used to define said immune cells.

Intracellular Cytokine Staining (ICS)

Peripheral blood mononuclear, lymph node, lung, chorionic villus, and bronchoalveolar lavage cells were dissociated from original samples and were left unstimulated or stimulated overnight with 10 ng/mL PMA (Sigma) and 1 lg/mL ionomycin (Life Technologies) in supplemented RPMI-1640. All samples were treated overnight with 1 μg/mL brefeldin A (Sigma) and in the presence of CD107a antibody (eBioH4A3; eBioscience). Viability was assessed using a live/dead stain (Life Technologies) and cells were stained using the surface markers CD45, CD3, CD4, CD8, γδ T cell receptor (TCR), CD25, Ki67, CD107a, and CD127. Definitions of immune cells using these surface markers are summarized in Table 2.4. Cells were fixed and permeabilized with True-Nuclear Transcription Buffer Set (BioLegend) and stained for the intranuclear transcription factor FoxP3 (206D; BioLegend), and for intracellular cytokines IL-17, IL-22, and TGF-β1. Samples were acquired on an LSRII (BD

Biosciences) and analyzed using FlowJo software version 9.9.4 (FlowJo; LLC). This protocol was adapted from a collaborator's publication.[156]

Immunophenotyping (IMP)

In our effort to characterize the immune response in our NHP subjects, we would be remiss to not quantify frequencies from leukocytes of interest. To do this, we depended on a collaboration with Dr. Deb Fuller's group to carry out immunophenotyping and intracellular cytokine staining assays. Whole blood and cells from lymph nodes, lung, placenta (basal plate, chorionic villous tissues), and the bronchoalveolar lavage were assessed for viability using Acridine Orange/Propidium Iodide (Nexcelom Bioscience LLC) and then stained with a panel of antibodies in Brilliant Stain Buffer (BD Biosciences) for 20 minutes to identify immune cells as previously described[157]. Antibodies used included BD Biosciences: CD3 (SP34-2)-BV650, CD8 (RPA-T8)-BUV395, CD11b (ICRF44)-AP-Cy7, CD11c (SHCL-3)-PE, CD45 (D058-1283)-PE-CF594, CD86 (IT2.2)-PE-Cy5, TCRγδ (B1)-FITC; BioLegend: CD4 (OKT4)-BV605, CD14 (M5E2)-BV785, CD16 (3G8)-Alexa Flour 700, CD20 (2H7)- BV570, HLA-DR (L243)-BV71; Invitrogen: CD123 (6H6)-eFlour 450, LIVE/DEAD Fixable Aqua for 405nm excitation; Beckman Coulter: CD159a (Z199)-PC7; and Miltenyi: CD66 (TET2)-APC. Definitions of immune cells using these surface markers are summarized in Table 2.4. After the assessment of viability, cells were resuspended in 2% FBS in PBS. To identify immune cells in whole blood, blood was stained with all antibodies listed except CD11c and CD123, permeabilized with FACS Lysing Solution (BD Biosciences), stained with CD11c and CD123, and then fixed in 1% paraformaldehyde. All samples were acquired on a Symphony A3 (BD Biosciences) using FACS Diva 8 (BD Biosciences). Samples were analyzed using FlowJo 10.9.0 (FlowJo, LLC). All events were first gated on FSC singlets, CD45+ leukocytes, live, and then FSC-A and SSC-A profiles. Populations were excluded from analysis if they did not meet the minimum threshold of >100 cells in their parent gate.

Total RNA-Seq Library Preparation and Analysis

Placental total RNA sequencing was done to generate a high-definition snapshot of the immune pathways relevant in organs of interest. We used 100ng of RNA with RIN>3 as input for RNA library prep using KAPA RNA HyperPrep kit with RiboErase HMR (Roche, #08098131702). The kit was designed for human, mouse and rat samples, but also effectively reduces ribosomal RNA in NHP RNA isolates. Libraries were prepared following the manufacturer standard protocol. Library quantity and quality was evaluated using Qubit and Tapestation. Constructed libraries were sequenced on NovaSeq 6000 platform (Illumina, #20012850), producing 2x100nt stranded paired end reads.

Raw sequences were aligned to the *Macaca nemestrina* reference genome from Ensembl (Mnem_1.0, INSDC Assembly GCA_000956065.1) utilizing STAR in Partek, a bioinformatics software suite (Partek, Inc.). Ensembl gene symbol conversions were employed for consistency across all gene ID's. Given a quality score greater than 35 across all samples, no bases were trimmed, and 100% of sequencing bases overlapped with read lengths of the reference genome. The raw count matrix was downloaded from Partek and subsequent statistical processing and analysis of bulk RNA-sequencing count data was done with the R statistical computing environment (R version 4.4.0). Gene counts were filtered by a row mean of 10 or greater, then normalized using edgeR to implement TMM normalization. Counts were transformed into log2 counts using voom to create a normalized count matrix.[158,159] Differential Expression (DE) analysis compared samples from infected animals against controls from uninfected animals. Comparisons were based on a linear model fit for each gene using Limma. Criteria for all DE analyses were an absolute fold change of 2 and a p-value < 0.05. Gene Set Enrichment Analysis was conducted across the comparison group using fgsea with the Broad Institute Molecular Signatures databases[160].

Nanostring nCounter

To quantify gene transcripts and verify results from bulk RNA sequencing, we required a multiplex transcriptomic method which was exactly what the nCounter platform provides. In addition, the assay we used was formulated for macaque RNA samples. Total RNA samples from adult lung tissue were analyzed using Nanostring nCounter NHP Immunology V2 gene expression codeset (Nanostring, #11500276). RNA hybridization reactions were done according to manufacturer's protocol. Probe-target RNA complexes from all reactions were processed and immobilized on nCounter Cartridges using nCounter Prep Station and quantified with nCounter Digital Analyzer (Nanostring, #MAN-C0035-07).

Single-cell RNA Sequencing

Single cell reads were aligned to the Macaca nemestrina version 1.0.11 genome with CellRanger version 7.2.0. Counts were combined into one count matrix using the CellRanger aggr command. Using Seurat version 5.0 we filtered out cells from the analysis that had less than 200 or greater than 6,500 genes detected and a mitochondrial DNA percentage greater than 2.5%. We used Seurat to normalize (SCTransform) and perform dimensionality reduction (UMAPs). scDEED was then used to identify and correct dubious cluster assignments. Clusters of interest were identified via UMAP and FindMarkers() from Seurat was used to identify DE genes.

Statistical analysis

All statistical analyses were performed in Rstudio (using R version 4.4.0) or nSolver (nCounter data only, recommended by Nanostring), both of which use R programming language. A p-value of <0.05 was considered significant and $0.05<p<0.1$ was considered noteworthy. Comparisons between two groups were done with Wilcoxon rank-sum test; comparisons involving three or more groups used the Kruskal-Wallis test. Spearman's rank correlation coefficient used for direct correlation calculations between two variables. Data visualizations were done with ggplot2, ggpmisc, and ComplexHeatmaps packages and their derivatives.[161,162]

Chapter III: IMPACT OF INFLUENZA A VIRUS INFECTION ON THE LUNG

Aim 1: Determine pregnancy-specific differences in the early pulmonary immune response to pandemic IAV infection.

- *Hypothesis 1A: Pregnant macaques will have greater disease severity than non-pregnant females at 5 days post-infection.*
- *Hypothesis 1B: Pregnant macaques will display lower Th17 and higher Treg frequencies in their lungs relative to non-pregnant females.*
- *Hypothesis 1C: Pregnant macaques will have lower expression of interferon-stimulated genes in their lungs relative to non-pregnant females.*
- *Hypothesis 1D: Pregnant macaques' macrophage populations are higher in animals with a higher lung viral load.*

Introduction

Influenza A viruses (IAV), which include the 2009 H1N1 pandemic virus and the emerging H5N1 highly pathogenic avian influenza virus, constitute a perennial threat to global health. IAV is a leading cause of annual death and morbidity in the U.S.A. for older adults, children, and pregnant women. Pregnant women are particularly susceptible to severe complications including maternal death, stillbirth, hospitalization, admission to the intensive care unit and preterm birth.[26,28-30,33,34,163] This problem is exacerbated during influenza pandemics, in which pregnant women have had higher risk of mortality, preterm birth, and stillbirth. For example, during the 2009 H1N1 IAV pandemic in the U.S.A., pregnant women were only 1% of the population yet accounted for 5% of pandemic-related deaths.[164,165] However, the immune correlates of this greater risk are still unknown.

In Chapter 1, we provided an overview of some of the changes to the maternal immune system that promote a tolerogenic immune environment for the fetus and may explain the greater

vulnerability in pregnant women. The hormones that drive these immunological changes also drive physiological changes in the pregnant woman to support the needs of the growing fetus.[22] Of particular interest are the changes to the cardiopulmonary system, which includes the added stress to take in and distribute greater levels of oxygen and blood throughout the pregnant body.[166,167] The physiologic changes that occur during human pregnancy include an increase in minute ventilation and oxygen uptake, to compensate for greater oxygen requirements as pregnancy progresses.[168] As the fetus grows, the diaphragm is elevated which reduces the functional residual capacity and residual lung volume.[169] Immunologically, Th1/Th17 cell-mediated immunity is downregulated by progesterone and estrogen, the sex hormones that most strongly influence pregnancy, to avoid strong inflammatory responses that could cause systemic tissue damage that could negatively impact the placenta and fetus.[99] Immune tolerance of the paternal alloantigens of the fetus is supported by the hormone-mediated upregulation of Th2 and immunoregulatory (Treg) immune responses.[22] Current work in the influenza field points towards an exacerbated inflammatory response as a major driving factor in severe disease risk in pregnant IAV-infected women.[170] However, the Type I IFN response seems to be suppressed in the lungs of pregnant mice infected with IAV while other markers of inflammation are elevated.[171] As the immunological correlates with influenza disease severity in pregnant women have not been decisively determined, our project interrogated possible differences between the immune responses to IAV infection in pregnant and non-pregnant female primates using a highly translational pigtail macaque (*Macaca nemestrina*) model of infection.

Results

Pulmonary physiology testing results and correlations

Pregnant and non-pregnant macaques were inoculated with H1N1pdm A/California/07/2009 at $10^{7.4}$ pfu as described in Chapter 2. Other than 1 non-pregnant subject (FLU 29) which developed

such severe symptoms that the veterinary staff believed it appropriate to euthanize at 3 days post-infection (dpi), all other subjects were euthanized at 5 days post-infection for tissue collection. Endpoint age and endpoint weight were not significantly different between pregnant and non-pregnant macaques (Fig 3.1A, 1B). Baseline adult weights were also not significantly different between the two infected groups. However, the change in weight was significantly different ($p<0.05$) in infected pregnant relative to non-pregnant animals and shows that the non-pregnant females generally lost a greater percentage of their initial weight than pregnant females (Fig 3.1C).

Figure 3.1. Physiological Variables of Infected Macaques

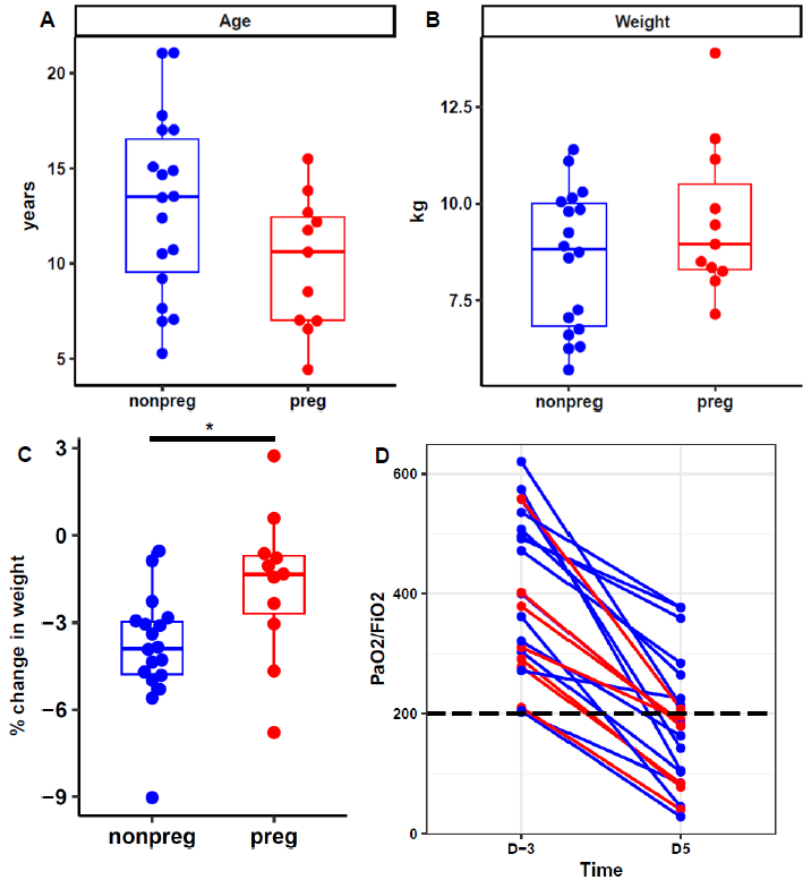

Endpoint adult age (A), weight (B), and percent change in weight (C) are represented between non-pregnant (blue) and pregnant (red) macaques. Pulmonary physiology metric of oxygenation, PaO_2/FiO_2 (D) is plotted between baseline (3 days pre-infection) and endpoint (5 days post-infection) with same color scheme. Dotted line at PaO_2/FiO_2 =200 to mark cutoff for hypoxemia.

We developed a clinical scoring system to score animal responsiveness, nasal discharge, skin condition, respiratory symptoms, food consumption, and fecal consistency. Clinical scores for the first 5 subjects demonstrated no significant change in scores from date of infection (0 dpi) through 5 dpi, which we attributed to macaque behavior to hide signs of disease that could make them vulnerable in the wild. Therefore, we implemented a pulmonary physiology

test at baseline (defined as a 3 to 7 days pre-infection) and endpoint (date of euthanasia), that would allow us to assess oxygenation, an important marker of lung health. The ratio of partial pressure of arterial oxygen (PaO_2) and fractional inspired oxygen (FiO_2) is frequently used to evaluate hypoxemia and is referred to as the PaO_2/FiO_2 (P/F) ratio (Fig 3.1D). Importantly, the PaO_2/FiO_2 ratio was the only measure from the pulmonary physiology testing battery where the relationship between endpoint and baseline values was consistent across all animals (i.e., uniform decrease at endpoint). The uninfected pregnant NHP experiments were performed before the pulmonary physiology testing protocol was ready for use, and so this data is lacking in a control group. Therefore, the pulmonary physiology test gives a more detailed picture of the general degradation in the pulmonary health of the NHP subjects in the pregnant versus non-pregnant animals when compared to the cage-side assessment scoring method.

Table 3.1. Correlations across Physiological Variables

	PaO2/FiO2 (endpoint)	PaO2/FiO2 (baseline)	Endpoint Age	Endpoint Weight
PaO2/FiO2 (endpoint)		0.59*	-0.39	-0.42*
PaO2/FiO2 (baseline)	0.59*		-0.12	0.46*
Endpoint Age	-0.39	-0.12		0.39*
Endpoint Weight	-0.42*	-0.46*	0.39*	

Spearman correlation coefficients were calculated between PaO2/FiO2 at baseline and endpoint, and endpoint adult age & weight. Coefficients with a (*) are significant ($p<0.05$).

The slope of the decrease in PaO_2/FiO_2 was fairly consistent across all animals, regardless of pregnancy status, with notable exceptions in some non-pregnant animals. Next, we asked if this value was influenced by age and weight. In respiratory infections, age and weight have been associated with disease severity in humans. Therefore, we calculated spearman correlation coefficients between age, weight, and PaO_2/FiO_2 at baseline and endpoint using values from all infected animals (Table 3.1). We found that PaO_2/FiO_2 at endpoint was significantly correlated with baseline PaO_2/FiO_2 (ρ=0.59) and endpoint weight (ρ=-0.42; $p<0.05$). This is important because the baseline PaO_2/FiO_2 ratio was lower in the pregnant animals for physiological reasons, but this may be a key factor in their clinical picture of ‘enhanced disease’

during IAV disease. The association between endpoint weight and endpoint PaO_2/FiO_2 is in line with previous work correlating higher body weight individuals with greater risk of hospitalization from respiratory infections and worse oxygenation.[172,173] These results suggest baseline PaO_2/FiO_2 and endpoint weight as viable predictors of endpoint PaO_2/FiO_2 in both pregnant and non-pregnant macaques.

Figure 3.2. RNA Viral Load in the Pulmonary System

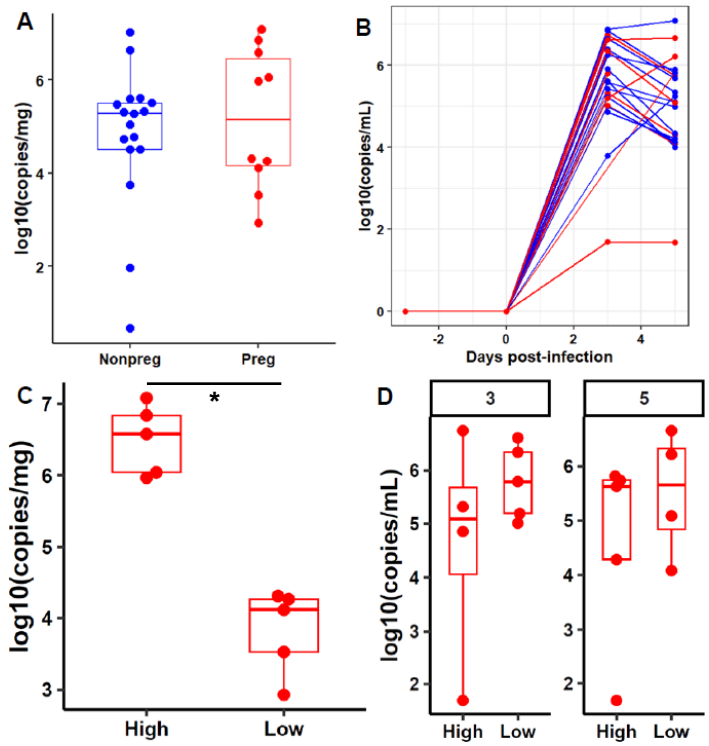

A H1-targeted qPCR assay was used to discern viral RNA concentrations in samples from adult lung (A) and BAL (B). Pregnant are in red and non-pregnant in blue. The viral RNA levels in pregnant macaques are represented between high and low bimodal distributions in the lung (C). The same animals in each group are used to plot RNA viral loads in the BAL at 3 and 5 dpi (D). Note we were not able to recover BAL samples from every animal at every timepoint.

Viral load in adult lungs and BAL

It was important to confirm evidence of viral infection, so we used reverse transcription quantitative PCR (RT-qPCR) to do so. We were interested in comparing the viral load between pregnant and non-pregnant infected groups to determine if either group had a higher infection burden. Bronchoalveolar lavage (BAL) samples were taken at baseline, 0, 3, and 5 dpi as described in Chapter 2. Lung tissue was excised from the organ at 5 dpi and preserved in RNALater solution for freezing. We performed RNA extraction from lung tissue and BAL; we performed molecular biology analyses to confirm RNA integrity and purity. cDNA was synthesized from these RNA samples for qPCR with the HKU primer-probe set.[174] We found that the viral RNA load in the lungs and BAL at the post-infection time points were not significantly different between non-pregnant and pregnant NHPs; however, there was a

notable bi-modal distribution of viral load in the lungs with a greater proportion of pregnant NHPs having a high IAV viral load (Fig 3.2A, B). Post-infection viral loads in the BAL and adult lungs did not correlate significantly with PaO_2/FiO_2 at endpoint, suggesting that viral burden does not affect the degradation in oxygenation in our model; however, this association may be confounded by physiologic compromise of lung function that is greater in the pregnant NHP group.

The bi-modal distribution of IAV RNA viral load in the infected pregnant dam lungs segregated into a high (~10^6 copies/mg) and low (~10^4 copies/mg) group (Fig 3.2C). A similar stratification was not observed in the viral loads in the BAL of either experimental group (Fig 3.2D); this may reflect the inability to recover BAL samples in some animals or the dilute nature of the BAL. Therefore, some of our further analysis in this chapter will focus on the lung viral loads of the pregnant adults to better understand the influence of the bimodal distribution we observed on scRNA-seq data and placental transcriptomics (Chapter 4).

Bulk mRNA sequencing analysis of adult lungs

We sought to use transcriptional analyses of the lungs to determine differences in gene expression and pathway upregulation between pregnant and non-pregnant macaques. Using mRNA samples from the lungs of infected and uninfected macaques, we generated RNA sequencing data for normalization. Principal component analysis (PCA) of the raw count matrices demonstrated there was a general separation between infected and uninfected tissues. PCA is useful for visualizing how different samples are from each other. However, there was a range in how different the transcriptomes of the infected pregnant and non-pregnant samples were from uninfected samples (Fig 3.3A). There was no clear separation between the PCA plot for uninfected pregnant and non-pregnant lung tissues; therefore, we combined these samples into a single uninfected control group.

Figure 3.3 Differential Gene Expression in the Adult Lung from RNAseq

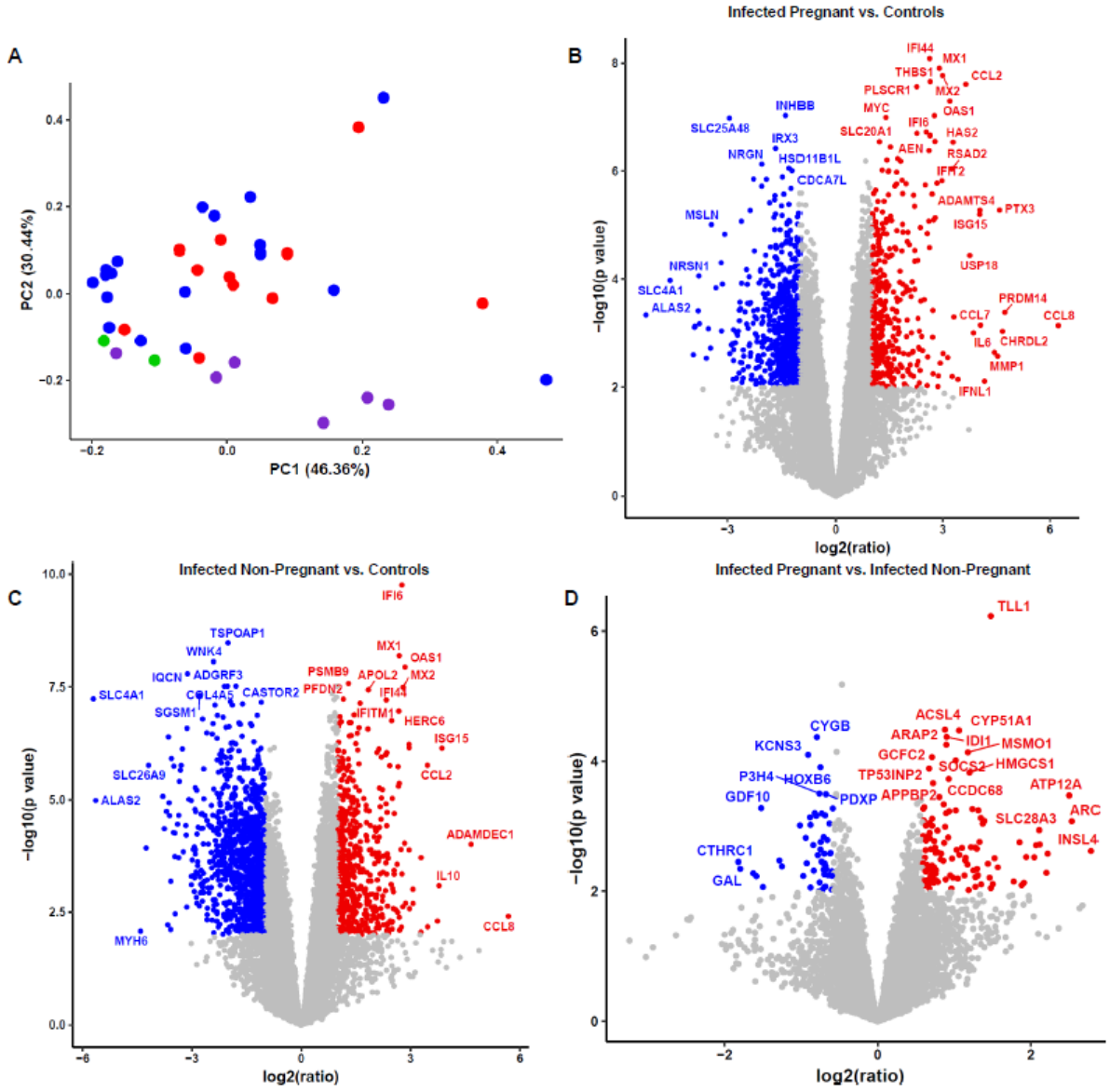

Adult lung RNA from uninfected controls and infected pregnant and non-pregnant subjects was used for bulk mRNA sequencing. Raw count matrices are represented per subject in a principal component analysis plot (A); blue is non-pregnant infected, red is pregnant infected, green is non-pregnant uninfected, and purple is pregnant uninfected. Volcano plots of infected non-pregnant group versus controls (B), infected pregnant versus controls (C), and infected pregnant versus non-pregnant (D) for comparison of differentially expressed genes. Ratio cutoff is 1.5/0.5 and significance cutoff is $p<0.01$; red is upregulated and blue is downregulated in these plots.

Analysis of the differentially expressed genes (DEG) in the lungs suggests a high degree of similarity in the transcriptional response between pregnant and non-pregnant infected macaques. Based on the PCA plot, we expected that the DEGs that emerge from comparing infected groups

to the uninfected group might be similar. DEGs were defined as genes that were expressed 50% greater or less in one group over the other and that the difference in expression was significant ($p<0.01$). Since all the animals showed a degradation in their pulmonary health, we also expected upregulation of genes related to a robust antiviral and inflammatory response. When compared to the transcriptomes of the control group, the infected pregnant and non-pregnant lungs demonstrated significant upregulation of some of the same interferon stimulated genes (ISGs), i.e. *MX1, IFI6, OAS1* (Fig 3.3B, 3C). In addition, when comparing the pregnant and non-pregnant to each other, the differentially expressed genes are not notable members of the innate antiviral immune response (Fig 3.3D). Taking the DEG analysis further, we carried out gene set enrichment analysis (GSEA) with the Gene Ontology: Biological Pathways gene sets. This further confirmed that in the lungs of infected macaques, regardless had similar level (NES>2) of enrichment for pathways related to the response of virus, negative regulation of viral genome

replication, and negative regulation of viral process, to name a few (Fig 3.4A, 4B). Due to the strong similarities in their lung transcriptomes, we found that at 5 dpi, pregnancy status does not lead to aberrations in regulation of genes of the antiviral innate immune response. This further suggests that it would be worthwhile to test which genes are associated with the lung disease severity metric (PaO2/FiO2) at 5 dpi, regardless of pregnancy status.

Next, we explored which gene sets were up or down regulated in infected pregnant macaques relative to non-pregnant. We found that the pathways that were significantly enriched in the lungs of infected pregnant over non-pregnant macaques were those related to lipid biosynthesis while lungs of non-pregnant macaques had higher enrichment of cellular respiration gene sets (Fig

Figure 3.4. Gene Set Enrichment and Overrepresentation Analyses

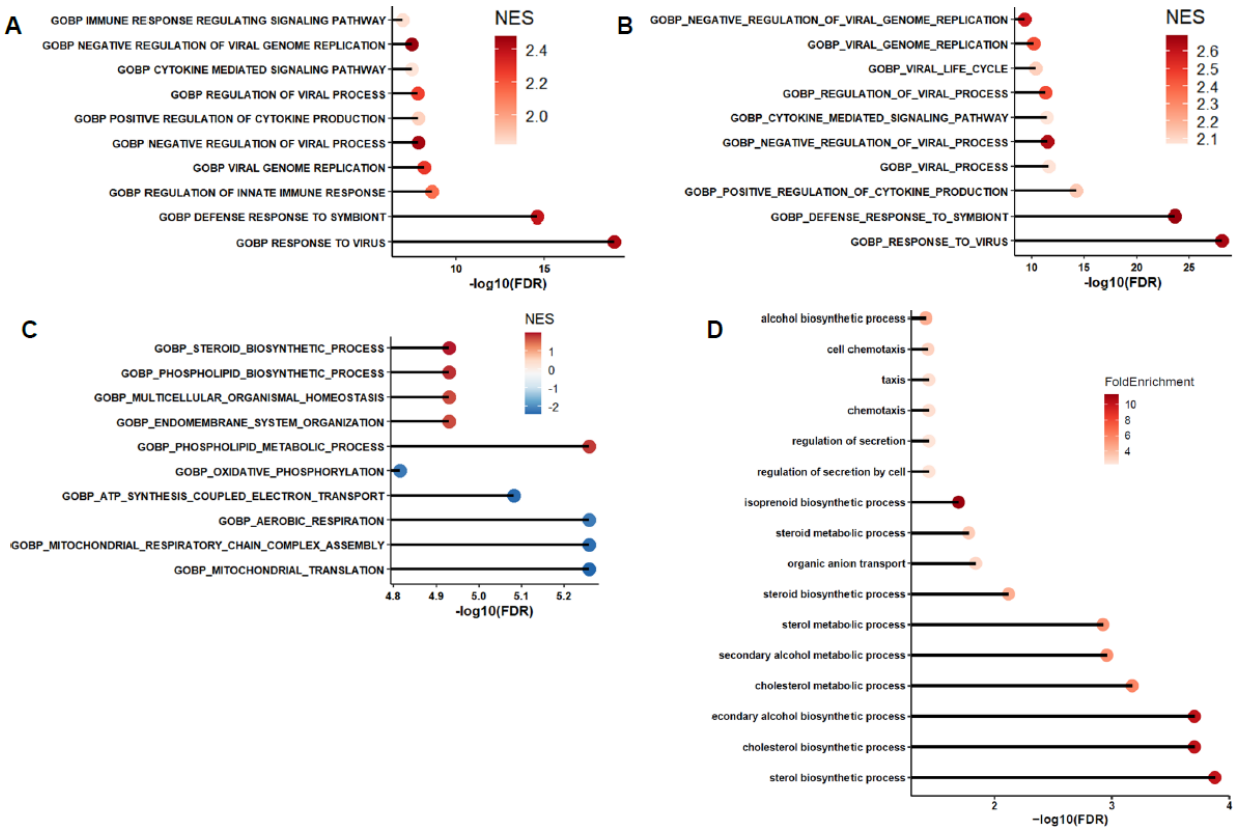

The list of DEGs and associated significance values were used to generate normalized enrichment scores (NES) of comparisons between infected pregnant versus controls (A), infected non-pregnant versus controls (B), and infected pregnant versus non-pregnant (C). ORA generated enrichment scores to validate pregnant versus non-pregnant infected (D).

3.4C). We decided not to compare uninfected pregnant to non-pregnant since we expected them to be too similar as observed in the PCA plot and there were only two uninfected non-pregnant animals in our study so any comparison would have been underpowered. Using overrepresentation analysis (ORA) to validate these results between the pregnancy status

Figure 3.5. Differential Gene Expression in the Lungs from nCounter Data

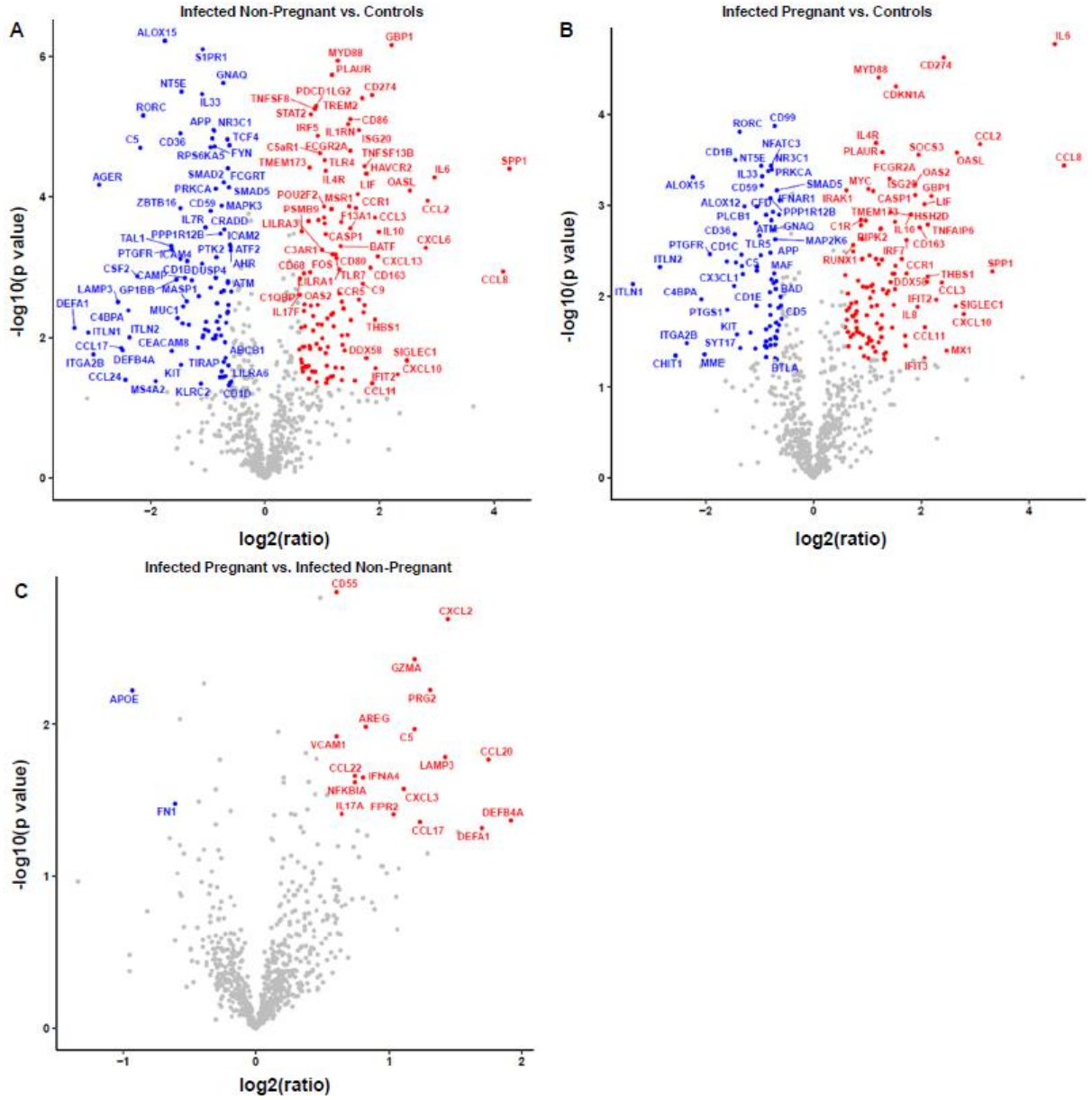

Figure 3.6. Average Cytokine Concentrations in the Lungs

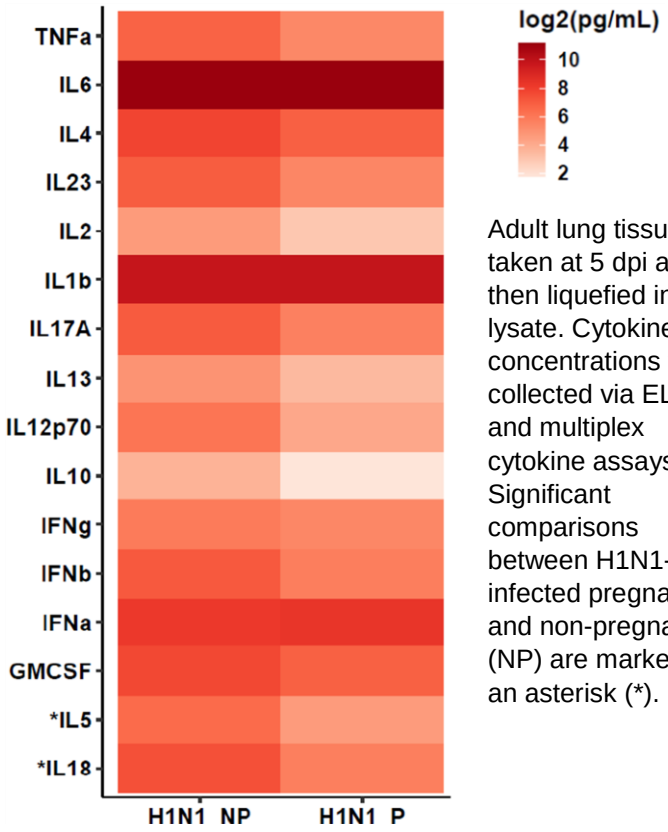

Adult lung tissue was taken at 5 dpi and then liquefied into lysate. Cytokine concentrations were collected via ELISA and multiplex cytokine assays. Significant comparisons between H1N1-infected pregnant (P) and non-pregnant (NP) are marked with an asterisk (*).

groups, we found that the lungs of the pregnant macaques were most significantly enriched for gene sets related to lipid biosynthesis (Fig 3.4D). Our bulk transcriptomics approach indicated strong similarities in the upregulation of the antiviral innate immune response, but significant differences in the regulation of lipid metabolic pathways between pregnant and non-pregnant macaques' lungs.

To validate our RNA sequencing and provide a useful dataset for correlations, we also utilized the Nanostring nCounter platform to generate insights into the immune transcriptome in the lungs of infected macaques. The nCounter platform is an alternative bulk transcriptomics approach that allowed us to collect direct counts of RNA transcripts of immune related genes. nCounter does not require amplification of the genetic material like RNA sequencing does and the technology is more sensitive to detection of low-expression genes. nCounter was also ideal at this stage because we only planned to focus on quantifying immune-related genes and Nanostring offered a panel targeting NHP genes specifically. Regardless, we also expected that we would observe the same similarity in the upregulation of antiviral genes in the infected pregnant and non-pregnant groups. DEG analysis between the infected non-pregnant and pregnant lungs and the controls demonstrated upregulation of genes related to antiviral immune response signaling (i.e. *MYD88, OASL, DDX58,*

IL6) in both infected groups' lungs (Fig 5A, 5B). Evaluating the DEGs in a comparison of infected lungs between pregnant and non-pregnant macaques shows only 20 genes and without the presence of many of the same actors of the antiviral signaling pathways for ISG expression (Fig 5C). Using a list of the DEGs from all our comparisons, we determined which genes yielded significant correlation coefficients with endpoint PaO_2/FiO_2 to generate a list of candidate predictor genes for linear regression modeling (Table 3.2). The DEG analysis results recapitulate what we observed in the RNA sequencing data and allowed us to proceed with our plan of using the gene count data to correlate with the PaO_2/FiO_2 data.

Cytokine concentrations in the adult lung

Comparing cytokine levels between infected groups would also allow us to determine if the differences in immune response variables we initially expected to find might appear post-translationally. We generated lysate from adult lung tissue and quantified cytokine levels via multiplex immunoassays and ELISAs. Cytokine concentrations in the adult lungs were higher on average in the non-pregnant group, but only IL-5 and IL-18 concentrations were significantly higher (Fig 3.6). The lack of significant differences in the Type I IFNs, IL-6, IL-1β and TNFα is largely in line with our findings in the lung transcriptome that the infected groups showed similar upregulation of antiviral and pro-inflammatory pathways. The outlier to this expected result is IL-18, a major product of the NLRP3 inflammasome pathway described in Chapter 1. This suggests that the mechanics of active IL-18 production and secretion in pregnant NHP lungs may merit further exploration. IL-5, a cytokine more closely associated with Type 2 immune responses, at lower levels in the pregnant NHPs may be a sign that the predominance of Type 2 immunity during pregnancy may be subverted during IAV infection. When accounting for all infected NHPs in our study, correlation analysis found that these cytokines were not significantly associated with PaO_2/FiO_2 and instead IL-23, IL-12p70 and IL-2 concentrations correlated significantly (Table 3.2). Previous work has associated IAV infection with reduced levels of these cytokines leading

to vulnerabilities to secondary bacterial infection.[175] Therefore, we plan to test these cytokines as potential predictors of disease severity in female macaques.

Figure 3.7. Th17 and Regulatory T cell Frequencies in Lungs

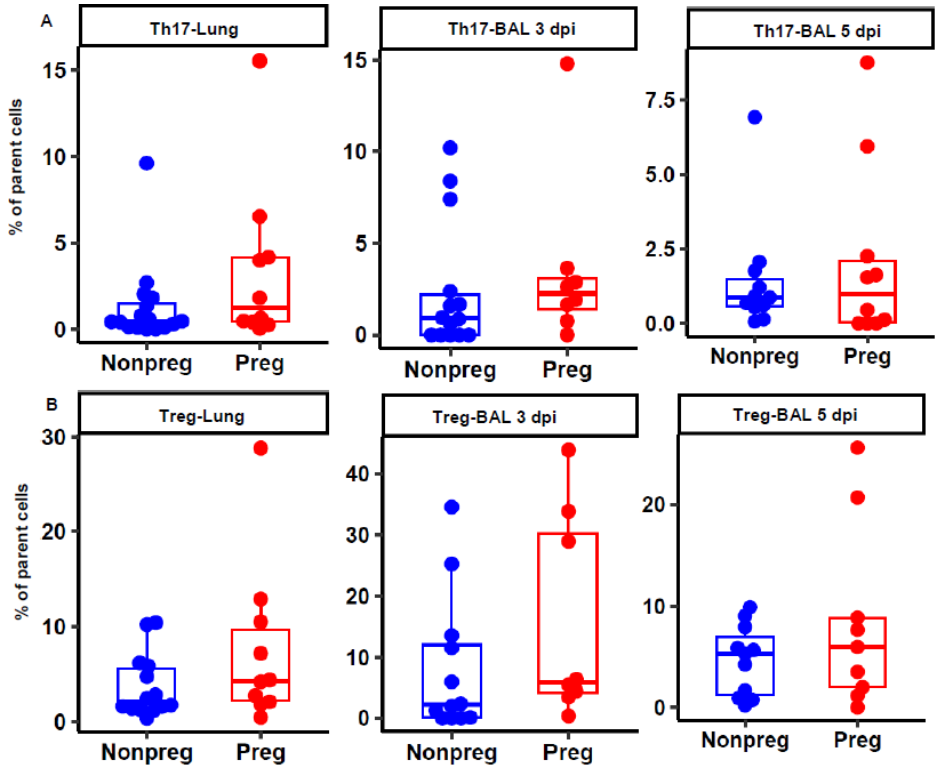

Intracellular cytokine staining assay was done on leukocytes dissociated from adult lung for quantification of (A) Th17 (CD3+CD4+IL-17+IL-22+) and (B) Treg (CD3+CD4+CD25+FOXP3+) frequencies.

Th17 and Regulatory T cell (Treg) Frequencies in the Adult Lungs

As explained in Chapter 1, Th17s and Tregs occupy important niches in the immunological response to IAV and pregnancy. Therefore, we were interested in verifying if Th17 frequencies were lower in infected pregnant NHP lungs while Tregs are higher in pregnant NHP lungs, in line with our hypothesis. To test this hypothesis, we quantified Th17 and Tregs in adult lung and BAL samples using intracellular cytokine staining (ICS) (see Chapter 2). Th17 and Treg frequencies were not significantly different between infected pregnant and non-pregnant infected macaques in either BAL or adult lung (Fig 3.7). This result was unexpected and counters our hypothesis, illustrating that at 5 dpi in the pulmonary system pregnant NHPs are not experiencing a muted Th17 response during IAV infection when compared to infected non-pregnant females. Since the control experiments were done before this study, we are unable to

Table 3.2. Immunological Variables Significantly Correlated with PaO_2/FiO_2 at 5 DPI

Variable	ρ coefficient	P-value
ICAM4 expression	0.52	0.014
ITLN2 expression	0.46	0.032
CX3CL1 expression	0.48	0.025
FCER1G expression	-0.52	0.014
IL1RL1 expression	-0.48	0.024
SIGLEC1 expression	-0.49	0.022
SYT17 expression	0.48	0.023
TLR9 expression	0.47	0.026
TNFSF8 expression	-0.48	0.023
IL-23 concentration	-0.45	0.04
IL-12p70 concentration	-0.67	0.001
IL-2 concentration	-0.45	0.04
Th17 freq. in lung	-0.45	0.029

Summary of Spearman correlation coefficients (ρ) and associated p-value.

present data on the frequencies of Th17 and Tregs in uninfected lungs. A future study could use the antibody panel for ICS of this study to compare the basal Th17 and Treg frequencies of the pregnant uninfected lung. Interestingly, we found that Th17 frequencies in the adult lungs, across all infected animals, were significantly and negatively correlated with endpoint PaO_2/FiO_2 (Table 3.2). The finding of a negative correlation between the frequency of lung Th17 cells and endpoint PaO2/FiO2 could represent a marker for IAV disease severity.[176]

Multi-variable Models of IAV-induced hypoxemia

Table 3.3. Summary of Linear Regression Models for PaO_2/FiO_2 at 5 DPI

Variable	Residual standard error	F-statistic p-value	R^2 (multiple/adjusted)
PaO_2/FiO_2 baseline	86.41	0.002	0.363/0.332
Adult weight	91.05	0.011	0.255/0.221
ICAM4 expression	98.16	0.053	0.174/0.132
ITLN2 expression	104.8	0.273	0.059/0.012
CXCL3 expression	102.8	0.164	0.094/0.048
FCER1G expression	96.6	0.036	0.200/0.160
IL1RL1 expression	89.86	0.007	0.308/0.273
SIGLEC1 expression	102.6	0.158	0.097/0.051
SYT17 expression	99.38	0.071	0.153/0.111
TLR9 expression	96.66	0.037	0.199/0.159
TNFSF8 expression	96.45	0.035	0.202/0.163
Th17 freq. in lung	97.66	0.068	0.143/0.104
IL-23 concentration	97.24	0.104	0.147/0.097
IL-12p70 concentration	93.93	0.080	0.160/0.113
IL-2 concentration	94.59	0.093	0.148/0.101

Summary of linear regression model metrics: residual standard error (standard deviation of the residuals), F-statistic p-value (p-value for the whole model), and R-squared values (measure of how much variance is explained by the model).

We observed that most of the immunological variables that we tested, antiviral genes, cytokines, and immune cells, were not significantly different between infected pregnant and non-pregnant NHPs. Therefore, we were interested in testing a new idea: could these variables be consistent biomarkers for predicting disease severity, regardless of pregnancy status? To test our variables, we decided to use linear regression modeling. Linear regression models are the next step after finding a correlation since significant correlations by themselves only demonstrate the presence of a relationship between the two tested variables. On the other hand, a variable that yields a significant linear regression model for an outcome variable can be considered a valid predictor variable. In addition, using all our subjects for linear regression modeling would enhance the power of our calculations. Since we did not have data for all these variables for all the uninfected animals, we had to exclude them from this analysis. Table 3.2

contains the list of immunological variables that demonstrated a significant relationship to PaO_2/FiO_2 at 5 dpi via Spearman correlation and using the pooled observations from all infected macaques, regardless of pregnancy status. We then calculated linear regression models for the endpoint PaO_2/FiO_2 outcome using these variables, baseline PaO_2/FiO_2, and adult weight (Table 3.3). Considering that PaO_2/FiO_2 at baseline was the linear regression model with the highest R^2 and lowest p-value over the other predictor candidates, we attempted to improve the predictive potential of the model by combining it with the other predictor variables into a multiple linear regression model (Table 3.4). If we could find an improved model, it would be more robust in explaining the variance in our dataset by integrating different independent variables. ANOVA comparison tests determined that combining *TLR9* counts with baseline PaO_2/FiO_2 generated the only significant improvement over using only baseline PaO_2/FiO_2. Despite this last result, it is still noteworthy that all these variables independently generated significant linear regression models that could predict endpoint PaO_2/FiO_2. This opens up opportunities to study potential mechanisms by which each of these variables influence IAV disease progression in both pregnant and non-pregnant females.

Table 4. Multivariate Linear Regression Models for PaO_2/FiO_2 at 5 DPI

Variable	Residual standard error	F-statistic p-value	R^2 (multiple/adjusted)
IL1RL1 + PF Baseline	85.58	0.006	0.447/0.379
TLR9 + PF Baseline	68.88	0.0001	0.532/0.391
FCER1G + PF Baseline	87.92	0.017	0.413/0.344
TNFSF8 + PF Baseline	91.64	0.021	0.363/0.288
Weight + PF Baseline	83.47	0.004	0.436/0.376
PaO_2/FiO_2 baseline	**86.41**	**0.002**	**0.363/0.332**

Summary of multivariate linear regression models built off results in Table 2. Models highlighted in green are a significant improvement, based on ANOVA testing, over univariate model using PaO_2/FiO_2 (PF) at baseline.

Single Cell RNA sequencing analysis of adult lungs

Considering the bi-modal distribution in the viral load of the pregnant animals, we investigated whether infected cell populations differed between pregnant and non-pregnant animals. We dissociated lung tissue at the endpoint into single-cell suspensions and then processed them through the single-cell RNA sequencing (scRNA-seq) pipeline described in Chapter 2. We then attempted to build an atlas of clusters identified through our bioinformatics approaches (Fig 3.8A). We also quantified the average percentage of cells in infected pregnant and non-pregnant NHPs positive for viral RNA (*PB2* gene). Of the cell types in our IAV-infected single-cell lung atlas, we found that monocyte-derived alveolar macrophages (MDAM) had the highest difference between infected pregnant and non-pregnant groups, with pregnant NHPs generally having a higher percentage of their MDAMs infected with IAV (Fig 3.8B). We then used significance tests to assess which clusters were significantly different between the two groups. The frequency of several populations of MDAMs was significantly different between the infected pregnant and non-

Figure 3.8. Single Cell RNA Sequencing Analysis of Adult Lungs

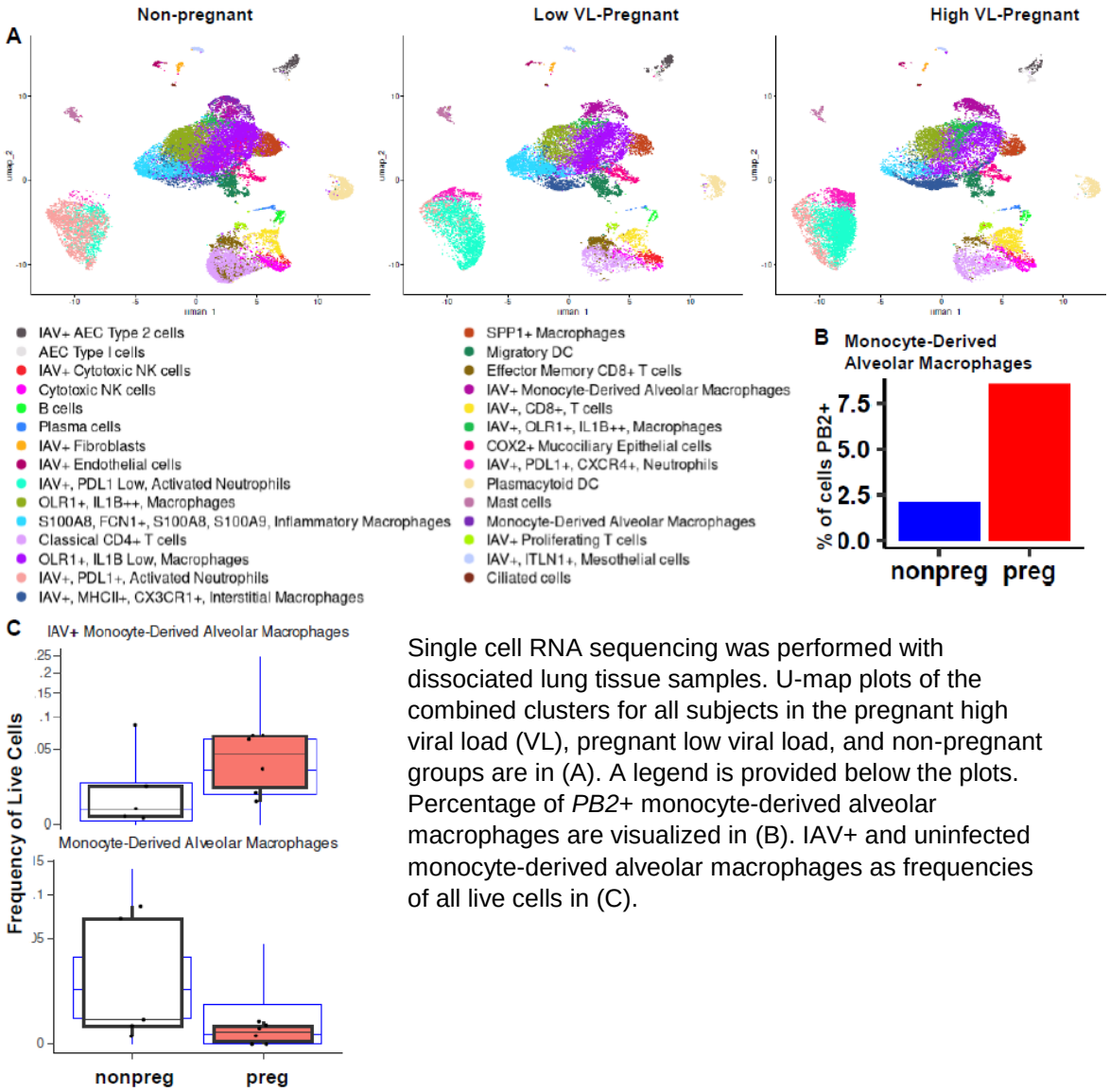

Single cell RNA sequencing was performed with dissociated lung tissue samples. U-map plots of the combined clusters for all subjects in the pregnant high viral load (VL), pregnant low viral load, and non-pregnant groups are in (A). A legend is provided below the plots. Percentage of *PB2*+ monocyte-derived alveolar macrophages are visualized in (B). IAV+ and uninfected monocyte-derived alveolar macrophages as frequencies of all live cells in (C).

pregnant groups (Fig 3.8C). The frequency of IAV+ MDAMs was significantly higher in infected pregnant NHPs; the uninfected MDAM population was also significantly lower in infected pregnant versus non-pregnant NHPs (both $p<0.05$). Our scRNA-seq analysis is still in progress as we incorporate data from the final animals in this study. We anticipate that adding these animals will strengthen our current findings that MDAMs are more permissive to IAV infection in pregnant NHPs relative to non-pregnant NHPs. Once those subjects are added to our scRNA-seq dataset, we will also go deeper into our analysis of which single cell populations are found in significantly

different frequencies in pregnant females with a focus on infected and uninfected monocyte and macrophage cells.

Discussion

The lung is the target organ of IAV and represents a primary organ of interest in determining differences between the pathogenesis of disease in pregnant and non-pregnant NHPs. We hypothesized initially that we would observe significant differences in disease severity and innate immunity biomarkers between pregnant and non-pregnant animals. We also hypothesized that these differences would be most pronounced in the Th17/Treg populations based on initial observations. Ultimately, we found no significant differences in the disease severity or immune response between pregnant and non-pregnant macaques at 5 dpi; however, we found that the proportion of infected and uninfected MDAMs in the lung were significantly different by pregnancy status. This suggests that there may be a fundamental difference in cellular permissivity to IAV during pregnancy, which may contribute to enhanced disease.

The finding that infected monocyte-derived alveolar macrophages were significantly higher in pregnant versus non-pregnant NHPs may be a key factor in the propensity of pregnant macaques to develop greater IAV-associated lung disease. To better understand this dynamic it will be necessary to study the mechanisms unique to the pregnant primate's lungs that would improve permissiveness to IAV infection. MDAMs are known to be permissive to IAV infection, but a greater viral burden in pregnant animals may result in an impaired pulmonary innate immune response.[195] Studies have further shown that influenza-experienced MDAMs can better help protect against secondary bacterial infections and coordinate epithelial tissue repair.[196,197] In contrast, other studies have found that in the context of IAV infections during pregnancy, MDAMs experience a shift to an anti-inflammatory phenotype, prolonging IAV disease and potentially contributing to offspring vulnerability to early-life infections.[186,198] As we continue our analysis of

alveolar macrophages with the scRNAseq data, we will plan to better characterize any potential dysregulation differences based on viral load differences in the pregnant NHP lungs.

Influenza researchers are aware of the risk of higher mortality and morbidity for pregnant women, especially in the third trimester, after pandemic IAV infection when compared to non-pregnant women. Early in the 2009 H1N1 pandemic, CDC researchers were able to detect that pregnant women were being hospitalized at higher rates for severe IAV infection than the general population.[30] In line with those observations, we decided to use pregnant pigtail macaques at the third trimester gestational period for their species. Interestingly, we did not find a significantly more severe disease phenotype in pregnant versus non-pregnant macaques at 5 dpi. In humans infected with pandemic IAV, illness can last a median of 7-11 days before death.[180,181] Pregnant women infected with pandemic IAV have been found to be at greatest risk of mortality >4 days from symptom onset, even with treatment.[33] These studies suggest that, even with our high viral dose model, it would be advisable to test an endpoint after 5 days post-infection and up to 11 days post-infection to more accurately recapitulate a fatal IAV disease time course.

We found no significant difference in hypoxemia as a function of the animal's weight, which was surprising since we were expecting that the pregnant animals might weigh more since they carried a third-trimester fetus. However, we found that adult weight significantly correlated with age and baseline/endpoint PaO_2/FiO_2. In humans, and likely in NHPs, adult weight increases with age and the non-pregnant females were generally older than the pregnant females. In addition, weight by itself was a significant predictor in a linear regression model for clinical disease severity at endpoint, regardless of pregnancy status. Therefore, adult age must be better controlled to account for its strong influence on adult weight in our model. In humans, clinical evidence suggests that higher body weight is a risk factor for severe IAV disease during the 2009 H1N1 [illegible] These studies support our conclusion that weight likely diminished differences that could have arisen between pregnancy status groups in terms of disease severity.

The mechanisms behind the differences between the immunologic and disease response between pregnant and non-pregnant people infected with IAV has been explored using mouse models. Specifically, the 2009 H1N1pdm IAV has been found to replicate to higher titers and stimulate the release of higher levels of inflammatory cytokines than seasonal H1N1 in pregnant mice.[27] Pregnant mice demonstrate higher levels of pro-inflammatory cytokines and more intense IAV disease phenotypes than non-pregnant mice.[184,185] In addition, mouse studies have shown that pregnant mice may shift the behavior of innate immune cells such as alveolar macrophages that makes them effective at antiviral functions.[186] However, viral load was not usually significantly different between pregnant and non-pregnant NHPs. An 8-day experiment found no significant differences in measures of pulmonary function such as lung compliance after infection in pregnant mice.[187] However, the non-pregnant infected mice did demonstrate a depreciation in lung compliance, minute ventilation, and oxygen diffusion compared to their baseline values. This suggests that pregnancy may actually have a physiological protective effect against IAV disease severity. However, other studies have demonstrated that pregnant mice generate significantly lower innate immune responses, especially Type I ISG expression, leading to increased mortality to H1N1 infection.[188] In fact, IAV infection caused enough damage systemically to lead to developmental delays in offspring and lower levels of circulating progesterone in dams.[189] In our results, we demonstrated that Type I IFN responses were elevated to a similar degree in the transcriptomes of pregnant and non-pregnant macaque lungs. In addition, pro-inflammatory cytokines and Th17/Treg frequencies were similar in the lungs and BAL of our experimental groups. Our results run counter to the expectation set by previous literature, but this likely stems from species-specific differences (mice vs. macaques) and other nuances of experimental design.[190,191] We believe that the similarity in t immune response is related to the strong antiviral response to a high viral inoculum; future experiments could attempt different endpoints or viral inoculation titers.

Through linear regression analysis, we were able to determine that a model including TLR9 gene expression and baseline PaO2/FiO2 was the best predictor for endpoint PaO2/FiO2 regardless of pregnancy status. This is an interesting finding since TLR9 binds unmethylated CpG DNA and not viral RNA like TLR3, 7/8. However, TLR9 could detect cell-free DNA due to cell death or neutrophil extracellular traps and may be necessary to prevent excessive lung injury.[126,192] A future experiment could verify if the increase in TLR9 expression may not instead prime vulnerability to secondary bacterial infections as has been observed in mice.[193] The aerosolized delivery of TLR9 agonists may be a protective countermeasure to severe IAV disease if administered early in the infection.[194] While the multiple linear regression model we formulated may have been the most significant, further study of the other linear regression model candidates could yield insights into the mechanisms that influence IAV disease progression in female primates.

A strength of our study was the development and use of the pulmonary physiology testing protocol allowed us to assess various metrics of oxygenation, respiration, and compliance and determine a measure of clinically relevant disease severity metric. We have previously published the methodology to allow other researchers to apply pulmonary physiology testing to other macaque models of respiratory disease.[147] Our protocol is minimally invasive, does not require training the NHPs, and nor does it need any specially manufactured equipment. Previous efforts to adapt forced oscillation techniques (FOT) or whole-body plethysmography (WBP) to NHPs can result in useful data but do not assess gas exchange and require specially engineered equipment.[177-179] In comparison, our method requires materials and equipment, specifically a mechanical ventilator, readily available at primate centers with associated medical institutions. The metrics we decided to focus on in the results, the static lung compliance, alveolar-arterial oxygen difference, and PaO_2/FiO_2 show a significant difference between baseline and endpoint values, regardless of pregnancy status and so demonstrate our success in producing a working model of IAV disease

severity. Since PaO_2/FiO_2 showed the expected trend in all NHPs and the other two major metrics did not, we decided to move forward with PaO_2/FiO_2 as our benchmark of clinical severity as it would allow us to include the most macaques possible in our correlation and linear regression analyses.

A final strength of this study is that we are the first to investigate the links between pregnancy, IAV pathogenesis, and disease severity in an NHP model. While our original hypotheses were proven wrong, we uncovered results that can drive promising research directions. Future studies could analyze the connection between estrogen and progesterone levels at different trimesters, cellular permissivity, and vulnerability to severe IAV infection. Due to the strong influence of estrogen and progesterone in shaping the immunological landscape, as described in Chapter 1, it is important to consider that different levels may not have the same effects across trimesters as has been shown in mouse models.[199,200] Simulating the concentration of circulating estrogen or progesterone levels and then infecting with IAVs is a strategy already pioneered in mice but needs the translational impact that only NHP models can provide.[201]

Chapter IV: IMPACT OF INFLUENZA A VIRUS INFECTION ON THE PLACENTA (adapted from manuscript in submission)

Aim 2: Determine the impact of maternal influenza A virus infection on placental health, innate immune activation, and transcriptional programs.

Hypothesis 2A: Maternal influenza A virus infection induces placental histopathologic injury, cytokine release and a placental antiviral response.

Hypothesis 2B: Severity of the lung infection correlates with placental antiviral response and injury.

Introduction

Influenza A virus (IAV) infections remain a global public health threat, which is especially pronounced in vulnerable populations like pregnant women.[202,203] IAV is a negative-sense, single-stranded RNA virus composed of eight segments. Pandemics have occurred when reassortment of the viral segments occurs to produce new combinations of its surface glycoproteins hemagglutinin (HA) and neuraminidase (NA). Epidemiologic evidence from several IAV pandemics (e.g., 1918, 1957, 1968, 2009) support the conclusion that IAV infections in pregnancy impart a greater risk of maternal morbidity, mortality and adverse pregnancy outcomes, such as stillbirth[204]. The risk for maternal mortality was further enhanced by the presence of comorbidities.[205] Studies done in the wake of the 2009 H1N1 IAV pandemic found that pregnant women admitted to the hospital with H1N1 infection had higher than expected rates of preterm birth, stillbirth, and neonatal death.[206-209] Maternal immune activation generally during pregnancy can lead to developmental deficiencies in infants.[210,211] Vaccination has been documented as an effective intervention to reduce the risk of hospitalization among pregnant women and infants, but vaccine skepticism remains an obstacle for high uptake among pregnant women.[212-214]

Vertical transmission of IAV is a possibility due to documented evidence of trophoblast (placental cell) susceptibility to IAV infection. Avian influenza H5N1 was detected in the Hofbauer cells (fetal macrophages) and cytotrophoblast cells of the placenta, as well as the fetal lungs, after a fatal human infection case.[41] A study using human placental explant tissue showed that trophoblasts were permissive for infection with 2009 H1N1 IAV.[215] IAV infection in pregnant mice can lead to smaller placentas with underdeveloped vascular labyrinth, especially when infection is at earlier gestational periods.[216] IAV infection during pregnancy could spread to the placenta and negatively affect placental integrity.

With growing interest in the effects of IAV infections during pregnancy, there is a need for animal models with strong anatomical similarities to humans, which recapitulate the pathology of IAV infection. Nonhuman primates (NHPs) have the most similar pregnancies and demonstrate similar pathogenesis during IAV infection to humans.[3,132] NHP IAV studies have thus far used pregnant NHPs to understand therapeutic pharmacokinetics, complement activation, and infant brain development.[140-142] However, the impact of IAV infection during pregnancy on the placenta has not been characterized. Mice remain the most commonly used animal model for IAV in pregnancy studies because of their accessibility, but their reproductive anatomy is dissimilar to primates. Mouse studies have demonstrated that maternal IAV infection can lead to greater maternal mortality and placental damage from hypercytokinemia, but not placental infection.[184,189,217] While these studies are important steps in understanding IAV pathogenesis during pregnancy, it is necessary to use a model that can be extrapolated to expected outcomes in humans.

Our study utilizes a translational animal model, the pigtail macaque, which shares many similarities in the realm of pregnancy (placentation, physiology, maternal-fetal interface, fetal development timeline)[218-220]. The pigtail macaque has a 23 to 26-week gestation and highly similar placental structure to humans. For this study we use samples from the chorionic villous (region of the placenta where maternal-fetal nutrient exchange occurs) tissue. Our research group and

collaborators have ample experience with using pigtail macaques as a model of infections during pregnancy.[1,221-224] Equipped with our experience, techniques, and highly translatable pregnancy model, we interrogated innate immune responses to IAV H1N1 infection in the NHP placenta with the objective of studying the systems immunology linking antiviral immune response and damage to the placenta.

Table 4.1. Overview of Pathology in H1N1-Infected Dams

ExpID	Gestational Age at Endpoint (days)	Fetal Sex	Maternal Age (years)	Stillbirth	Histopathology on Dam Lungs	Placental Pathology
FLU1	130	M	12.19	No	Pneumonia, multifocal to coalescing, mild to moderate, mixed, with multifocal pleural fibrosis	No pathology observed
FLU2	131	F	12.68	No	Pneumonia, multifocal to diffuse, interstitial, mild to moderate, mixed, with multifocal pleural fibrosis	No pathology observed
FLU3	132	F	6.56	No	Pneumonia, interstitial to diffuse, mild (left) to severe (right), with alveolar edema and hyaline membranes	Multiple infarctions in disc with eosinophils in decidua
FLU4	143	F	15.5	No	Mild interstitial pneumonitis, mixed, with mild deep alveolar edema	Small foci of active inflammation in villi
FLU5	139	F	10.61	No	Pneumonia, multifocal, moderate, mixed, with edema and respiratory epithelial hyperplasia	Single focus of necrosis and active inflammation in decidua basalis with basal perivillous fibrin deposition
FLU6	140	M	7.02	No	Pneumonia, neutrophilic to mixed, severe, with edema	Two foci of subacute placental infarction
FLU7	134	M	13.83	Yes	Pneumonia, interstitial, mild, chronic to mixed, with peribronchial lymphoid hyperplasia	Multiple large foci of subacute placental infarction, thrombi in decidual vessels
FLU8	132	M	8.52	No	Pneumonia, interstitial, mild to severe, neutrophilic to mixed, with alveolar edema and fibrin	Placental necrosis with fibrin and active inflammation in superficial disc, possible subacute infarction
FLU9	121	M	6.99	Yes	Severe pneumonia with pleural effusion and hilar lymphadenopathy	Placental necrosis with fibrin and active inflammation in disc, possible subacute infarction, some hemosiderin-laden histiocytes in fetal membranes
FLU10	131	F	4.43	No	Pneumonia, multifocal, mild to moderate, interstitial, neutrophilic to mixed, with alveolar edema	Focal active inflammation in decidua
FLU11	139	M	11.75	No	Severe pneumonia with pleural effusion and hilar lymphadenopathy	No pathology observed

Summary of histopathology reports and other physiological variables.

Table 4.2. Clinical Observation Scores

	Total Score					
ID	0 DPI	1 DPI	2 DPI	3 DPI	4 DPI	5 DPI
FLU1	N.C.	N.C.	1	0	3	2
FLU2	0	1	0	0	4	2
FLU3	N.C.	0	N.C.	0	0	N.C.
FLU4	0	0	0	0	0	0
FLU5	0	0	1	3	4	0
FLU6	0	0	0	0	0	0
FLU7	0	0	1	N.C.	0	0
FLU8	0	N.C.	3	4	6	4
FLU9	0	0	2	2	4	3
FLU10	0	0	0	0	0	0
FLU11	0	1	3	0	0	0

Observations were conducted once per day and each score is a cumulative assessment of symptoms covering appetite, fecal consistency, respiratory effort, alertness, and coughing. N.C. stands for days in which a score was not collected. DPI stands for days post-infection.

Results

Impact of Influenza A Viral Disease on Pregnancy Outcome

A total of 11 pigtail macaque pregnancies were inoculated with IAV H1N1 between 116-138 days gestation (third trimester) and reached the study endpoint 5 days after inoculation, at which time Cesarean section was performed (Table 4.1). Stillbirth occurred in two pregnancies, which was detected at the time of Cesarean section. Maternal pneumonia was diagnosed in both cases of stillbirth; one case had mild, multifocal pneumonia and the other had severe pneumonia with pleural effusion and hilar lymphadenopathy. Preterm birth was not observed.

Table 4.3. Summary of Pathology in Controls

ID	Placental Pathology
CTRL3	Some marginal fibrin deposition and neutrophilic inflammation in decidua
CTRL4	Tiny focus of decidual necrosis and active inflammation
CTRL6	Remote subchorionic hemorrhage associated with membranes
CTRL7	Foci of neutrophil-rich inflammation in & around necrotic villi
CTRL8	Tiny focus of decidual necrosis and active inflammation
CTRL9	2 adjacent foci of active inflammation in subchorionic space without associated chorionic plate inflammation
CTRL10	No pathology observed
CTRL11	Large areas of transmural subacute placental infarction and subchorionic fibrin

Summary of histopathology analysis of a subset of control subjects' placentas.

Illness of the dam was documented using daily clinical scores and vital signs taken at the time of sedation and study endpoint on Day 5 post-inoculation (Table 4.2). The animals with the greatest illness based on the cage-side IAV disease clinical scoring system were FLU8 and FLU9. Neither of these cases experienced a stillbirth.

Table 4.4. Summary of H1N1 Viral Presence in Placentas

ID	Positive in Chorionic Villous (CV) Tissues
FLU1	Yes
FLU2	No
FLU3	No
FLU4	No
FLU5	No
FLU6	No
FLU7	No
FLU8	No
FLU9	No
FLU10	No
FLU11	No

qPCR was done for samples from placental chorionic villous tissue from placentas of H1N1 infected dams. This table summarizes if samples came back positive for viral RNA.

Placental histopathology was evaluated to determine if maternal IAV infection could induce pathologic changes that might contribute to stillbirth. To that end, random sections of the placental membrane, chorionic villous, and umbilical cord were evaluated for pathology using diagnostic criteria from the Amsterdam classification system and Redline scoring criteria (Table 4.1)[225-227] Most placentas from IAV-infected animals had evidence of either placental necrosis, chronic villitis, placental infarction, and or chronic deciduitis (6/11, 55%; Figure 2.1A-C). Four of the 11 placentas (5/11, 45%) had either a single focus of inflammation or no observable pathology. None of the placentas demonstrated active chorioamniotic inflammation. Placental histopathology in the two cases of stillbirth (FLU7, FLU9, Table 4.1) overlapped with that observed in other IAV-infected animals, and some controls (Table 4.3).

IAV H1N1 Viral RNA in Placenta

To determine the extent of IAV infection, we performed an RT-qPCR assay targeting the H1 gene in placental (chorionic villous) tissue. All infected animals had detectable IAV vRNA in their lungs

Figure 4.1. Pathology and Viral Load

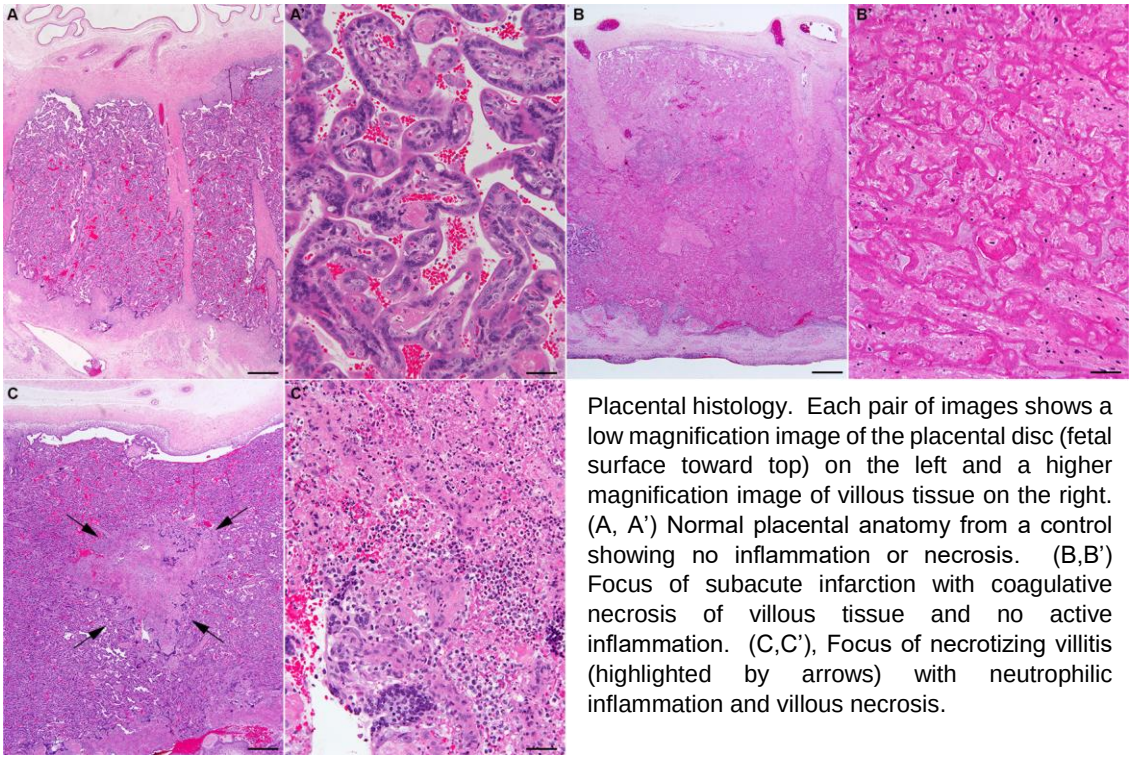

Placental histology. Each pair of images shows a low magnification image of the placental disc (fetal surface toward top) on the left and a higher magnification image of villous tissue on the right. (A, A') Normal placental anatomy from a control showing no inflammation or necrosis. (B,B') Focus of subacute infarction with coagulative necrosis of villous tissue and no active inflammation. (C,C'), Focus of necrotizing villitis (highlighted by arrows) with neutrophilic inflammation and villous necrosis.

(Chapter 3). There was a bimodal distribution of lung vRNA data with half having a maximum viral load exceeding 900,000 copies/mg and half with a viral load less than 20,000 copies/mg. In placental chorionic villous tissue, IAV vRNA was not detected except in one case (FLU1) with a very low copy number (Table 4.4). Fetal tissue samples from the brain, spinal cord, lungs, liver, heart, spleen and thymus were negative for H1 viral RNA across the entire cohort.

Placental Transcriptional Profile

To define the transcriptional signature in the placentas from infected animals, we performed bulk RNA sequencing on placental chorionic villous tissues from infected and control animals and then

Figure 4.2. Transcriptional Immunology in the Placenta

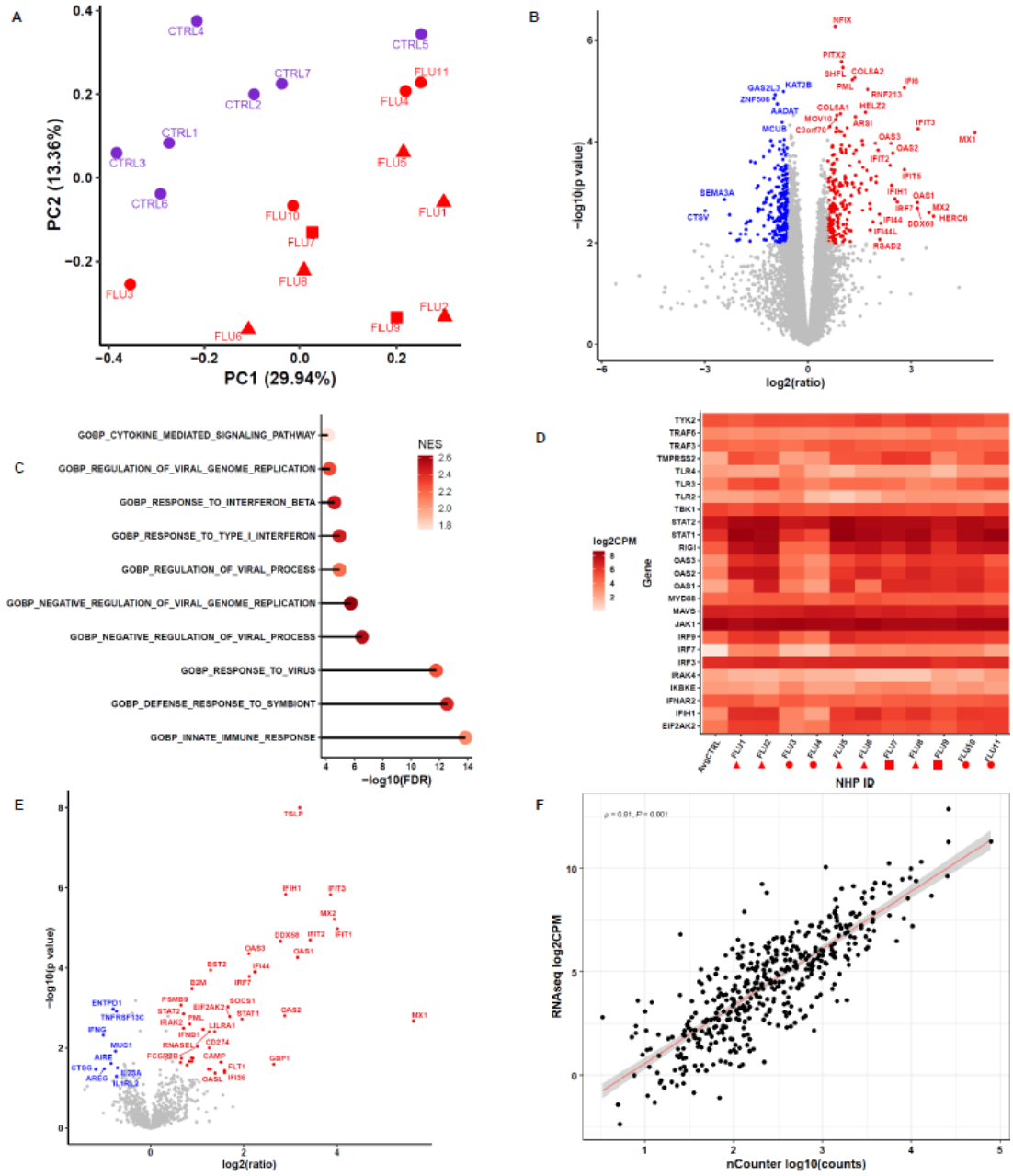

RNA for transcriptomics was taken from tissue samples taken at endpoint from infected and uninfected placentas. 2A shows a PCA of normalized RNAseq results from placentas with infected dams represented in red and uninfected dams in purple. In the infected group, dots represent low lung viral load, triangles represent high lung viral load, and squares represent stillbirths. 2B shows DEGs from bulk RNAseq data; red are upregulated and blue are down regulated in placentas from infected dams vs uninfected. 2C visualizes GSEA analysis. A heat map of the gene expression values for Type I ISGs is presented in 2D. 2E shows the DEG analysis result with nCounter data. 2F is a scatter plot of average nCounter and RNAseq expression values.

quantified differences in gene expression using differential expression analysis. Principal

component analysis of the normalized transcriptional profiles of the placentas demonstrated a clear division between the two experimental groups (Figure 4.2A). In addition, there was a separation along the principal components between the placentas from uninfected controls (Figure 4.2A, purple) and IAV-infected dams with low lung viral loads (Figure 4.2A, red circles) and those with high lung viral load (Figure 4.2A, red triangle) or stillbirth, which both had low lung viral loads (Figure 4.2A, red square). A similar number of genes were upregulated (262) as were downregulated (271) in placental chorionic villous tissues of infected animals relative to controls (Figure 4.2B). We observed that several IFN stimulated genes (ISGs) such as *IFIT3, MX1*, and *OAS2* were among the genes with the greatest positive log2 ratio, meaning that they had far greater expression in placentas from infected animals relative to control placentas. These results were supported by the nCounter assay differential gene expression results on the same samples (Figure 2B). Taking this observation to the next level, we did gene set enrichment analysis (GSEA) using the Gene Ontology: Biological Processes (GO:BP) (Figure 4.2C). In line with our observations from the differential gene expression analysis, pathways related to the negative regulation of viral process/genome replication/entry and Type I IFN response were significantly and positively enriched in the placentas of infected NHPs. We highlighted the expression levels of genes from the Type I IFN signaling pathways, as defined by the WikiPathways database, and compared expression between the average across controls and each infected animal (Figure 4.2D). From this visualization we can observe that the enrichment of these pathways was not driven uniformly by all genes in these pathways, but instead by several key genes and in certain animals from the infected group. In fact, FLU3 and FLU4 had a similar expression of genes in this pathway as controls. RNA sequencing analysis demonstrated upregulation of antiviral response pathways in the placental chorionic villous tissues of most infected NHPs.

RNA from placental chorionic villous tissues from infected NHPs and control NHPs was analyzed for RNA transcripts related to immune activity using the Nanostring nCounter system. A 770-plex

assay specific for NHP gene targets was used to determine differentially expressed genes between the two experimental groups. The profile of significantly differentially expressed genes includes an upregulation of genes related to the Type I interferon (IFN) signaling pathway (e.g. *DDX58, STAT2, IRF7*) ($p<0.01$) and several ISGs (e.g. *OAS1, IFIH1, IFIT1*) ($p<0.0001$) (Figure 4.2E). Next, we validated the total RNA-Seq using the Nanostring nCounter platform, which yields a direct gene count that would be useful for correlation calculations. RNA sequencing and nCounter count data were significantly correlated ($p<0.001$, $r=0.81$) across all NHP samples used (Figure 4.2F). The nCounter analysis validated the results from our RNA sequencing effort and provided a gene expression variable we could use for associations with other immunological variables.

Cytokine Concentrations in the Placenta

With the transcriptome showing a clear antiviral immunological signature, it was necessary to determine if the cytokinome also showed a significant increase relative to baseline. Lysates prepared from placental chorionic villous tissues of NHP subjects were quantified for cytokines via 14-plex cytokine assay or ELISAs. Comparisons between control samples (n=4) and infected animals (n=11) were done using Wilcoxon rank-sum test for significance. Placental chorionic villous tissues from infected NHPs had significantly greater concentrations of pro-inflammatory cytokines IL-18 and IL-1β ($p<0.05$) (Figure 4.3A). The median of IL-1β in infected NHP placental chorionic villous tissues was 22.02 pg/mL while the median in controls was 7.57 pg/mL. For IL-18, infected NHPs' placental chorionic villous tissues had a median and mean of 7.18 pg/mL and 10.48 pg/mL while these values were 2.49 pg/mL and 2.7 pg/mL in controls, respectively. The concentration of IFNβ, IL-6, and TNFα were not significantly different between placentas of infected and control NHPs but were generally higher (Figure 4.3A). However, only IL-6 and TNFα concentrations were significantly and negatively correlated with lung viral load in the dams via Spearman correlation calculation (Figure 4.3B). These results indicate that the placentas of

infected animals are natively producing higher inflammasome products (IL-1β and IL-18). However, the levels of other inflammatory mediators (IL-6 and TNFα) in the placenta are inversely influenced by viral burden in the dam lungs.

Myeloid Cell Frequencies

Table 4.5. Correlations Between Gene Expression and Innate Immune Cells

Plasmacytoid dendritic cells (pDCs)		
Gene	ρ coefficient	p-value
DDIT3	-0.76	0.037
IFIH1	0.90	0.005
IFIT3	0.86	0.011
Myeloid dendritic cells (mDCs)		
Gene	ρ coefficient	p-value
DDIT3	0.90	0.002
IFIH1	-0.74	0.035
IFIT3	-0.74	0.035
Classical monocytes		
Gene	ρ coefficient	p-value
MX1	0.81	0.022
DDX58	0.81	0.022
TSLP	0.86	0.011

Spearman correlation coefficients that were significant ($p<0.05$) or close to significance ($0.1>p>0.05$) between gene expression (log10(gene counts)) and frequency of immune cell populations expressed as percentage of live CD45+ leukocytes.

To discern if the gene expression and cytokine levels were tied to innate immune cell activity, we assessed placental chorionic villous tissue for immune cell frequencies via an immunophenotyping assay. The control samples were processed at a different timepoint than for the H1N1-infected group, and the antibody panel used was not configured for quantifying granulocytes. The frequencies of plasmacytoid dendritic cells (pDC) (CD45+/CD20-CD3-/HLA-DR+/CD14-/CD123−CD11c-) and myeloid dendritic cells (mDC) (CD45+/CD20-CD3-/HLA-DR+/CD14-/CD123−CD11c+) were not significantly different between infected and control groups (Figure 4.3C). However, classical monocytes (CD45+/CD20-CD3-/HLA-DR+/CD14+CD16-) were detected in greater frequencies from in the placental chorionic villous tissues from controls versus IAV-infected dams. This could be due to the trafficking of monocytes into the IAV-infected lungs. None of the immune cells assessed were significantly correlated with the lung viral load.

Figure 4.3. Cytokine Concentrations and Immune Cell Subsets of Interest

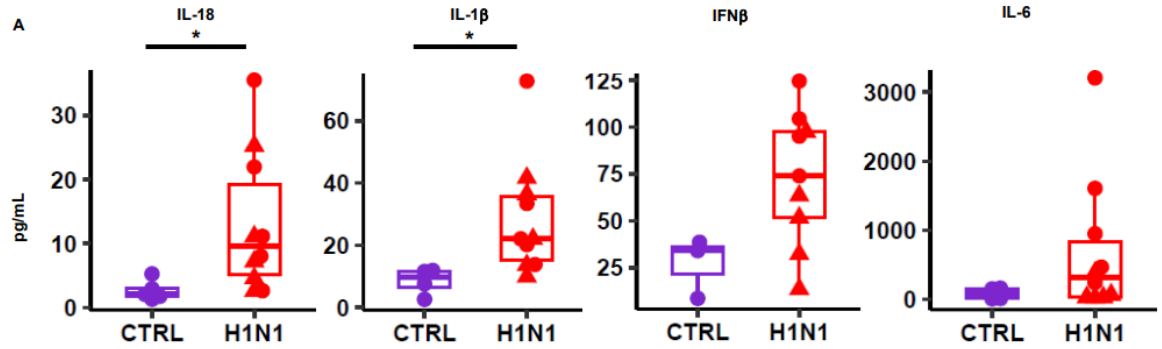

B

Cytokine	ρ coefficient	p value
IL-6	-0.74	0.01
TNFα	-0.81	0.004

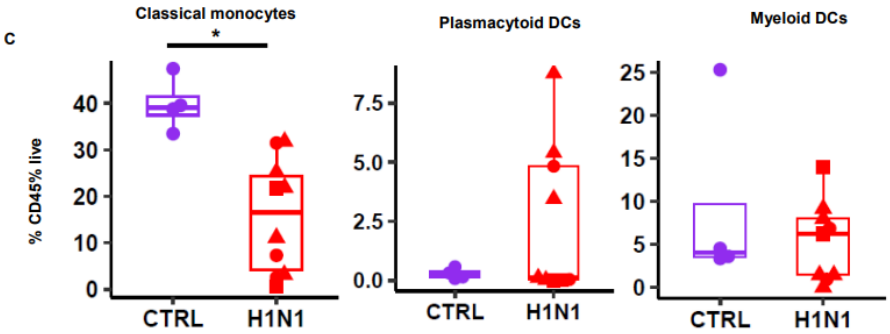

Lysates generated from placental tissue samples were tested for cytokine concentrations via immunoassays. 3A shows cytokine concentrations (pg/mL) in the placenta between uninfected (CTRL) and infected (H1N1). Triangles signify high lung viral load, circle is low viral load or control. 3B shows Spearman correlation coefficents (ρ) and associated p-values for cytokines significantly correlated with dam lung viral load. 3C shows immune cell frequencies from immunophenotyping of the CV tissue with the same groups. N.A. signifies that we were not able to generate frequencies for that group.

We were also interested in understanding the relationships between myeloid immune cells and placental transcription. pDC frequencies were significantly positively correlated to *DDIT3*, *IFIT3,* and *IFIH1* (r=-0.76, 0.86, 0.9; p=0.03, 0.005, 0.01 respectively) (Table 4.5). On the other hand, mDCs were significantly correlated with *DDIT3, IFIH1, and IFIT3* in the opposite direction (r=0.9, -0.74, -0.74; p=0.002, 0.03, 0.03 respectively). When compared to frequencies of classical monocytes, the gene expression of *DDX58, MX1*, and *TSLP* was significantly positively correlated

(r=0.81, 0.81, 0.86; p=0.02, 0.02, 0.01 respectively). These correlations suggest that pDCs and classical monocytes in the placenta had a positive relationship with the upregulation of ISGs while mDCs had a negative relationship with the upregulation of ISGs.

Association between lung viral load and placental gene expression

Considering the strong upregulation of the Type I IFN response in the placentas of infected dams, we were curious to see if there was an association with other variables we collected. We were

Figure 4.4. Clustermap of Placental Gene Expression

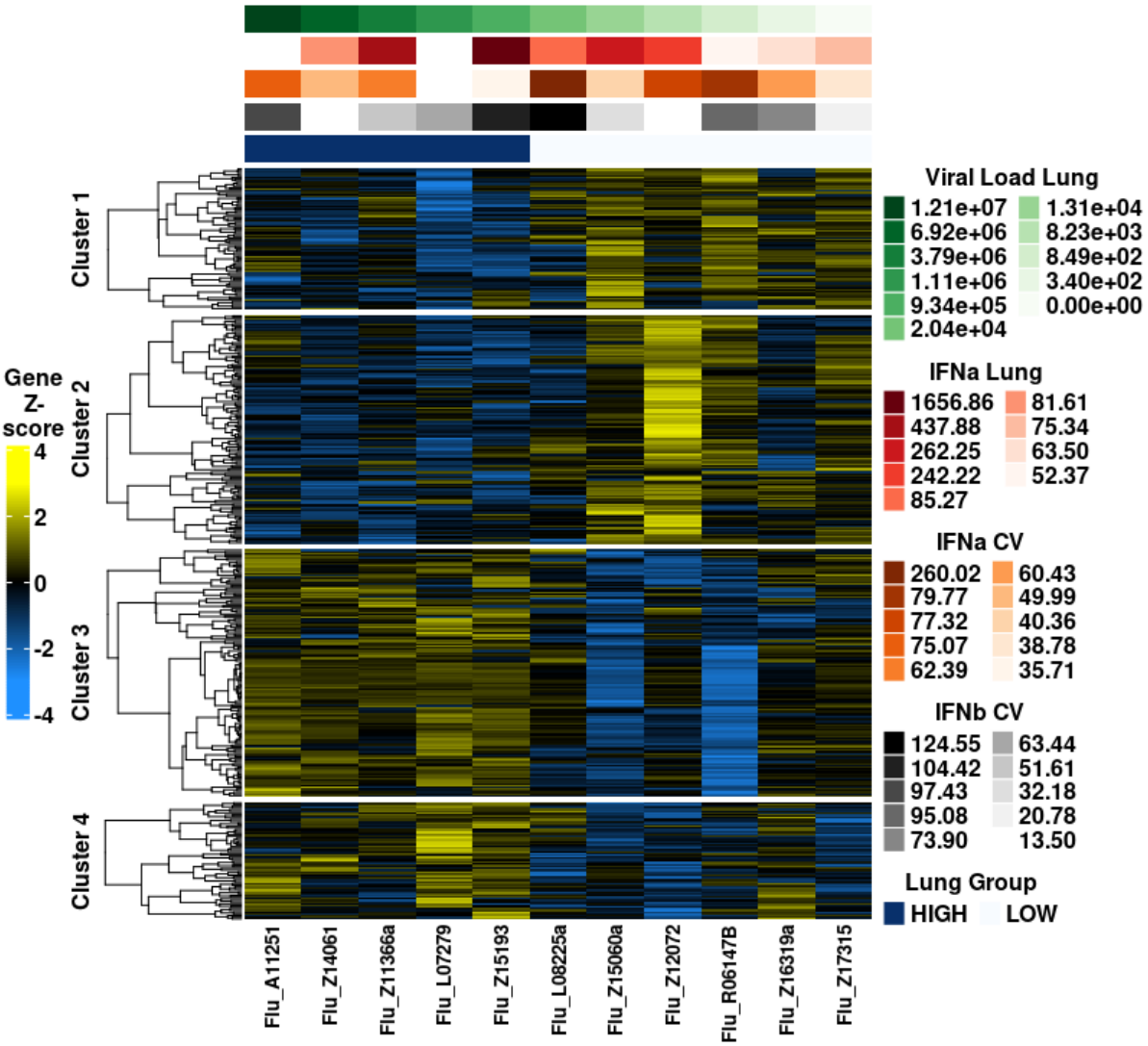

Viral load and Type I IFN concentrations in placenta and lung were used in generation of a clustered heatmap using the ComplexHeatmaps package.

particularly interested in determining whether the bi-modal distribution in the lung viral load could be correlated with the expression of antiviral innate immune response genes in the placenta. We constructed a clustered heatmap and observed which immunological variables led to the best clustering of differentially expressed genes of the placenta (Figure 4.4). When ordering the heatmap by highest to lowest lung viral load, there was a clear difference in the placental transcriptional response between the high and low lung viral load groups. When the normalized placental bulk RNA-Seq gene counts were compared to the lung viral load (Spearman correlation), we found that placental ISG expression was significantly and positively correlated to the lung viral load (Table 4.6). Notably, PaO_2/FiO_2 at the 5-day endpoint did not correlate significantly with any of the genes related to innate immune response. These results suggest to us that the viral burden in the lung may be a more important correlate of placental antiviral transcriptional response than the oxygenation status of the animal.

Table 4.6. Correlations between Gene Expression and Maternal Viral Load

Gene	ρ coefficient	p-value
DDX60	0.81	0.003
IFI6	0.76	0.009
IFIH1	0.62	0.04
IFIT3	0.75	0.01
IRF3	0.61	0.04
IRF9	0.67	0.02
ISG15	0.62	0.04
MX1	0.81	0.003
MX2	0.65	0.03
RIGI	0.69	0.02
STAT1	0.70	0.02

Spearman correlation coefficients were calculated between normalized gene counts from bulk RNA sequencing data and dam lung viral load from qPCR data.

Discussion

Overall, our results indicate that there is a robust antiviral innate immune response in the chorionic villous tissue of the placenta after a maternal IAV infection plus histopathologic changes that may culminate in stillbirth. Pneumonia was observed in the dam lungs of all IAV-infected animals and in two cases, stillbirth occurred. Although there was a spectrum of pathology observed in the placentas, similar pathology was also observed in the controls and is present in some normal human pregnancies.[228,229] H1N1 viral RNA was detected in 1/11 subject placental chorionic villous tissue. In human cases of stillbirth, it is routine to extensively sample the placenta to survey

histopathology across the entire disc. More limited sampling of the placenta prevented a more confident determination of the underlying cause of the two stillbirths. However, the striking cytokine and transcriptomic signature of a Type I IFN response in the IAV cohort indicates that the placental innate immune response was activated in these cases and may have contributed to the placental pathology. Stillbirth cases only represented 2/11 pregnancies in the infected group which prevented us from being able to draw any statistically significant comparisons with non-stillbirth cases. However, due to the transcriptome difference between stillbirth and low dam viral load cases, we can speculate that high dam viral load cases may have eventually led to stillbirth before the pregnancies went to term. To better quantify the relationship between infection status and pregnancy complications, we would need to have extended the experimental timeline and done daily ultrasounds to monitor fetal viability. Furthermore, a future study should conduct a proteomic analysis of fetal serum and amniotic status to discover any biomarkers to distinguish stillbirth and live birth cases in infected mothers since we did not detect any major differences in ISG or pro-inflammatory cytokine levels between case groups in this study.

After quantifying cytokine concentrations, we found that IL-1β and IL-18 were at significantly greater levels in the placental chorionic villous tissue of infected NHPs versus controls, but that Type I IFNs, IL-6, and TNFα were not. The cytokine signature of elevated IL-1β and IL-18 is classic for NLRP3 inflammasome activation, which is known to restrict IAV infection and epithelial injury.[60,230] A future study should focus on finding the presence of components of the NLRP3 inflammasome such as caspase-1 and evidence of other products such as active gasdermin D.[58] Since neither cytokine was significantly correlated with dam lung viral load and placental viral burden was rare in our cohort, it is worthwhile to consider potential mechanisms of sterile inflammation as a trigger for inflammasome activity.[68] Immune cell subpopulations in the placental chorionic villous tissue were not significantly different between infected and control groups. Cytokines and leukocytes were significantly associated with ISGs and other elements of the Type

I IFN pathway, suggesting interconnectivity between these immunological variables, particularly in infected, pregnant NHPs.

Current literature supports that a Type I IFN response can occur in the context of some perinatal infections, but whether this response harms placental integrity may depend on the degree of antiviral innate immune response. In the context of Zika virus infection during early pregnancy in a mouse model, Type I IFN signaling was associated with malformation of the placenta architecture and resorption of the fetus.[85] The experimental infections in this thesis were performed in the third trimester, when stillbirth (fetal resorption, miscarriage) is rare. However, injury to the placental architecture is a likely outcome of a robust Type I IFN response within the placenta. Nonetheless, a Type I IFN response may also be necessary to mitigate maternal mortality and vertical transmission, as observed in a model of murine herpes virus infection.[81]

The human placenta has been identified as a permissive organ to IAV infection, although documentation of this phenomenon has been rare.[19] The preferred entry factor for human IAV infection, α-2, 6 sialic acid glycans are found in the respiratory tract, but also in the placenta and many other organs.[20] The human placenta presents α-2, 6 sialic acid and can sustain infection with IAV H1N1 2009.[215] In our model, placental infection was only detected in 1/11 NHPs, but this could reflect an uneven distribution of infected tissue as observed with other viral infections or the resolution of viral infection by study endpoint (5 dpi).[43,231] Other researchers have advanced a theory of a “vascular storm” in which the blood vessels of the circulatory system become infected, triggering the influx of proinflammatory cells and mediators such as monocytes, neutrophils, and chemokines throughout the body. This was associated with placental hypoxia and stunting of placental growth even though the placentas were not infected.[170] This hypothesis may explain the results of a cohort study of placentas from pregnant patients infected with influenza during the 2009 pandemic. The study found that while 47% of the placentas had features consistent with chronic villitis, none tested positive for IAV H1N1.[232] Several placental cells have been shown to

be permissive to different IAV subtypes in vitro and induce an antiviral innate immune response. In human chorionic cells, IAV H1N1 infection leads to a robust Type I IFN and pro-inflammatory response.[233] IAV H3N2 infection of first trimester trophoblast cell lines instead found that trophoblasts at this stage were more vulnerable to mass apoptosis in response to the virus.[234] IAV H3N2 has also been shown to be capable of inducing increased neutrophil infiltration, necrosis, mineralization and inflammatory gene expression after sublethal infection in pregnant mice.[88] In our study, we did not examine trophoblast subsets separately, but we did find that IFN pathway genes were upregulated in placentas from infected NHPs (*DDX58, IRF7, TLR3).* Furthermore, we found an association between viral load levels in the lung and placental ISG expression. Higher lung viral load clustered with higher placental ISG expression, suggesting a systemic immune response that spreads to the placenta as the lung's viral burden increases. Similar work has linked IAV infection to the spread of pro-inflammatory, antiviral cytokines through the circulatory system and causing injury to the placenta in a murine model of IAV infection during pregnancy.[237,238]

No previous publications have examined cellular responses to IAV infection in the placenta. However, we can compare our results to studies in pregnancy models of other viral infections. Zika virus has demonstrated the tendency to infect monocytes and could be using them to cross the placental barrier, leading to increased neutrophil infiltration and inflammatory cytokine secretion.[239,240] Future research should investigate the mechanism for how ISG expression promotes the expansion of classical monocyte populations in the placenta during IAV infection. The role of pDCs as a part of the placental response to viral infections has not been well-explored in the past. pDC function and role in the placenta may be dependent on the type of infectious agent, as its frequencies decrease during hepatitis C virus infection, but its maturation is promoted during malarial infection.[242,243] Our study is thus the first to identify pDCs and a prominent Type I IFN response signature in the placenta during an IAV infection. The mDC relationship to placental gene expression is an inversion of what we found with the pDCs with the mDC frequencies

correlating negatively with ISG production. Previous work has uncovered a similar inverse relationship between mDCs and ISGs in the context of other viral infections.[244-246] Investigating long-term changes to the placental immune landscape as a result of innate immune activation may be illuminating if done when considering infection in earlier trimesters. We hypothesize that pregnancies affected by IAV infection lead to placental innate immune activation and have increased risk of preterm birth. Furthermore, we speculate that associating pDC and classical monocyte levels in the placenta with preterm birth cases can lead to a model of the immune changes that place pregnancies at risk for complications.

The main strength of our study is the translational nature of the NHP model to human pregnancy in which we can model an IAV infection. NHPs are highly similar to humans both genetically and physiologically, which extends to their pregnancies.[1] The macaque placenta has similar placental architecture to humans and a long gestational period. Another strength is the ability to study the placental antiviral immune response at a defined time after infection onset, which is not possible during human pregnancy. We also conducted our study in the third trimester of pregnancy, which is the time period when pregnant women experience the greatest rate of maternal morbidity and mortality.[33] Collectively, these features of the pregnant NHP model of IAV infection increase the translational relevance of this model and the impact of our findings.

An important limitation was that we did not study endpoints earlier or later than five days post-infection limiting our ability to determine the trajectory of the antiviral response. Due to ethical and budgetary limitations, we also used pregnant NHP controls from our research program that did not receive the same bronchoalveolar lavage procedures as the study animals. Our study design also predisposed to rapid and severe IAV disease with a high inoculum administered via several routes. Therefore, we did not evaluate the impact of a greater spectrum of IAV disease phenotypes that might occur after a natural infection on placental IFN signaling, as has been observed in mild/asymptomatic SARS-CoV-2 pregnant people.[247] Many of these limitations are

inherent to the use of a pregnant NHP model, which also provides unique insight into the pathogenesis of infectious disease.

In our study, we did not examine the post-birth effects of this immune activation during gestation on the development of the fetus. It has been hypothesized that immune activation from IAV infection during pregnancy is linked to neurodevelopmental issues in developing children.[141,248]. Our current study was not designed to investigate these research questions, but future studies could investigate possible effects of placental immune activation and inflammation on the heatlh and development of the fetal brain. Future work should also focus on testing vaccines using pregnant NHPs as a model for pregnant women.

Chapter V: CONCLUSIONS

Overview of Results

Pregnancy, particularly in the third trimester, has been identified as a risk factor for severe IAV disease and death due to IAV infection during the major IAV pandemics of the last over a hundred years. The basis for the enhanced pathogenesis of disease in pregnancy is unknown. This dissertation project was designed to investigate the nature of IAV pathogenesis in pregnant women with a focus on differences in the innate immune response and transcriptional programs in the lungs and placenta. The recent spread of highly pathogenic avian IAV H5N1 in the United States' wild bird populations, poultry flocks, and dairy cattle is highly concerning for the potential development of a new pandemic. Therefore, developing a stronger understanding of IAV pathogenesis and disease manifestations in vulnerable populations, like pregnant women, is of critical importance.

We used a highly translational model of IAV infection, the pigtail macaque (*Macaca nemestrina*), to evaluate innate immune responses within multiple organs and compartments across a 5-day time period after inoculation. While mice are a common model to study IAV pathogenesis and have even been used to study infection in the pregnancy context, they do not recapitulate important elements of human IAV pathogenesis and have major differences in their pregnancies compared to humans. In contrast, NHPs share highly similar anatomy, immunology, and pregnancies relative to humans and have been used successfully to model IAV infection. The central hypothesis of this dissertation is that aberrations in the pregnant primate's innate immune response to IAV H1N1 predisposes to severe IAV lung disease and aberrant placental function in pregnant nonhuman primates (NHPs). In Chapter 2, we described the protocols and methodology employed to do this work. Our initial hypothesis was that the lungs of pregnant animals would

have attenuated antiviral immune responses and elevated Treg levels, leading to a more severe disease phenotype.

The first major advance of this thesis was the development of the pulmonary physiology testing protocol described in Chapter 2. With the guidance of pulmonologists at the University of Washington, we developed a protocol to assess metrics of oxygenation, ventilation, and pulmonary mechanics in pregnant and non-pregnant macaques. This protocol is an optimized version of what is used with ventilated human patients of acute respiratory illness. In brief, we sedated and paralyzed macaques to place them on a mechanical ventilator and collect various measures to calculate PaO_2/FiO_2, alveolar-arterial oxygen difference, and static lung compliance. We can also use this protocol to generate scalar tracings of flow-volume and pressure-volume loops. Our protocol generates a diverse set of quantitative data that can be used assess the progress of infection and is superior to the simple observations we relied on previously.

Pregnant women are known to have a greater burden of IAV lung disease than non-pregnant individuals. However, it is unknown the extent to which physiologic changes in pregnancy and sociodemographic factors interact to set the stage for enhanced lung disease. In Chapter 3, we initially focused our investigation of IAV lung disease by analyzing the relationships between age, weight, pregnancy status, and lung physiologic disease correlates (e.g., PaO_2/FiO_2 ratio). Physiologically, we found that adult age and weight were not significantly different between the two infected groups, but non-pregnant females did lose a greater percentage of the initial body weight during infection. PaO_2/FiO_2, a measure of oxygenation and disease severity, was significantly decreased between endpoint and baseline measurement time points across all animals. Interestingly, PaO_2/FiO_2 at endpoint and baseline was not significantly different between pregnant and non-pregnant animals at 5 dpi. Our initial hypothesis that disease severity would be greater in pregnant versus non-pregnant NHPs was disproven. However, the initial PaO_2/FiO_2 ratio was lower in pregnant versus non-pregnant animals suggesting that in pregnancy there was

pre-existing atelectasis from the pressure of the growing uterus on the lungs that made these animals more vulnerable to enhanced IAV disease. Whether enhanced IAV disease in pregnant animals required a longer time course to become apparent in relation to IAV disease in non-pregnant animals is unknown.

Both infected pregnant and non-pregnant animals had a robust antiviral response to IAV in their lungs. Notably, we found that in the pregnant animals' lungs, there was a bi-modal distribution of viral load values, with a high and low viral load group. The differences in Th17 and Treg frequencies we expected to detect between pregnancy status groups were not significant in the lungs and BAL. IL-5 and IL-18 concentrations were significantly higher in the lungs of infected non-pregnant relative to pregnant animals, but IL-17 and IL-23 concentrations were not. As the infected pregnant and non-pregnant animals demonstrate similar immune responses to IAV infection in their lungs, we planned to test which immunological variables could serve as predictors as disease severity in female macaques, regardless of pregnancy status. To do this, we used the variables (genes, cytokines, cell subsets, adult weight) significantly correlated to PaO2/FiO2 at the O2 at the endpoint and calculated linear regression models based on each of these variables. We found that adult weight at endpoint, PaO_2/FiO_2 at baseline, and gene expression (*FCER1G, TLR9, TNSF8, IL1RL1*) were significant predictors of endpoint PaO_2/FiO_2. We decided to take these analyses further by combining PaO_2/FiO_2 at baseline, the model which had the best parameters, with the other variables to generate multivariate linear regressions. We determined that combining *TLR9* expression with baseline PaO_2/FiO_2 was a significantly improved predictive model than baseline PaO_2/FiO_2 alone. This finding justifies studying the link between TLR9 expression and protection from enhanced disease in pregnant and non-pregnant NHPs. We also think that the immunologic differences we expected to find may not manifest by 5 days post-infection. A longer infection time course and more thorough interrogation of the adaptive

immune response may better explain the enhanced mortality and morbidity risk in pregnant women.

Next, we analyzed single cell RNA-Seq data from the lung tissues of infected pregnant and non-pregnant NHPs. We also leveraged an analysis technique to identify and quantify frequencies of cell populations that were infected with IAV. Our data currently supports that infected alveolar macrophage frequencies are higher in infected pregnant versus non-pregnant NHPs; in tandem, the uninfected macrophage cell population frequencies are significantly fewer. This data supports the RT-qPCR observation of a bi-modal distribution in the lung viral loads of pregnant NHPs with very high levels in some cases. The reason for the potential greater permissivity of these cells in the pregnant group may be related to hormonal changes in pregnancy. Since scRNA-seq allows us to quantify a more diverse set of leukocytes, there is a possibility that we may find the immunological differences between pregnancy status groups that we were unable to find with our other tools. In future analyses, we also expect to find a connection to the disease severity metric PaO_2/FiO_2.

In Chapter 4, we discussed the impact of IAV infection on placental immune response and transcriptional programs in the placenta. We hypothesized that infected animals would have greater evidence of placental injury than uninfected placentas and that placentas from infected animals would have robust antiviral responses. We found that most placentas from infected (8/11) and uninfected (7/8) NHPs had similar evidence of placental injury. However, two of the 11 pregnancies in the infected NHP group experienced a stillbirth by the endpoint, which is a known complication of IAV disease. Fetal organs were negative for the presence of viral RNA. Viral detection was rare in the placentas from infected animals, but there was a robust antiviral transcriptomic signature via bulk RNAseq and nCounter. DEG and gene set enrichment analysis revealed that placentas from infected NHPs had significantly greater upregulation of interferon stimulated genes (ISG) and pathways related to innate antiviral defense. The inflammasome

products, cytokines IL-1β and IL-18, were both elevated in placentas from infected relative to uninfected placentas. This data suggests that direct viral infection of the placenta is not necessary to provoke a robust antiviral immune response in the placenta and that stimulus may be related to other organs in the infected pregnant NHPs.

Next, we explored host-pathogen crosstalk between the lung and placenta by testing correlations between lung viral load and our immunological variables. Lung viral load correlated significantly and positively with ISG expression in the placenta. In addition, the frequencies of pDCs and classical monocytes in the placentas of infected NHPs were significantly correlated with ISG expression but not with lung viral load. This data supports the new hypothesis that lung viral load in pregnant NHPs is contributing to the change in placental transcriptional programs to promote transcription of antiviral innate immune genes. Future research should focus on the mechanism of crosstalk between the viral lung burden and placental immune activation, possibly through proteomic analyses of the maternal/fetal plasma and amniotic fluid. The next step should be to identify therapeutic interventions that can disrupt this mechanism and thereby reduce fetal morbidity/mortality associated with maternal IAV infection. Since viral infection of the placenta and fetus was rare and placental injury was similar to uninfected controls, we cannot be sure of what the direct impact could be on fetal development. The two stillbirth cases showed similar immunology in their placentas as the others in the infected group. A future study could plan to have the infected mothers deliver at term to evaluate whether pregnancy complications (preeclampsia, preterm birth, stillbirth) are increased; performing developmental tests of infant NHPs to record any developmental deficiencies would provide more definitive answers regarding the impact of in utero exposure to a maternal influenza infection on postnatal development. Together with the data in Chapter 4, this would better answer the question of how placental immune activation affects fetal health even without fetal or placental infection.

Limitations and Future Directions

Non-human primate models carry greater risk than other traditional models of IAV infection. Out of the traditional animal models, using NHPs are the most expensive per animal due to their husbandry costs. Each animal experiment was expensive since we were not only paying for the animal but for the high costs of housing and husbandry staff. Based on estimates for other NHP models, we would likely have only spent ~5% of that value per animal if we had used mice instead of macaques.[251] Therefore, we did not have the financial flexibility to include *in vitro* experiments with human or other primate cell lines to verify our results. Future experiments could take a targeted approach to better flesh out the mechanisms that we found to be relevant to lung and placenta injury using *in vitro* and *ex vivo* approaches.

The outbred genetics of our macaque population is an advantage in better modeling the fact that human population are outbred, but makes it harder get normally distributed results that we would expect in inbred models like mice strains. To make up for the outbred nature of our animals, we made sure to work with a statistician before the experiments started to ensure our study had adequate power. Due to the age and environment of the macaques, it is likely that epigenetic influences on the innate immune system is likely behind our unexpected results.[252,253] The distinctions between primate and mouse immune systems is likely behind the differences in our results and previous work in mouse models of IAV infection during pregnancy.[254] However, we strongly recommended that future experimental plans use different endpoints before and after 5 days post-infection to see if the disease severity risk for pregnant women is more relevant at different stages of the infection. Another interesting experimental option would be to employ aerosolized delivery of IAV. Our 4-pronged conventional infection protocol is typical in the field and was necessary since our facilities are not at the required biosafety level for aerosolized delivery. We also recommend ensuring that all animals are closer in age due to the influence that age had on weight, which was then significantly associated with endpoint oxygenation.

In summary, we identified promising predictors of severe lung injury and placental immune activation, which merit further investigation within the context of primate pregnancy. We implemented a novel pulmonary physiology testing protocol to collect data on measures such as oxygenation and compliance that can be used by other researchers to study infections, asthma, and inhaled pollutants. We found that non-pregnant and pregnant macaques developed similar innate immune responses to IAV infection and that TLR9 expression with baseline PaO_2/FiO_2 can predict extent of disease severity (endpoint PaO_2/FiO_2), regardless of pregnancy status. This result can be taken further to test mechanisms by which TLR9 expression affects lung tissue repair and the mitigation of lung injury. This line of investigation has the potential to come across therapeutic interventions that can be applied to both pregnant and non-pregnant women. Interestingly, we encountered a bimodal distribution of lung viral load in the infected pregnant group and are in the process of evaluating its impact on the immunological landscape of the adult lung. Better understanding the mechanisms and cell types behind the range in viral loads in pregnant NHPs should be a goal of future investigations. Even though we did not observe significant differences in placental injury with uninfected controls or positive viral load in most placentas, we found that macaque placentas have robust upregulation of antiviral gene expression. Furthermore, the expression of ISGs in the placenta was significantly associated with lung viral load of dams. Future research should focus on explaining the potential triggers behind this relationship and how it may be tied to cellular immunology of the dam lung. We did not find a significant association between pulmonary disease severity and placental upregulation of antiviral gene expression, but believe it would be worthwhile to study the effect of placental immune activation on offspring development and possible pregnancy complications. It is my hope that the work in this dissertation can inspire further infectious disease work with NHPs, a valuable model of infection and pregnancy.

Chapter VI: Bibliography

1. Li, M.*, et al.* Non-human Primate Models to Investigate Mechanisms of Infection-Associated Fetal and Pediatric Injury, Teratogenesis and Stillbirth. *Front Genet* **12**, 680342 (2021).
2. Kroeze, E.J., Kuiken, T. & Osterhaus, A.D. Animal models. *Methods Mol Biol* **865**, 127-146 (2012).
3. Nguyen, T.Q., Rollon, R. & Choi, Y.K. Animal Models for Influenza Research: Strengths and Weaknesses. *Viruses* **13**(2021).
4. Javanian, M.*, et al.* A brief review of influenza virus infection. *J Med Virol* **93**, 4638-4646 (2021).
5. Paules, C. & Subbarao, K. Influenza. *Lancet* **390**, 697-708 (2017).
6. Taubenberger, J.K. & Morens, D.M. Influenza: the once and future pandemic. *Public Health Rep* **125 Suppl 3**, 16-26 (2010).
7. Microbial, I.o.M.U.F.o. & Threats. The Threat of Pandemic Influenza: Are We Ready? Workshop Summary. (2005).
8. Eisfeld, A.J.*, et al.* Pathogenicity and transmissibility of bovine H5N1 influenza virus. *Nature* **633**, 426-432 (2024).
9. Yoo, D.S.*, et al.* Bridging the Local Persistence and Long-Range Dispersal of Highly Pathogenic Avian Influenza Virus (HPAIv): A Case Study of HPAIv-Infected Sedentary and Migratory Wildfowls Inhabiting Infected Premises. *Viruses* **14**(2022).
10. Brüssow, H. The Arrival of Highly Pathogenic Avian Influenza Viruses in North America, Ensuing Epizootics in Poultry and Dairy Farms and Difficulties in Scientific Naming. *Microb Biotechnol* **17**, e70062 (2024).
11. Caserta, L.C.*, et al.* Spillover of highly pathogenic avian influenza H5N1 virus to dairy cattle. *Nature* **634**, 669-676 (2024).
12. Burrough, E.R.*, et al.* Highly Pathogenic Avian Influenza A(H5N1) Clade 2.3.4.4b Virus Infection in Domestic Dairy Cattle and Cats, United States, 2024. *Emerg Infect Dis* **30**, 1335-1343 (2024).
13. Relations, C.M. First H5 Bird Flu Death Reported in United States. (Centers for Disease Control and Prevention, cdc.gov, 2025).
14. Relations, C.M. CDC Confirms First Severe Case of H5N1 Bird Flu in the United States. (cdc.gov, 2024).
15. Bouvier, N.M. & Palese, P. The biology of influenza viruses. *Vaccine* **26 Suppl 4**, D49-53 (2008).
16. Das, K., Aramini, J.M., Ma, L.C., Krug, R.M. & Arnold, E. Structures of influenza A proteins and insights into antiviral drug targets. *Nat Struct Mol Biol* **17**, 530-538 (2010).
17. Prevention, C.f.D.C.a. Types of Influenza Viruses. (CDC, 2024).
18. Krammer, F.*, et al.* Influenza. *Nat Rev Dis Primers* **4**, 3 (2018).
19. Zhang, H. Tissue and host tropism of influenza viruses: importance of quantitative analysis. *Sci China C Life Sci* **52**, 1101-1110 (2009).
20. Sempere Borau, M. & Stertz, S. Entry of influenza A virus into host cells - recent progress and remaining challenges. *Curr Opin Virol* **48**, 23-29 (2021).
21. Liang, Y. Pathogenicity and virulence of influenza. *Virulence* **14**, 2223057 (2023).
22. Cervantes, O.*, et al.* Role of hormones in the pregnancy and sex-specific outcomes to infections with respiratory viruses. *Immunol Rev* **308**, 123-148 (2022).
23. Bourne, A.W. Influenza: pregnancy, labour, the puerperium, and diseases of women. in *Influenza: essays by several authors* (ed. Crookshank, F.G.) 433-443 (Heinemann, London, 1922).
24. Harris, J.W. Influenza occurring in pregnant women: a statistical study of thirteen hundred and fifty cases. *JAMA* **72**, 978-980 (1919).
25. Freeman, D.W. & Barno, A. Deaths from Asian influenza associated with pregnancy. *American journal of obstetrics and gynecology* **78**, 1172-1175 (1959).

26. Hardy, J.M., Azarowicz, E.N., Mannini, A., Medearis, D.N., Jr. & Cooke, R.E. The effect of Asian influenza on the outcome of pregnancy, Baltimore, 1957-1958. *Am J Public Health Nations Health* **51**, 1182-1188 (1961).
27. Kim, H.M., Kang, Y.M., Song, B.M., Kim, H.S. & Seo, S.H. The 2009 pandemic H1N1 influenza virus is more pathogenic in pregnant mice than seasonal H1N1 influenza virus. *Viral Immunol* **25**, 402-410 (2012).
28. Mosby, L.G., Rasmussen, S.A. & Jamieson, D.J. 2009 pandemic influenza A (H1N1) in pregnancy: a systematic review of the literature. *Am J Obstet Gynecol* **205**, 10-18 (2011).
29. Centers for Disease, C. & Prevention. 2009 pandemic influenza A (H1N1) in pregnant women requiring intensive care - New York City, 2009. *MMWR Morb Mortal Wkly Rep* **59**, 321-326 (2010).
30. Jamieson, D.J.*, et al.* H1N1 2009 influenza virus infection during pregnancy in the USA. *Lancet* **374**, 451-458 (2009).
31. Centers for Disease, C. & Prevention. Novel influenza A (H1N1) virus infections in three pregnant women - United States, April-May 2009. *MMWR Morb Mortal Wkly Rep* **58**, 497-500 (2009).
32. Jimenez, M.F.*, et al.* Outcomes for pregnant women infected with the influenza A (H1N1) virus during the 2009 pandemic in Porto Alegre, Brazil. *Int J Gynaecol Obstet* **111**, 217-219 (2010).
33. Siston, A.M.*, et al.* Pandemic 2009 influenza A(H1N1) virus illness among pregnant women in the United States. *JAMA* **303**, 1517-1525 (2010).
34. Pierce, M.*, et al.* Perinatal outcomes after maternal 2009/H1N1 infection: national cohort study. *BMJ* **342**, d3214 (2011).
35. Louie, J.K., Acosta, M., Jamieson, D.J., Honein, M.A. & California Pandemic Working, G. Severe 2009 H1N1 influenza in pregnant and postpartum women in California. *N Engl J Med* **362**, 27-35 (2010).
36. Ribeiro, A.F.*, et al.* Severe influenza A(H1N1)pdm09 in pregnant women and neonatal outcomes, State of Sao Paulo, Brazil, 2009. *PLoS One* **13**, e0194392 (2018).
37. Mertz, D.*, et al.* Populations at risk for severe or complicated influenza illness: systematic review and meta-analysis. *BMJ* **347**, f5061 (2013).
38. Purcell, R., Giles, M.L., Crawford, N.W. & Buttery, J. Systematic Review of Avian Influenza Virus Infection and Outcomes during Pregnancy. *Emerg Infect Dis* **31**, 50-56 (2025).
39. Wang, J.*, et al.* Influenza A virus infection disrupts the function of syncytiotrophoblast cells and contributes to adverse pregnancy outcomes. *J Med Virol* **96**, e29687 (2024).
40. Xu, L., Bao, L., Deng, W. & Qin, C. Highly pathogenic avian influenza H5N1 virus could partly be evacuated by pregnant BALB/c mouse during abortion or preterm delivery. *Virol J* **8**, 342 (2011).
41. Gu, J.*, et al.* H5N1 infection of the respiratory tract and beyond: a molecular pathology study. *Lancet* **370**, 1137-1145 (2007).
42. Zhao, Y.*, et al.* Neutrophils may be a vehicle for viral replication and dissemination in human H5N1 avian influenza. *Clin Infect Dis* **47**, 1575-1578 (2008).
43. Baas, T.*, et al.* Integrated molecular signature of disease: analysis of influenza virus-infected macaques through functional genomics and proteomics. *J Virol* **80**, 10813-10828 (2006).
44. StatPearls. (2025).
45. Davies, A.*, et al.* Extracorporeal Membrane Oxygenation for 2009 Influenza A(H1N1) Acute Respiratory Distress Syndrome. *JAMA* **302**, 1888-1895 (2009).
46. Ranieri, V.M.*, et al.* Acute respiratory distress syndrome: the Berlin Definition. *JAMA* **307**, 2526-2533 (2012).
47. Matthay, M.A.*, et al.* A New Global Definition of Acute Respiratory Distress Syndrome. *Am J Respir Crit Care Med* **209**, 37-47 (2024).

48. Morton, B.*, et al.* Performance of influenza-specific triage tools in an H1N1-positive cohort: P/F ratio better predicts the need for mechanical ventilation and critical care admission. *Br J Anaesth* **114**, 927-933 (2015).
49. Suttapanit, K., Boriboon, J. & Sanguanwit, P. Risk factors for non-invasive ventilation failure in influenza infection with acute respiratory failure in emergency department. *Am J Emerg Med* **45**, 368-373 (2021).
50. Sanders, C.J.*, et al.* Compromised respiratory function in lethal influenza infection is characterized by the depletion of type I alveolar epithelial cells beyond threshold levels. *Am J Physiol Lung Cell Mol Physiol* **304**, L481-488 (2013).
51. LoMauro, A. & Aliverti, A. Respiratory physiology of pregnancy: Physiology masterclass. *Breathe (Sheff)* **11**, 297-301 (2015).
52. Gilroy, R.J., Mangura, B.T. & Lavietes, M.H. Rib cage and abdominal volume displacements during breathing in pregnancy. *Am Rev Respir Dis* **137**, 668-672 (1988).
53. Weinberger, S.E., Weiss, S.T., Cohen, W.R., Weiss, J.W. & Johnson, T.S. Pregnancy and the lung. *Am Rev Respir Dis* **121**, 559-581 (1980).
54. Richardson, P., Wyman, M.L. & Jung, A.L. Functional residual capacity and severity of respiratory distress syndrome in infants. *Crit Care Med* **8**, 637-640 (1980).
55. Jensen, D.*, et al.* Physiological mechanisms of hyperventilation during human pregnancy. *Respir Physiol Neurobiol* **161**, 76-86 (2008).
56. Contreras, G.*, et al.* Ventilatory drive and respiratory muscle function in pregnancy. *Am Rev Respir Dis* **144**, 837-841 (1991).
57. Taverne, J.*, et al.* High incidence of hyperventilation syndrome after COVID-19. *J Thorac Dis* **13**, 3918-3922 (2021).
58. Tate, M.D. & Mansell, A. An update on the NLRP3 inflammasome and influenza: the road to redemption or perdition? *Curr Opin Immunol* **54**, 80-85 (2018).
59. Pothlichet, J.*, et al.* Type I IFN triggers RIG-I/TLR3/NLRP3-dependent inflammasome activation in influenza A virus infected cells. *PLoS Pathog* **9**, e1003256 (2013).
60. Allen, I.C.*, et al.* The NLRP3 inflammasome mediates in vivo innate immunity to influenza A virus through recognition of viral RNA. *Immunity* **30**, 556-565 (2009).
61. McAuley, J.L.*, et al.* Activation of the NLRP3 inflammasome by IAV virulence protein PB1-F2 contributes to severe pathophysiology and disease. *PLoS Pathog* **9**, e1003392 (2013).
62. Ichinohe, T., Pang, I.K. & Iwasaki, A. Influenza virus activates inflammasomes via its intracellular M2 ion channel. *Nat Immunol* **11**, 404-410 (2010).
63. Bauer, R.N.*, et al.* Influenza enhances caspase-1 in bronchial epithelial cells from asthmatic volunteers and is associated with pathogenesis. *J Allergy Clin Immunol* **130**, 958-967.e914 (2012).
64. Guo, J.*, et al.* The Serum Profile of Hypercytokinemia Factors Identified in H7N9-Infected Patients can Predict Fatal Outcomes. *Sci Rep* **5**, 10942 (2015).
65. Ren, R.*, et al.* The H7N9 influenza A virus infection results in lethal inflammation in the mammalian host via the NLRP3-caspase-1 inflammasome. *Sci Rep* **7**, 7625 (2017).
66. Coates, B.M.*, et al.* Inhibition of the NOD-Like Receptor Protein 3 Inflammasome Is Protective in Juvenile Influenza A Virus Infection. *Front Immunol* **8**, 782 (2017).
67. Tate, M.D.*, et al.* Reassessing the role of the NLRP3 inflammasome during pathogenic influenza A virus infection via temporal inhibition. *Sci Rep* **6**, 27912 (2016).
68. Gomez-Lopez, N.*, et al.* Inflammasomes: Their Role in Normal and Complicated Pregnancies. *J Immunol* **203**, 2757-2769 (2019).
69. Romero, R.*, et al.* A Role for the Inflammasome in Spontaneous Labor at Term. *Am J Reprod Immunol* **79**, e12440 (2018).

70. Gomez-Lopez, N.*, et al.* Gasdermin D:. *J Matern Fetal Neonatal Med* **34**, 569-579 (2021).
71. Gotsch, F.*, et al.* Evidence of the involvement of caspase-1 under physiologic and pathologic cellular stress during human pregnancy: a link between the inflammasome and parturition. *J Matern Fetal Neonatal Med* **21**, 605-616 (2008).
72. Romero, R.*, et al.* Interleukin-1 alpha and interleukin-1 beta in preterm and term human parturition. *Am J Reprod Immunol* **27**, 117-123 (1992).
73. Cardenas, I.*, et al.* Placental viral infection sensitizes to endotoxin-induced pre-term labor: a double hit hypothesis. *Am J Reprod Immunol* **65**, 110-117 (2011).
74. C Weel, I.*, et al.* Increased expression of NLRP3 inflammasome in placentas from pregnant women with severe preeclampsia. *J Reprod Immunol* **123**, 40-47 (2017).
75. Gomez-Lopez, N.*, et al.* A Role for the Inflammasome in Spontaneous Preterm Labor With Acute Histologic Chorioamnionitis. *Reprod Sci* **24**, 1382-1401 (2017).
76. Pontillo, A.*, et al.* Bacterial LPS differently modulates inflammasome gene expression and IL-1β secretion in trophoblast cells, decidual stromal cells, and decidual endothelial cells. *Reprod Sci* **20**, 563-566 (2013).
77. Wu, W. & Metcalf, J.P. The Role of Type I IFNs in Influenza: Antiviral Superheroes or Immunopathogenic Villains? *J Innate Immun* **12**, 437-447 (2020).
78. Ezeonwumelu, I.J., Garcia-Vidal, E. & Ballana, E. JAK-STAT Pathway: A Novel Target to Tackle Viral Infections. *Viruses* **13**(2021).
79. Husain, M. Influenza Virus Host Restriction Factors: The ISGs and Non-ISGs. *Pathogens* **13**(2024).
80. van de Sandt, C.E., Kreijtz, J.H. & Rimmelzwaan, G.F. Evasion of influenza A viruses from innate and adaptive immune responses. *Viruses* **4**, 1438-1476 (2012).
81. Racicot, K.*, et al.* Cutting Edge: Fetal/Placental Type I IFN Can Affect Maternal Survival and Fetal Viral Load during Viral Infection. *J Immunol* **198**, 3029-3032 (2017).
82. Casazza, R.L., Lazear, H.M. & Miner, J.J. Protective and Pathogenic Effects of Interferon Signaling During Pregnancy. *Viral Immunol* **33**, 3-11 (2020).
83. Crow, Y.J.*, et al.* Characterization of human disease phenotypes associated with mutations in TREX1, RNASEH2A, RNASEH2B, RNASEH2C, SAMHD1, ADAR, and IFIH1. *Am J Med Genet A* **167A**, 296-312 (2015).
84. Andrade, D.*, et al.* Interferon-alpha and angiogenic dysregulation in pregnant lupus patients who develop preeclampsia. *Arthritis Rheumatol* **67**, 977-987 (2015).
85. Yockey, L.J.*, et al.* Type I interferons instigate fetal demise after Zika virus infection. *Sci Immunol* **3**(2018).
86. Park, H.*, et al.* A distinct lineage of CD4 T cells regulates tissue inflammation by producing interleukin 17. *Nat Immunol* **6**, 1133-1141 (2005).
87. Ivanov, II*, et al.* The orphan nuclear receptor RORgammat directs the differentiation program of proinflammatory IL-17+ T helper cells. *Cell* **126**, 1121-1133 (2006).
88. Antonson, A.M.*, et al.* Moderately pathogenic maternal influenza A virus infection disrupts placental integrity but spares the fetal brain. *Brain Behav Immun* **96**, 28-39 (2021).
89. Li, C.*, et al.* IL-17 response mediates acute lung injury induced by the 2009 pandemic influenza A (H1N1) virus. *Cell Res* **22**, 528-538 (2012).
90. Bermejo-Martin, J.F.*, et al.* Th1 and Th17 hypercytokinemia as early host response signature in severe pandemic influenza. *Crit Care* **13**, R201 (2009).
91. Choi, G.B.*, et al.* The maternal interleukin-17a pathway in mice promotes autism-like phenotypes in offspring. *Science (New York, N.Y.)* **351**, 933-939 (2016).
92. McKinstry, K.K.*, et al.* IL-10 deficiency unleashes an influenza-specific Th17 response and enhances survival against high-dose challenge. *J Immunol* **182**, 7353-7363 (2009).

93. Sakaguchi, S., Yamaguchi, T., Nomura, T. & Ono, M. Regulatory T cells and immune tolerance. *Cell* **133**, 775-787 (2008).
94. Smigiel, K.S., Srivastava, S., Stolley, J.M. & Campbell, D.J. Regulatory T-cell homeostasis: steady-state maintenance and modulation during inflammation. *Immunol Rev* **259**, 40-59 (2014).
95. Fontenot, J.D., Gavin, M.A. & Rudensky, A.Y. Foxp3 programs the development and function of CD4+CD25+ regulatory T cells. *Nat Immunol* **4**, 330-336 (2003).
96. Williams, L.M. & Rudensky, A.Y. Maintenance of the Foxp3-dependent developmental program in mature regulatory T cells requires continued expression of Foxp3. *Nat Immunol* **8**, 277-284 (2007).
97. Li, M.O., Wan, Y.Y. & Flavell, R.A. T cell-produced transforming growth factor-beta1 controls T cell tolerance and regulates Th1- and Th17-cell differentiation. *Immunity* **26**, 579-591 (2007).
98. Rubtsov, Y.P*., et al.* Regulatory T cell-derived interleukin-10 limits inflammation at environmental interfaces. *Immunity* **28**, 546-558 (2008).
99. Saito, S., Nakashima, A., Shima, T. & Ito, M. Th1/Th2/Th17 and regulatory T-cell paradigm in pregnancy. *Am J Reprod Immunol* **63**, 601-610 (2010).
100. Figueiredo, A.S. & Schumacher, A. The T helper type 17/regulatory T cell paradigm in pregnancy. *Immunology* **148**, 13-21 (2016).
101. Vermillion, M.S., Ursin, R.L., Attreed, S.E. & Klein, S.L. Estriol Reduces Pulmonary Immune Cell Recruitment and Inflammation to Protect Female Mice From Severe Influenza. *Endocrinology* **159**, 3306-3320 (2018).
102. Burzyn, D*., et al.* A special population of regulatory T cells potentiates muscle repair. *Cell* **155**, 1282-1295 (2013).
103. Dial, C.F., Tune, M.K., Doerschuk, C.M. & Mock, J.R. Foxp3(+) Regulatory T Cell Expression of Keratinocyte Growth Factor Enhances Lung Epithelial Proliferation. *Am J Respir Cell Mol Biol* **57**, 162-173 (2017).
104. Arpaia, N*., et al.* A Distinct Function of Regulatory T Cells in Tissue Protection. *Cell* **162**, 1078-1089 (2015).
105. Varanasi, S.K., Rajasagi, N.K., Jaggi, U. & Rouse, B.T. Role of IL-18 induced Amphiregulin expression on virus induced ocular lesions. *Mucosal Immunol* **11**, 1705-1715 (2018).
106. Garnier, L*., et al.* Estrogen Signaling in Bystander Foxp3(neg) CD4(+) T Cells Suppresses Cognate Th17 Differentiation in Trans and Protects from Central Nervous System Autoimmunity. *J Immunol* **201**, 3218-3228 (2018).
107. Polanczyk, M.J., Hopke, C., Huan, J., Vandenbark, A.A. & Offner, H. Enhanced FoxP3 expression and Treg cell function in pregnant and estrogen-treated mice. *J Neuroimmunol* **170**, 85-92 (2005).
108. Mjosberg, J*., et al.* Systemic reduction of functionally suppressive CD4dimCD25highFoxp3+ Tregs in human second trimester pregnancy is induced by progesterone and 17beta-estradiol. *J Immunol* **183**, 759-769 (2009).
109. Haghmorad, D*., et al.* Pregnancy level of estrogen attenuates experimental autoimmune encephalomyelitis in both ovariectomized and pregnant C57BL/6 mice through expansion of Treg and Th2 cells. *J Neuroimmunol* **277**, 85-95 (2014).
110. Shirshev, S.V., Nekrasova, I.V., Gorbunova, O.L. & Orlova, E.G. Effect of Estriol, Chorionic Gonadotropin, and Oncostatin M on the Expression of Recombinase RAG-1 in Regulatory T Lymphocyte Subpopulations. *Bull Exp Biol Med* **167**, 57-61 (2019).
111. Nekrasova, I. & Shirshev, S. Estriol in regulation of cell-mediated immune reactions in multiple sclerosis. *J Neuroimmunol* **349**, 577421 (2020).
112. Lee, J.H., Ulrich, B., Cho, J., Park, J. & Kim, C.H. Progesterone promotes differentiation of human cord blood fetal T cells into T regulatory cells but suppresses their differentiation into Th17 cells. *J Immunol* **187**, 1778-1787 (2011).

113. Black, A., Bhaumik, S., Kirkman, R.L., Weaver, C.T. & Randolph, D.A. Developmental regulation of Th17-cell capacity in human neonates. *Eur J Immunol* **42**, 311-319 (2012).
114. Engler, J.B.*, et al.* Glucocorticoid receptor in T cells mediates protection from autoimmunity in pregnancy. *Proc Natl Acad Sci U S A* **114**, E181-E190 (2017).
115. Mao, G.*, et al.* Progesterone increases systemic and local uterine proportions of CD4+CD25+ Treg cells during midterm pregnancy in mice. *Endocrinology* **151**, 5477-5488 (2010).
116. Karlsson, E.A.*, et al.* Influenza virus infection in nonhuman primates. *Emerg Infect Dis* **18**, 1672-1675 (2012).
117. Paungpin, W.*, et al.* Evidence of Influenza A Virus Infection in Cynomolgus Macaques, Thailand. *Vet Sci* **9**(2022).
118. Nakayama, M. & Itoh, Y. Lectin Staining to Detect Human and Avian Influenza Virus Receptors in the Airway of Nonhuman Primates. *Methods Mol Biol* **2556**, 37-43 (2022).
119. Mooij, P.*, et al.* Pandemic Swine-Origin H1N1 Influenza Virus Replicates to Higher Levels and Induces More Fever and Acute Inflammatory Cytokines in Cynomolgus versus Rhesus Monkeys and Can Replicate in Common Marmosets. *PLoS One* **10**, e0126132 (2015).
120. Nguyen, C.T.*, et al.* Efficacy of Neuraminidase Inhibitors against H5N6 Highly Pathogenic Avian Influenza Virus in a Nonhuman Primate Model. *Antimicrob Agents Chemother* **64**(2020).
121. Bahl, K.*, et al.* Preclinical and Clinical Demonstration of Immunogenicity by mRNA Vaccines against H10N8 and H7N9 Influenza Viruses. *Mol Ther* **25**, 1316-1327 (2017).
122. Impagliazzo, A.*, et al.* A stable trimeric influenza hemagglutinin stem as a broadly protective immunogen. *Science* **349**, 1301-1306 (2015).
123. Chertow, D.S.*, et al.* Influenza A and methicillin-resistant Staphylococcus aureus co-infection in rhesus macaques - A model of severe pneumonia. *Antiviral Res* **129**, 120-129 (2016).
124. Herfst, S.*, et al.* Pandemic 2009 H1N1 influenza virus causes diffuse alveolar damage in cynomolgus macaques. *Vet Pathol* **47**, 1040-1047 (2010).
125. Baskin, C.R.*, et al.* Early and sustained innate immune response defines pathology and death in nonhuman primates infected by highly pathogenic influenza virus. *Proc Natl Acad Sci U S A* **106**, 3455-3460 (2009).
126. Corry, J.*, et al.* Infiltration of inflammatory macrophages and neutrophils and widespread pyroptosis in lung drive influenza lethality in nonhuman primates. *PLoS Pathog* **18**, e1010395 (2022).
127. Watanabe, T.*, et al.* Experimental infection of Cynomolgus Macaques with highly pathogenic H5N1 influenza virus through the aerosol route. *Sci Rep* **8**, 4801 (2018).
128. Fukuyama, S.*, et al.* Pathogenesis of Influenza A(H7N9) Virus in Aged Nonhuman Primates. *J Infect Dis* **222**, 1155-1164 (2020).
129. Iwatsuki-Horimoto, K.*, et al.* The Marmoset as an Animal Model of Influenza: Infection With A(H1N1)pdm09 and Highly Pathogenic A(H5N1) Viruses via the Conventional or Tracheal Spray Route. *Front Microbiol* **9**, 844 (2018).
130. Moncla, L.H.*, et al.* A novel nonhuman primate model for influenza transmission. *PLoS One* **8**, e78750 (2013).
131. Holbrook, B.C.*, et al.* Nonhuman primate infants have an impaired respiratory but not systemic IgG antibody response following influenza virus infection. *Virology* **476**, 124-133 (2015).
132. Carter, A.M. Animal models of human placentation--a review. *Placenta* **28 Suppl A**, S41-47 (2007).
133. Andersen, M.D.*, et al.* Animal Models of Fetal Medicine and Obstetrics. (InTech, 2018).
134. Machado, D.A., Ontiveros, A.E. & Behringer, R.R. Mammalian uterine morphogenesis and variations. *Curr Top Dev Biol* **148**, 51-77 (2022).
135. Rinkenberger, J. & Werb, Z. The labyrinthine placenta. *Nat Genet* **25**, 248-250 (2000).

136. Roberts, V.H.J*., et al.* Rhesus macaque fetal and placental growth demographics: A resource for laboratory animal researchers. *Am J Primatol* **85**, e23526 (2023).
137. Matsumoto, S., Okamura, E., Muto, M. & Ema, M. Similarities and differences in placental development between humans and cynomolgus monkeys. *Reprod Med Biol* **22**, e12522 (2023).
138. Hoo, R., Nakimuli, A. & Vento-Tormo, R. Innate Immune Mechanisms to Protect Against Infection at the Human Decidual-Placental Interface. *Front Immunol* **11**, 2070 (2020).
139. Haider, S*., et al.* Self-Renewing Trophoblast Organoids Recapitulate the Developmental Program of the Early Human Placenta. *Stem Cell Reports* **11**, 537-551 (2018).
140. Mayer, A.E. & Parks, G.D. An AGM model for changes in complement during pregnancy: neutralization of influenza virus by serum is diminished in late third trimester. *PLoS One* **9**, e112749 (2014).
141. Short, S.J*., et al.* Maternal influenza infection during pregnancy impacts postnatal brain development in the rhesus monkey. *Biol Psychiatry* **67**, 965-973 (2010).
142. Loukotková, L*., et al.* Pharmacokinetics of oseltamivir phosphate and oseltamivir carboxylate in non-pregnant and pregnant rhesus monkeys. *Regul Toxicol Pharmacol* **112**, 104569 (2020).
143. Sirianni, J.E., Newell-Morris, L. & Campbell, M. Growth of the fetal pigtailed macaque (Macaca nemestrina) I. Cephalofacial dimensions. *Folia Primatol (Basel)* **35**, 65-75 (1981).
144. Koday, M.T*., et al.* Multigenic DNA vaccine induces protective cross-reactive T cell responses against heterologous influenza virus in nonhuman primates. *PLoS One* **12**, e0189780 (2017).
145. Go, J.T*., et al.* 2009 pandemic H1N1 influenza virus elicits similar clinical course but differential host transcriptional response in mouse, macaque, and swine infection models. *BMC Genomics* **13**, 627 (2012).
146. Itoh, Y*., et al.* In vitro and in vivo characterization of new swine-origin H1N1 influenza viruses. *Nature* **460**, 1021-1025 (2009).
147. Cervantes, O*., et al.* Testing pulmonary physiology in ventilated non-human primates. *J Med Primatol* **53**, e12694 (2024).
148. Ferguson, N.D*., et al.* The Berlin definition of ARDS: an expanded rationale, justification, and supplementary material. *Intensive Care Med* **38**, 1573-1582 (2012).
149. Nuckton, T.J*., et al.* Pulmonary dead-space fraction as a risk factor for death in the acute respiratory distress syndrome. *N Engl J Med* **346**, 1281-1286 (2002).
150. Kallet, R.H., Alonso, J.A., Pittet, J.F. & Matthay, M.A. Prognostic value of the pulmonary dead-space fraction during the first 6 days of acute respiratory distress syndrome. *Respir Care* **49**, 1008-1014 (2004).
151. Kallet, R.H*., et al.* The association between physiologic dead-space fraction and mortality in subjects with ARDS enrolled in a prospective multi-center clinical trial. *Respir Care* **59**, 1611-1618 (2014).
152. Lapinsky, S.E. Acute respiratory failure in pregnancy. *Obstet Med* **8**, 126-132 (2015).
153. Amato, M.B*., et al.* Driving pressure and survival in the acute respiratory distress syndrome. *N Engl J Med* **372**, 747-755 (2015).
154. Villar, J*., et al.* A Quantile Analysis of Plateau and Driving Pressures: Effects on Mortality in Patients With Acute Respiratory Distress Syndrome Receiving Lung-Protective Ventilation. *Crit Care Med* **45**, 843-850 (2017).
155. Bellani, G*., et al.* Driving Pressure Is Associated with Outcome during Assisted Ventilation in Acute Respiratory Distress Syndrome. *Anesthesiology* **131**, 594-604 (2019).
156. O'Connor, M.A*., et al.* Mucosal T Helper 17 and T Regulatory Cell Homeostasis Correlate with Acute Simian Immunodeficiency Virus Viremia and Responsiveness to Antiretroviral Therapy in Macaques. *AIDS Res Hum Retroviruses* **35**, 295-305 (2019).

157. O'Connor, M.A.*, et al.* Early cellular innate immune responses drive Zika viral persistence and tissue tropism in pigtail macaques. *Nat Commun* **9**, 3371 (2018).
158. Robinson, M.D., McCarthy, D.J. & Smyth, G.K. edgeR: a Bioconductor package for differential expression analysis of digital gene expression data. *Bioinformatics* **26**, 139-140 (2010).
159. Law, C.W., Chen, Y., Shi, W. & Smyth, G.K. voom: Precision weights unlock linear model analysis tools for RNA-seq read counts. *Genome Biol* **15**, R29 (2014).
160. Subramanian, A*., et al.* Gene set enrichment analysis: a knowledge-based approach for interpreting genome-wide expression profiles. *Proc Natl Acad Sci U S A* **102**, 15545-15550 (2005).
161. Gu, Z., Eils, R. & Schlesner, M. Complex heatmaps reveal patterns and correlations in multidimensional genomic data. *Bioinformatics* **32**, 2847-2849 (2016).
162. Aphalo, P.J. *Learn R: As a Language*, (Chapman and Hall/CRC Press, Boca Raton and London, 2024).
163. Nishiura, H. Excess risk of stillbirth during the 1918-1920 influenza pandemic in Japan. *Eur J Obstet Gynecol Reprod Biol* **147**, 115 (2009).
164. Rasmussen, S.A. & Jamieson, D.J. Influenza and pregnancy in the United States: before, during, and after 2009 H1N1. *Clin Obstet Gynecol* **55**, 487-497 (2012).
165. Rasmussen, S.A., Jamieson, D.J. & Uyeki, T.M. Effects of influenza on pregnant women and infants. *American Journal of Obstetrics and Gynecology* **207**, S3-S8 (2012).
166. Costantine, M.M. Physiologic and pharmacokinetic changes in pregnancy. *Front Pharmacol* **5**, 65 (2014).
167. Soma-Pillay, P., Nelson-Piercy, C., Tolppanen, H. & Mebazaa, A. Physiological changes in pregnancy. *Cardiovasc J Afr* **27**, 89-94 (2016).
168. Laibl, V. & Sheffield, J. The management of respiratory infections during pregnancy. *Immunol Allergy Clin North Am* **26**, 155-172, viii (2006).
169. Harris, J. & Sheiner, E. Does an upper respiratory tract infection during pregnancy affect perinatal outcomes? A literature review. *Curr Infect Dis Rep* **15**, 143-147 (2013).
170. Liong, S*., et al.* Influenza A virus causes maternal and fetal pathology via innate and adaptive vascular inflammation in mice. *Proc Natl Acad Sci U S A* **117**, 24964-24973 (2020).
171. Vanders, R.L*., et al.* Inflammatory and antiviral responses to influenza A virus infection are dysregulated in pregnant mice with allergic airway disease. *Am J Physiol Lung Cell Mol Physiol* **325**, L385-L398 (2023).
172. Bohrmann, B., Massa, M.S., Ross, S., Lewington, S. & Lacey, B. Body Mass Index and Risk of Hospitalization or Death Due to Lower or Upper Respiratory Tract Infection. *JAMA* **329**, 1512-1514 (2023).
173. Hedenstierna, G*., et al.* Oxygenation Impairment during Anesthesia: Influence of Age and Body Weight. *Anesthesiology* **131**, 46-57 (2019).
174. Poon, L.L*., et al.* Molecular detection of a novel human influenza (H1N1) of pandemic potential by conventional and real-time quantitative RT-PCR assays. *Clin Chem* **55**, 1555-1558 (2009).
175. Loughran, S.T*., et al.* Influenza infection directly alters innate IL-23 and IL-12p70 and subsequent IL-17A and IFN-γ responses to pneumococcus in vitro in human monocytes. *PLoS One* **13**, e0203521 (2018).
176. Yu, Z.X*., et al.* The ratio of Th17/Treg cells as a risk indicator in early acute respiratory distress syndrome. *Crit Care* **19**, 82 (2015).
177. Bassett, L*., et al.* Non-invasive measure of respiratory mechanics and conventional respiratory parameters in conscious large animals by high frequency Airwave Oscillometry. *J Pharmacol Toxicol Methods* **70**, 62-65 (2014).
178. Obot Akata, C.J*., et al.* Development of a head-out plethysmograph system for non-human primates in an Animal Biosafety Level 3 facility. *J Pharmacol Toxicol Methods* **55**, 96-102 (2007).

179. Foster, C.D., Hunter, T.C., Gibbs, P.H. & Leffel, E.K. Whole-body plethysmography in African green monkeys (Chlorocebus aethiops) with and without jackets. *J Am Assoc Lab Anim Sci* **47**, 52-55 (2008).
180. Shieh, W.J.*, et al.* 2009 pandemic influenza A (H1N1): pathology and pathogenesis of 100 fatal cases in the United States. *Am J Pathol* **177**, 166-175 (2010).
181. Klugman, K.P., Astley, C.M. & Lipsitch, M. Time from illness onset to death, 1918 influenza and pneumococcal pneumonia. *Emerg Infect Dis* **15**, 346-347 (2009).
182. Yu, H.*, et al.* Risk factors for severe illness with 2009 pandemic influenza A (H1N1) virus infection in China. *Clin Infect Dis* **52**, 457-465 (2011).
183. Louie, J.K.*, et al.* A novel risk factor for a novel virus: obesity and 2009 pandemic influenza A (H1N1). *Clin Infect Dis* **52**, 301-312 (2011).
184. Chan, K.H.*, et al.* Wild type and mutant 2009 pandemic influenza A (H1N1) viruses cause more severe disease and higher mortality in pregnant BALB/c mice. *PLoS One* **5**, e13757 (2010).
185. Marcelin, G.*, et al.* Fatal outcome of pandemic H1N1 2009 influenza virus infection is associated with immunopathology and impaired lung repair, not enhanced viral burden, in pregnant mice. *J Virol* **85**, 11208-11219 (2011).
186. Lauzon-Joset, J.F.*, et al.* Pregnancy induces a steady-state shift in alveolar macrophage M1/M2 phenotype that is associated with a heightened severity of Influenza infection: mechanistic insight using mouse models. *J Infect Dis* (2018).
187. Vermillion, M.S.*, et al.* Pregnancy preserves pulmonary function following influenza virus infection in C57BL/6 mice. *Am J Physiol Lung Cell Mol Physiol* **315**, L517-L525 (2018).
188. Engels, G.*, et al.* Pregnancy-Related Immune Adaptation Promotes the Emergence of Highly Virulent H1N1 Influenza Virus Strains in Allogenically Pregnant Mice. *Cell Host Microbe* **21**, 321-333 (2017).
189. Creisher, P.S.*, et al.* Suppression of progesterone by influenza A virus mediates adverse maternal and fetal outcomes in mice. *mBio* **15**, e0306523 (2024).
190. Chronopoulos, J.*, et al.* Pregnancy enhances antiviral immunity independent of type I IFN but dependent on IL-17-producing γδ. *Sci Adv* **10**, eado7087 (2024).
191. Vanders, R.L., Gibson, P.G., Wark, P.A. & Murphy, V.E. Alterations in inflammatory, antiviral and regulatory cytokine responses in peripheral blood mononuclear cells from pregnant women with asthma. *Respirology* **18**, 827-833 (2013).
192. Kim, J.*, et al.* Damage sensing through TLR9 Regulates Inflammatory and Antiviral Responses During Influenza Infection. *bioRxiv* (2024).
193. Martínez-Colón, G.J.*, et al.* Influenza-induced immune suppression to methicillin-resistant Staphylococcus aureus is mediated by TLR9. *PLoS Pathog* **15**, e1007560 (2019).
194. Tuvim, M.J., Gilbert, B.E., Dickey, B.F. & Evans, S.E. Synergistic TLR2/6 and TLR9 activation protects mice against lethal influenza pneumonia. *PLoS One* **7**, e30596 (2012).
195. David, C., Verney, C., Si-Tahar, M. & Guillon, A. The deadly dance of alveolar macrophages and influenza virus. *Eur Respir Rev* **33**(2024).
196. Pervizaj-Oruqaj, L.*, et al.* Alveolar macrophage-expressed Plet1 is a driver of lung epithelial repair after viral pneumonia. *Nat Commun* **15**, 87 (2024).
197. Aegerter, H.*, et al.* Influenza-induced monocyte-derived alveolar macrophages confer prolonged antibacterial protection. *Nat Immunol* **21**, 145-157 (2020).
198. Jacobsen, H.*, et al.* Offspring born to influenza A virus infected pregnant mice have increased susceptibility to viral and bacterial infections in early life. *Nat Commun* **12**, 4957 (2021).

199. Davis, S.M., Sweet, L.M., Oppenheimer, K.H., Suratt, B.T. & Phillippe, M. Estradiol and progesterone influence on influenza infection and immune response in a mouse model. *Am J Reprod Immunol* **78**(2017).
200. Robinson, D.P., Lorenzo, M.E., Jian, W. & Klein, S.L. Elevated 17beta-estradiol protects females from influenza A virus pathogenesis by suppressing inflammatory responses. *PLoS Pathog* **7**, e1002149 (2011).
201. Finch, C.L.*, et al.* Pregnancy level of estradiol attenuated virus-specific humoral immune response in H5N1-infected female mice despite inducing anti-inflammatory protection. *Emerg Microbes Infect* **8**, 1146-1156 (2019).
202. Le, T.V.*, et al.* Fatal avian influenza A(H5N1) infection in a 36-week pregnant woman survived by her newborn in Soc Trang Province, Vietnam, 2012. *Influenza Other Respir Viruses* **13**, 292-297 (2019).
203. Rasmussen, S.A., Jamieson, D.J. & Bresee, J.S. Pandemic influenza and pregnant women. *Emerg Infect Dis* **14**, 95-100 (2008).
204. Miller, A.C.*, et al.* Novel influenza A(H1N1) virus among gravid admissions. *Arch Intern Med* **170**, 868-873 (2010).
205. Ng, K.O.*, et al.* Case report: the management for a gestational hypertensive woman with influenza A virus pneumonia and peripartum cardiomyopathy. *BMC Pregnancy Childbirth* **22**, 497 (2022).
206. Wang, R., Yan, W., Du, M., Tao, L. & Liu, J. The effect of influenza virus infection on pregnancy outcomes: A systematic review and meta-analysis of cohort studies. *Int J Infect Dis* **105**, 567-578 (2021).
207. Fell, D.B.*, et al.* Maternal influenza and birth outcomes: systematic review of comparative studies. *BJOG* **124**, 48-59 (2017).
208. Kanmaz, H.G.*, et al.* Placental transmission of novel pandemic influenza a virus. *Fetal Pediatr Pathol* **30**, 280-285 (2011).
209. Cetinkaya, M., Ozkan, H., Celebi, S., Koksal, N. & Hacimustafaoglu, M. Human 2009 influenza A (H1N1) virus infection in a premature infant born to an H1N1-infected mother: placental transmission? *Turk J Pediatr* **53**, 441-444 (2011).
210. Lacaille, H.*, et al.* Impaired Interneuron Development in a Novel Model of Neonatal Brain Injury. *eNeuro* **6**(2019).
211. Weckman, A.M., Ngai, M., Wright, J., McDonald, C.R. & Kain, K.C. The Impact of Infection in Pregnancy on Placental Vascular Development and Adverse Birth Outcomes. *Front Microbiol* **10**, 1924 (2019).
212. Holstein, R.*, et al.* Characteristics and Outcomes of Hospitalized Pregnant Women With Influenza, 2010 to 2019 : A Repeated Cross-Sectional Study. *Ann Intern Med* **175**, 149-158 (2022).
213. Sahni, L.C.*, et al.* Maternal Vaccine Effectiveness Against Influenza-Associated Hospitalizations and Emergency Department Visits in Infants. *JAMA Pediatr* **178**, 176-184 (2024).
214. Marshall, H., McMillan, M., Andrews, R.M., Macartney, K. & Edwards, K. Vaccines in pregnancy: The dual benefit for pregnant women and infants. *Hum Vaccin Immunother* **12**, 848-856 (2016).
215. Xiao, Y.N., Yu, F.Y., Xu, Q. & Gu, J. Tropism and Infectivity of Pandemic Influenza A H1N1/09 Virus in the Human Placenta. *Viruses* **14**(2022).
216. Van Campen, H.*, et al.* Maternal Influenza A Virus Infection Restricts Fetal and Placental Growth and Adversely Affects the Fetal Thymic Transcriptome. *Viruses* **12**(2020).
217. Littauer, E.Q.*, et al.* H1N1 influenza virus infection results in adverse pregnancy outcomes by disrupting tissue-specific hormonal regulation. *PLoS Pathog* **13**, e1006757 (2017).
218. Furukawa, S., Kuroda, Y. & Sugiyama, A. A comparison of the histological structure of the placenta in experimental animals. *J Toxicol Pathol* **27**, 11-18 (2014).

219. Grigsby, P.L. Animal Models to Study Placental Development and Function throughout Normal and Dysfunctional Human Pregnancy. *Semin Reprod Med* **34**, 11-16 (2016).
220. Stouffer, R.L. & Woodruff, T.K. Nonhuman Primates: A Vital Model for Basic and Applied Research on Female Reproduction, Prenatal Development, and Women's Health. *ILAR J* **58**, 281-294 (2017).
221. Tisoncik-Go, J.*, et al.* Disruption of myelin structure and oligodendrocyte maturation in a pigtail macaque model of congenital Zika infection. *bioRxiv* (2023).
222. McCartney, S.A.*, et al.* Amniotic fluid interleukin 6 and interleukin 8 are superior predictors of fetal lung injury compared with maternal or fetal plasma cytokines or placental histopathology in a nonhuman primate model. *Am J Obstet Gynecol* **225**, 89 e81-89 e16 (2021).
223. Coleman, M.*, et al.* Hyaluronidase Impairs Neutrophil Function and Promotes Group B Streptococcus Invasion and Preterm Labor in Nonhuman Primates. *mBio* **12**(2021).
224. Coleman, M.*, et al.* A Broad Spectrum Chemokine Inhibitor Prevents Preterm Labor but Not Microbial Invasion of the Amniotic Cavity or Neonatal Morbidity in a Non-human Primate Model. *Front Immunol* **11**, 770 (2020).
225. Khong, T.Y.*, et al.* Sampling and Definitions of Placental Lesions: Amsterdam Placental Workshop Group Consensus Statement. *Arch Pathol Lab Med* **140**, 698-713 (2016).
226. Redline, R.W.*, et al.* Maternal vascular underperfusion: nosology and reproducibility of placental reaction patterns. *Pediatr Dev Pathol* **7**, 237-249 (2004).
227. Redline, R.W., Ravishankar, S., Bagby, C.M., Saab, S.T. & Zarei, S. Four major patterns of placental injury: a stepwise guide for understanding and implementing the 2016 Amsterdam consensus. *Mod Pathol* **34**, 1074-1092 (2021).
228. Cline, J.M.*, et al.* The placenta in toxicology. Part III: Pathologic assessment of the placenta. *Toxicol Pathol* **42**, 339-344 (2014).
229. Hirsch, A.J.*, et al.* Zika virus infection in pregnant rhesus macaques causes placental dysfunction and immunopathology. *Nat Commun* **9**, 263 (2018).
230. Ichinohe, T., Lee, H.K., Ogura, Y., Flavell, R. & Iwasaki, A. Inflammasome recognition of influenza virus is essential for adaptive immune responses. *J Exp Med* **206**, 79-87 (2009).
231. Deinhardt-Emmer, S.*, et al.* Early postmortem mapping of SARS-CoV-2 RNA in patients with COVID-19 and the correlation with tissue damage. *Elife* **10**(2021).
232. Meijer, W.J., Wensing, A.M., Bruinse, H.W. & Nikkels, P.G. High rate of chronic villitis in placentas of pregnancies complicated by influenza A/H1N1 infection. *Infectious diseases in obstetrics and gynecology* **2014**, 768380 (2014).
233. Kumar, S.R., Biswas, M. & Elankumaran, S. Pandemic H1N1 influenza A virus induces a potent innate immune response in human chorionic cells. *Viral Immunol* **27**, 129-137 (2014).
234. Trinh, Q.D.*, et al.* H3N2 influenza A virus replicates in immortalized human first trimester trophoblast cell lines and induces their rapid apoptosis. *Am J Reprod Immunol* **62**, 139-146 (2009).
235. Komine-Aizawa, S.*, et al.* H1N1/09 influenza A virus infection of immortalized first trimester human trophoblast cell lines. *Am J Reprod Immunol* **68**, 226-232 (2012).
236. Wang, Y.*, et al.* Cell-type specific distribution and activation of type I IFN pathway molecules at the placental maternal-fetal interface in response to COVID-19 infection. *Front Endocrinol (Lausanne)* **13**, 951388 (2022).
237. Liong, S.*, et al.* Influenza A virus causes maternal and fetal pathology via innate and adaptive vascular inflammation in mice. *Proceedings of the National Academy of Sciences* **117**, 24964-24973 (2020).
238. Oseghale, O.*, et al.* Influenza A virus elicits peri-vascular adipose tissue inflammation and vascular dysfunction of the aorta in pregnant mice. *PLoS Pathog* **18**, e1010703 (2022).

239. McDonald, E.M., Anderson, J., Wilusz, J., Ebel, G.D. & Brault, A.C. Zika Virus Replication in Myeloid Cells during Acute Infection Is Vital to Viral Dissemination and Pathogenesis in a Mouse Model. *J Virol* **94**(2020).
240. Michlmayr, D., Andrade, P., Gonzalez, K., Balmaseda, A. & Harris, E. CD14(+)CD16(+) monocytes are the main target of Zika virus infection in peripheral blood mononuclear cells in a paediatric study in Nicaragua. *Nature microbiology* **2**, 1462-1470 (2017).
241. Winkler, C.W., Evans, A.B., Carmody, A.B. & Peterson, K.E. Placental Myeloid Cells Protect against Zika Virus Vertical Transmission in a Rag1-Deficient Mouse Model. *J Immunol* **205**, 143-152 (2020).
242. Hurtado, C.W.*, et al.* Innate immune function in placenta and cord blood of hepatitis C--seropositive mother-infant dyads. *PLoS One* **5**, e12232 (2010).
243. Fievet, N.*, et al.* Plasmodium falciparum exposure in utero, maternal age and parity influence the innate activation of foetal antigen presenting cells. *Malar J* **8**, 251 (2009).
244. Sun, X.*, et al.* Transcriptional Changes during Naturally Acquired Zika Virus Infection Render Dendritic Cells Highly Conducive to Viral Replication. *Cell Rep* **21**, 3471-3482 (2017).
245. Cui, A.*, et al.* Single-cell atlas of the liver myeloid compartment before and after cure of chronic viral hepatitis. *J Hepatol* **80**, 251-267 (2024).
246. van der Wijst, M.G.P.*, et al.* Type I interferon autoantibodies are associated with systemic immune alterations in patients with COVID-19. *Sci Transl Med* **13**, eabh2624 (2021).
247. Sureshchandra, S.*, et al.* Single-cell RNA sequencing reveals immunological rewiring at the maternal-fetal interface following asymptomatic/mild SARS-CoV-2 infection. *Cell Rep* **39**, 110938 (2022).
248. Jash, S. & Sharma, S. Pathogenic Infections during Pregnancy and the Consequences for Fetal Brain Development. *Pathogens* **11**(2022).
249. ACOG Committee Opinion No. 732 Summary: Influenza Vaccination During Pregnancy. *Obstet Gynecol* **131**, 752-753 (2018).
250. Zaman, K.*, et al.* Effectiveness of maternal influenza immunization in mothers and infants. *N Engl J Med* **359**, 1555-1564 (2008).
251. Fitzgerald, T.A. Comparison of research cost: man--primate animal--other animal models. *J Med Primatol* **12**, 138-145 (1983).
252. Wang, J.*, et al.* DNA methylation and transcriptome analysis reveal epigenomic differences among three macaque species. *Evol Appl* **17**, e13604 (2024).
253. Zhang, Q. & Cao, X. Epigenetic regulation of the innate immune response to infection. *Nat Rev Immunol* **19**, 417-432 (2019).
254. Bouvier, N.M. & Lowen, A.C. Animal Models for Influenza Virus Pathogenesis and Transmission. *Viruses* **2**, 1530-1563 (2010).